Chapter 6: Paleoclimate

Coordinating Lead Authors:
Eystein Jansen, Jonathan Overpeck

Lead Authors:
Keith R. Briffa, Jean-Claude Duplessy, Fortunat Joos, Valérie Masson-Delmotte, Daniel O. Olago, Bette Otto-Bliesner, Wm. Richard Peltier, Stefan Rahmstorf, Rengaswamy Ramesh, Dominique Raynaud, David H. Rind, Olga Solomina, Ricardo Villalba, De'er Zhang.

Contributing Authors:
Jean-Marc Barnola, Eva Bauer, Mark Chandler, Julia Cole, Edward R. Cook, Elsa Cortijo, Trond Dokken, Dominik Fleitmann, Myriam Khodri, Laurent Labeyrie, Anders Levermann, Øyvind Lie, Marie-France Loutre, Erik Monnin, Daniel Muhs, Tim Osborn, Frederic Parrenin, Gian-Kasper Plattner, Henry N. Pollack, Øyvind Paasche, Lowell Stott, Ellen Mosley-Thompson, Renato Spahni, Guo-Zheng-Tang, Lonnie Thompson, Claire Waelbroeck, Jim Zachos.

Review Editors: Jean Jouzel, John Mitchell

Date of Draft: 7 March 2006

Notes: TSU compiled version. See Appendix 6.A for terms used in this chapter.

Table of Contents

Executive Summary

What do paleoclimates before one million years ago reveal about the nature of atmospheric carbon dioxide and climate change?

- It is likely that all climates before one million years ago featuring higher than present atmospheric CO_2 concentrations were also significantly warmer than present. This is the case both for climate states stable over millions of years (e.g., the mid-Pliocene, 3.5 million years ago) and for warm events lasting a few hundred thousand years (i.e., the Paleocene-Eocene Thermal Maximum, 55 million years ago).

What is the significance of glacial-interglacial variability in atmospheric composition and climate?

- Post-industrial concentrations of atmospheric CO_2 and CH_4 have risen far above the natural variablity found in the longest ice-core records (650,000 years). Over these multi-millennial time scales, Antarctic temperature and CO_2 concentrations co-vary, and indicate a rather stable coupling between climate and the carbon cycle.

- It is virtually certain that the average rate of increase in radiative forcing from the three well-mixed greenhouse gases carbon dioxide (CO_2), methane (CH_4), and nitrous oxide (N_2O) is larger at present than at any time during the past 20,000 years.

- There is no evidence that the current warming will be mitigated by a natural cooling trend towards glacial conditions. It is very likely that the Earth would not naturally enter another ice age for at least 30,000 years.

- Global mean cooling and warming associated with past glacial maxima and minima are comparable in magnitude, but not in rate, to a projected global mean warming of several degrees over the 21st century. The temperature change since the Last Glacial Maximum (ca. 21,000 years ago) took place at a rate more than ten times slower than this projected future change.

- Climate models have proved capable of simulating the broad-scale spatial patterns of regional climate change recorded by paleoclimatic data to the radiative forcing and land surface changes of the Last Glacial Maximum, thus adequately representing the processes that determine this past climate state.

- During the past 120,000 years, and prior to 10,000 years ago, many large and abrupt climate shifts have occurred, such as 25 abrupt Greenland warmings known as Dansgaard-Oeschger events. During several of these events, the temperature over Greenland likely changed by between 8 and 16°C within a few decades. These events persisted for centuries and had global repercussions, such as major shifts in tropical rainfall patterns. It is unlikely that these events were associated with large changes in global mean temperature, but instead very likely involved a redistribution of heat between northern and southern hemisphere.

- Some large abrupt climate events of the past are very likely linked to changes in the Atlantic Ocean circulation, although details of the mechanism are still under discussion. Our current understanding suggests that the ocean circulation can become unstable and change rapidly when critical ocean temperature-salinity thresholds are crossed. It is unclear at present what and where these thresholds are, and how much they differ between glacial (cold) and interglacial (warm) climate.

- The recent collapse of the Antarctic Larsen B ice shelf is likely unprecedented in the last 10,000 years, and likely linked to recent enhanced warming in the Antarctic Peninsula region.

- Large-scale retreat of the south Greenland Ice Sheet and other Arctic ice fields during the previous interglacial (129 to 116 ka), confirmed by data and models, likely contributed between 2 and 3.5 meters to a total last interglacial sea level rise of 4 to 6 m above present day. This sea level rise was likely driven by warming in the Arctic latitudes of Greenland of 2 to 4°C. Paleoclimate observations also suggest that the Antarctic Ice Sheet likely also contributed to the last interglacial high stand. The rate of sea level rise leading to this high-stand may have exceeded 1 m/century.

What does the study of the current interglacial climate tell us?

- Variations of atmospheric greenhouse gas concentrations observed during the pre-industrial Holocene were small compared to industrial era greenhouse gas increases, and were likely due to mostly natural processes.

- During the last 10,000 years, different regions of the Earth underwent periods warmer and cooler than the 20th century because of changes in the Earth's orbit and the resulting seasonal and latitudinal distribution of incoming solar radiation. Commonly cited warm periods, including the Medieval Warm Period, Holocene Climate Optimum, Holocene Thermal Optimum, Altithermal, Hypsithermal and others, appear to have been distinct only regionally and asynchronously. Consistent with our understanding of past climate forcing, there are no known Holocene periods of synchronous global warmth comparable to the late 20th century.

- Glaciers of several mountain regions of the Northern Hemisphere retreated in response to warming, and were smaller in the early to mid-Holocene than at the end of 20th century, or were even absent. The present day near-global retreat of alpine glaciers cannot be attributed to the same natural causes: the decrease of summer insolation during the past few millennnia, especially in the Northern Hemisphere, should be, on the contrary, favorable to the growth of the glaciers.

- For the mid-Holocene (ca. 6000 years ago), coupled climate models are able to simulate most robust large-scale features of observed climate change, including mid-latitude warming with little change in global mean temperature (<0.4°C), as well as enhanced monsoons, consistent with our understanding of orbital forcing. Coupled climate models perform generally better than atmosphere-only models, and reveal the amplifying roles of ocean and land surface feedbacks in climate change.

- There is no evidence for interglacial centennial to millennial cycles of natural climate variability generating *global* warming and cooling in the past, or that could explain the majority of global warming of the last 100 years.

- The ability of climate and vegetation models to simulate past northward shifts of the boreal treeline under warming conditions supports the simulated significant northward (and upward) expansion of boreal trees in the Northern Hemisphere under global warming. Paleoclimatic results also indicated that these treeline shifts likely result in significant positive climate feedback.

- The strength and frequency of El Niño-Southern Oscillation (ENSO) extremes have varied in response to past changes in orbital forcing, indicating that ENSO variability will likely change as background climate and forcings change.

- Abrupt shifts in the frequency of regional hurricanes, floods, and decadal droughts very likely occurred during the past 10,000 years. However, the mechanisms behind these abrupt shifts are not well understood, nor captured by current climate models.

What does the climate of the last 2000 years tell us about 20th century climate change?

- It is virtually certain that the average rate of increase in carbon dioxide (CO_2), methane (CH_4) and nitrous oxide (N_2O) is larger at present than at any time during the past two millennia before the Industrial Era. It is very likely that the average rate of increase in radiative forcing from these well-mixed greenhouse gases is also at least six times faster at present than at any time during the past two millennia before the Industrial Era.

- It is very likely that the average rate of increase in atmospheric carbon dioxide is at least seven times faster at present than at any time during the past two millennia before the Industrial Era.

- The average rate of increase in atmospheric methane peaked around 1980, when it was very likely almost eight times higher than at any time during the past two millennia before the Industrial Era.

- It is likely that the average rate of increase in atmospheric nitrous oxide is at least three times faster at present than at any time during the past two millennia before the industrialisation.

- Ice core data from Greenland and Northern Hemisphere mid-latitudes show a rapid post-Industrial Era increase in sulfur concentrations above the pre-industrial background, as well as a recent decline, very likely consistent with independent estimates of anthropogenic sulphur dioxide emissions.

- Since the IPCC Third Assessment Report (TAR), there has been an expansion in the length and geographical coverage of high-resolution proxy data, as well as in the number of hemispheric temperature reconstructions using the available data.

- Some of the post-TAR studies indicate greater multi-centennial Northern Hemisphere temperature variability than was shown in the TAR, due to the particular proxies used, and the specific statistical methods of processing and/or scaling them to represent past temperatures. The additional variability implies mainly cooler temperatures (predominantly in the 12th-14th, 17th and 19th centuries) and only one new reconstruction suggests slightly warmer conditions (in the 11th century), but well within the uncertainty range indicated in the TAR.

- The TAR pointed to the "*exceptional warmth of the late 20th century, relative to the past 1000 years*". Subsequent evidence has provided more information. However, it is *very likely* that average Northern Hemisphere temperatures during the second half of the 20th century were warmer than any other 50-year period in the last 500 years. It is also *likely* that this was the warmest period in the past 1000 years and unusually warm compared with the last 1300 years. The regional extent of Northern Hemisphere warmth was very likely greater during the 20th century than in any other century during the last 1300 years. The uneven coverage and characteristics of the proxy data mean that these conclusions are most robust over summer, extra-tropical, land areas.

- Taken together, the very sparse evidence for Southern Hemisphere temperatures prior to the period of instrumental records indicates that it is as *likely as not* that the warmth of the last 50 years is unprecedented in a 350 to 1000 year context. More paleoclimatic records are needed to place the 20th century in a secure multi-century context.

- Paleoclimate simulations are consistent with the reconstructed NH temperatures over the last 1000 years, and the rise in surface temperatures observed since 1900 cannot be reproduced without including anthropogenic greenhouse gases in the model forcings.

- Small preindustrial variations in atmospheric carbon dioxide, methane, and nitrous oxide provide indirect evidence for a limited range of low-frequency climate variations over the last millennium prior to the industrialization. The amplitudes of the preindustrial, decadal-scale Northern Hemisphere temperature changes from the proxy-based reconstructions (<1°C) are broadly consistent with the ice core CO_2 record and the strength of the carbon cycle-climate feedback as found in the models used in the Chapter 10.

- Reconstructions of the behaviour of ENSO over the past millennium suggest greater variability in the frequency, amplitude, and climate teleconnections than is represented in the period of instrumental record.

- It is likely that the strength of the Asian summer monsoon, and hence precipitation amount, changed abruptly in the late Holocene. However, the mechanisms behind these abrupt shifts are not well understood, nor captured by current climate models.

- The paleoclimate records of northern and eastern Africa and of North America indicate that droughts lasting decades to centuries are a recurrent feature of climate in these regions under a wide range of climate forcing.

What does the paleoclimatic record reveal about biogeochemical and biogeophysical processes?

- Climate models and paleoclimate data confirm that the climate system reacts in a highly nonlinear manner to changes in the orbital forcing with positive feedbacks resulting in large changes in vegetation, snow and ice, atmospheric load of dust, and concentrations of greenhouse gases. It is likely that these feedbacks will amplify the future direct anthropogenic greenhouse gas forcing, thereby causing larger climatic changes than in the absence of these feedbacks.

- Paleoenvironmental data indicate that vegetation composition and structure are very likely sensitive to climate change, and can, in some cases, respond to climate change within decades, or even years.

- It is virtually certain that millennial-scale changes in atmospheric CO_2 associated with individual Antarctic warm events were less than 25 ppm during the last glacial period, despite strong changes in North Atlantic Deep Water formation and in the deposition of wind-borne iron into the Southern Ocean. This suggests, consistent with model results, a limited role of these processes in regulating future atmospheric CO_2 and climate.

- It is very likely that marine carbon cycle processes were primarily responsible for the glacial-interglacial CO_2 variations. The detailed explanation of these variations remains a difficult problem.

- Current models are capable of simulating climate, the vegetation structure and terrestrial carbon storage for the Last Glacial Maximum and the Holocene, periods characterized by markedly different forcing and climate. This strengthens the confidence in model formulations and in projections by these models and suggests that major unexpected feedbacks are very unlikely to occur over this century.

6.1 Introduction

This chapter assesses paleoclimatic data and knowledge of how the climate system changes across interannual to millennial time-scales, and how well these variations can be simulated with climate models. We highlight potential implications this knowledge has for the future, as well as for the credibility of projections into the future.

Paleoclimate science has made significant advances since the 1970's, when a primary focus was on the origin of the ice ages, the possibility of an imminent future ice age, and the first explorations of the so-called Little Ice Age and Medieval Warm Period. Even in the first IPCC assessment (1990), many climatic variations prior to the instrumental record were not that well known or understood. Fifteen years later, our understanding is much improved, quantitative and more integrated with respect to observations and modeling.

After a brief overview of paleoclimatic methods, including their strengths and weaknesses, we examine the paleoclimatic record in chronological order, from oldest to youngest. This approach was selected for a number of reasons, but primarily because the climate system varies and changes over all time scales, and it is instructive – e.g., for policy debates – to understand the contributions lower frequency patterns of climate change might make in influencing higher-frequency patterns of variability and change. Also, an examination of how the climate system has responded to large changes in climate forcing in the past is useful in assessing how the same climate system might respond to the large anticipated forcing changes in the future. We also devote the most chapter space to recent paleoclimatic history because uncertainties become smaller toward the present. Moreover, climate variation and change of the last 2000 years is of great relevance to policy making. Lastly, additional focused paleoclimatic perspectives are also included in other chapters of this volume: for example, Chapter 4, 9 and 10.

Cross-cutting our chronologically-based presentation are assessments of climate forcing and response, and of the ability of state-of-the-art climate models to simulate the responses. Perspectives from paleoclimatic observations, theory and modeling are integrated wherever possible to reduce uncertainty in our assessment. We consider the contemporary understanding of paleoclimates on both broad-scale (e.g., hemispheric) and regional scales. In several sections, we also assess the latest developments in the rapidly advancing area of abrupt climate change: i.e., *forced* or *unforced* climatic change that involves crossing a threshold to a new climate regime (e.g., new mean state or character of variability), often where the transition time to the new regime is short relative to duration of the regime (Rahmstorf, 2001; Alley et al., 2003; Overpeck and Trenberth, 2004).

6.2 Paleoclimatic Methods

6.2.1 Methods – Observations of Forcing and Response

The field of paleoclimatology has seen significant methodological advances since the TAR, and the purpose of this section is to emphasize these advances while giving an overview of the methods underlying the data used in this chapter. Many critical methodological details are presented in subsequent sections where needed. Thus, this methods section is designed to be more general, and to give readers of this chapter more insight and confidence in the findings of the chapter. Readers are referred to several useful books and special issues of journals for additional methodological detail (Bradley, 1999; Cronin, 1999; Fischer and Wefer, 1999; Ruddiman and Thomson, 2001; Alverson et al., 2003; Mackay et al., 2003; Kucera et al., 2005).

6.2.1.1 How do we know how climate forcing changed in the past?

Time series of astronomically driven insolation change are well known and can be calculated from celestial mechanics (see Box 6.1). The methods behind reconstructions of past solar and volcanic forcing continue to improve, although important uncertainties still exist (see Section 6.6).

6.2.1.2 How do we know past changes in global atmospheric composition?

Perhaps one of the most important aspects of modern paleoclimatology is that it is possible to derive time series of atmospheric trace gases and aerosols for the period ca. 650,000 years to present from air trapped in polar ice (see Sections 6.4 to 6.6 for more methodological citations). As is common in paleoclimatic studies of the Late Quaternary, the quality of forcing and response series are verified against recent (i.e., post 1950) measurements made by direct instrumental sampling. Section 6.3 cites several papers that reveal how atmospheric CO_2 concentrations can be inferred back millions of years, with much lower accuracy than the ice core estimates. As is common across all aspects of the field, paleoclimatologists seldom rely on one method or proxy, but rather several. This potentially provides a richer and more encompassing view of climatic change that would be available from a single proxy. In this way, results can be cross-checked and uncertainties better understood. In the case of pre-Quaternary CO_2, multiple geochemical and biological methods provide reasonable constraints on past CO_2 variations, but, as pointed out in Section 6.3, the quality of the estimates is somewhat limited.

6.2.1.3 How precisely can paleoclimatic records of forcing and response be dated?

Much has been researched and written on the dating methods associated with paleoclimatic records, and readers are referred to the background books cited in the first paragraph of this section for more detail. In general, time control gets weaker farther back in time. Tree-ring records are generally the best, and are accurate to the year, or season of a year (even back thousands of years). There are a host of other proxies that also have annual layers or bands – e.g., corals, varved sediments, some cave deposits, some ice cores – but the age models are not always exact to a specific year. Again, paleoclimatologists always strive to generate age information from multiple sources to reduce age uncertainty, and most paleoclimatic interpretations must take into account uncertainties in time control.

There continue to be significant advances in radiometric dating. Each radiometric system has ranges over which the system is useful, and paleoclimatic studies almost always publish analytical uncertainties. Because there can be additional uncertainties, methods have been developed for checking assumptions and cross-verifying with independent methods. For example, secular variations in the radiocarbon clock over the last 15,000 years are very well known, and fairly well understood over the last 35,000 years. These variations, and the quality of the radiocarbon clock, have both been well demonstrated via comparisons with age models derived from precise tree-ring and varved sediment records, as well as with age determinations derived from independent radiometric systems such as uranium-series; note, however, that for each specific proxy record, the quality of the radiocarbon chronology also depends on the density of dates, the material available for dating and knowledge about the radiocarbon age of the carbon that was incorporated into the dated material.

6.2.1.4 How good are the methods used to reconstruct past climate dynamics?

Most of the methods behind the paleoclimatic reconstructions assessed in this chapter are described in some detail in the aforementioned books, as well as in the citations of each chapter section. In some sections, important methodological background and controversies are discussed where such discussions help assess paleoclimatic uncertainties.

Paleoclimatic reconstruction methods have matured greatly in the past decades and range from direct measurements of past change, as in the case of ground temperature variations, gas content in ice core air bubbles, ocean sediment pore-water change, and glacier extent changes, to proxy measurements involving the change in chemical, physical and biological parameters that reflect – often in a quantitative and well-understood manner – past change in the environment where the proxy grew or existed. In addition to these methods paleoclimatologists also use documentary data, e.g., in the form of specific observations, logs, harvest data for reconstructions of past climates. While a number of uncertainties remain, it is now well accepted and verified that many biological organisms (e.g., trees, corals, plankton, insects and other organisms) alter their growth and/or population dynamics in response to changing climate, and that these climate-induced changes are well-recorded in past growth in living and dead (fossil) specimens or assemblages of organisms. Tree-rings, ocean and lake plankton and pollen are some of the best-known and best-developed proxy sources of past climate going back centuries and millennia. Networks of tree-ring width and tree-ring density chronologies are used to infer past temperature changes based on comprehensive calibration with temporally overlapping instrumental data. Past distributions of pollen and plankton from sediment cores can be used to derive quantitative estimates of past temperature, salinity or precipitation via statistical transfer functions which are calibrated against their modern distribution and associated climate parameters. The chemistry of several biological and physical entities reflects well understood thermodynamic processes that can be transformed into estimates of climate parameters such as temperature. Key examples are: Oxygen-isotope ratios in coral and foraminiferal carbonate to infer past temperature and salinity, Mg/Ca and Sr/Ca ratios in carbonate for temperature estimates, alkenone saturation indices from marine organic molecules to infer past sea surface temperature (SST), O and H-isotopes and combined N and Ar-isotope studies in ice cores to infer temperature and atmospheric transport. Lastly, many physical systems (e.g., sediments and aeolian deposits) change in predictable ways that can be used to infer past climate change. While these methods are heavily used, there is ongoing work on further development and refinement, and there are remaining research issues concerning the degree to which the methods have spatial and seasonal biases. Therefore, in many recent paleoclimatic studies, a combination of methods is applied since multi-proxy series provide more rigorous estimates than single proxy and this approach may identify possible seasonal biases in the estimates. No paleoclimatic method is foolproof, and knowledge of the underlying methods and processes is required when using paleoclimatic data.

Not surprisingly, the field of paleoclimatology depends heavily on replication and cross-verification between paleoclimate records from independent sources in order to build confidence in inferences about past climate variability and change. In this chapter, the most weight is placed on those inferences that have been made with particularly robust or replicated methodologies; the assessed quality of methods used is reflected in the confidence placed on the paleoclimatic inferences.

6.2.2 Methods – Paleoclimate Modeling

Climate models are used to simulate episodes of past climate (e.g., the Last Glacial Maximum, the last interglacial period, or abrupt climate events) to help understand the mechanisms of past climate changes. Models are the only way to test physical hypotheses quantitatively, such as the Milankovitch theory (Box 6.1). Models allow us to investigate the linkage of cause and effect in past climate change. Models also help to fill the gap between the local and global scale in paleoclimate, as paleoclimatic information is often sparse, patchy and seasonal. For example, long ice core records show a strong correlation between local temperature in Antarctica and the globally mixed gases CO_2 and methane, but the causal connections between these variables can only be explored with the help of models. Developing a quantitative understanding of mechanisms is the best way to learn from past climate for the future, since there are no direct analogues of the future in the past.

At the same time, paleoclimate reconstructions offer the possibility of testing climate models, particularly if the climate forcing can be appropriately specified, and the response is sufficiently well-constrained. For earlier climates (i.e., before the current “Holocene” interglacial), forcing and responses cover a much larger range, but data are more sparse and uncertain, while for recent millennia more records are available, but forcing and response are much smaller. Testing models with paleoclimatic data is important, as not all aspects of climate models can be tested against instrumental climate data. For example, good performance for present climate is not a conclusive test for a realistic sensitivity to CO_2 – to test this, simulation of a climate with very different CO_2 level can be used. Also, many empirical parameterizations describing sub-grid scale processes (e.g., cloud parameters, turbulent mixing) have been developed using present-day observations; hence climate states not used in model development provide an independent benchmark for testing models. Paleoclimate data are key to evaluating the ability of climate models to simulate realistic climate change.

In principle the same climate models that are used to simulate present-day climate, or scenarios for the future, are also used to simulate episodes of past climate. The difference is in the external forcing (e.g., solar radiation or greenhouse gas concentrations), and for the deep past (tens of millions of years ago), also in the configuration of oceans and continents. The full spectrum of models (see Chapter 8) is used (Claussen et al., 2002), ranging from simple conceptual models, through Earth system models of intermediate complexity (EMIC’s) and coupled general circulation models. Since long simulations (thousands of years) can be required for some paleoclimatic applications, and computer power is still a limiting factor, relatively "fast" coupled models are often used. Additional components that are not standard in models used for simulating present climate are also increasingly added for paleoclimate applications, e.g., continental ice sheet models or components that track the stable isotopes in the climate system (LeGrande et al., 2006). Vegetation, as well as terrestrial and marine ecosystem, modules are increasingly included, both to capture biophysical and biogeochemical feedbacks on climate, and to allow for validation of models against proxy ecological (e.g., pollen) data. The representation of biogeochemical tracers and processes is a particularly important new advance for paleoclimatic model simulations, as a rich body of information on past climate has emerged from proxy data from a variety of archives that are intrinsically linked to the cycling of carbon and other nutrients.

6.3 The Pre-Quaternary Climates

6.3.1 What is the Relationship Between CO_2 and Temperature in this Time Period?

Pre-Quaternary climates (prior to 3 Myr) were, by and large, warmer than today and associated with higher CO_2 levels (e.g., Figure 6.1). In that sense they have certain similarities with the anticipated future climate change (although the global biology and geography were increasingly different further back in time). In general, they verify that warmer climates are to be expected with increased greenhouse gas concentrations. As we look back in time beyond the reach of ice cores, i.e., prior to about one million years in the past, data on greenhouse gas concentrations in the atmosphere become much more uncertain. However, there are ingenious efforts to obtain quantitative reconstructions of the warm climates over the past 65 million years and in the following section we discuss two particularly relevant climate events of this period.

How accurately do we know the relationship between CO_2 and temperature? There are four primary proxies used for pre-Quaternary CO_2 levels (Royer et al., 2001; Royer, 2003). Two proxies apply the fact that biological entities in soils and seawater (Cerling, 1991; Freeman and Hayes, 1992; Yapp and Poths, 1992; Pagani et al., 2005) have carbon isotope ratios that are distinct from the atmosphere. The third proxy uses the ratio of boron isotopes (Pearson et al., 2001), while the fourth uses the empirical relationship between stomatal pores on tree leaves and atmospheric CO_2 content (McElwain and Chaloner, 1995; Royer, 2003). As shown in Figure 6.1 (bottom panel), while there is a wide range of reconstructed CO_2 values, magnitudes are generally higher than the interglacial, pre-industrial values seen in ice core data. Changes in CO_2 on these long time scales are thought to be driven by changes in tectonic processes (e.g., volcanic activity and weathering, e.g., (Ruddiman, 1997). Temperature reconstructions, such as that shown in Figure 6.1 (middle panel), are derived from oxygen isotopes, corrected for variations in the global ice volume. Indicators for the presence of continental ice on Earth show that the planet was mostly ice-free during geologic history, another indication of the general warmth. Major expansion of Antarctic glaciations starting around 35-40 Myr ago may have been a response, in part, to declining atmospheric CO_2 levels from their peak in the Cretaceous (~100 Myr) (DeConto and Pollard, 2003). The relationship between CO_2 and temperature can be traced further back in time as indicated in Figure 6.1 (top panel), which shows the warmth of the Mesozoic Periods (230-65 Myr) were associated with high levels of CO_2 and the major glaciations that occurred around 300 million years ago, coincided with relatively low CO_2 concentrations compared with surrounding epochs.

[INSERT FIGURE 6.1 HERE]

6.3.2 What Does the Record of the Mid-Pliocene Tell Us?

The Mid-Pliocene (ca. 3.3 to 3.0 Myr) is the most recent time in Earth's history when mean global temperatures were substantially warmer (estimated by GCMs to be 2°C to 3°C above pre-industrial (e.g. Chandler et al., 1994), providing an accessible example of a world that is similar in many respects to what models estimate will be the Earth of the late 21st century. The Pliocene is also recent enough that the continents and ocean basins had nearly reached their present geographic configuration. Taken together, the average of the warmest times during the middle Pliocene presents us with a view of the equilibrium state of a globally warmer world, in which CO_2 concentrations (estimated to be between 360–400 ppm) were likely higher than pre-industrial values (Raymo and Rau, 1992; Raymo et al., 1996) and geologic evidence and isotopes agree that sea level was at least 15–25 m above modern (Dowsett and Cronin, 1990; Shackleton et al., 1995), with correspondingly reduced ice sheets, and continental aridity was much lower (Guo et al., 2004).

Temperature reconstructions for this time period from both terrestrial and marine paleoclimate proxies (Thompson, 1991; Dowsett et al., 1996; Thompson and Fleming, 1996) show high latitudes were significantly warmer, but tropical SSTs and surface air temperatures were little different from modern. The result was a substantial decrease in the lower tropospheric latitudinal temperature gradient. For example, atmospheric GCM simulations driven by reconstructed SSTs from the Pliocene Research Interpretations and

Synoptic Mapping (PRISM) Group (Dowsett et al., 1996; Dowsett et al., 2005) produced winter surface air temperature warming of 10–20°C at high northern latitudes with 5–10°C increases over the northern North Atlantic (~60°N), whereas there was essentially no tropical surface air temperature change (or even slight cooling) (Chandler et al., 1994; Sloan et al., 1996; Haywood et al., 2000). In contrast, a coupled atmosphere-ocean experiment with 400 ppm CO_2 produced warming relative to pre-industrial times of 3–5°C in the northern North Atlantic, and 1–3°C in the tropics (Haywood et al., 2005).

The estimation of lack of tropical warming is a result of basing tropical SST reconstructions on marine microfaunal evidence. As in the case of the Last Glacial Maximum (see Section 6.4), we are uncertain whether tropical sensitivity is really as small as such reconstructions show. Haywood et al. (2005) found that alkenone estimates of tropical and subtropical temperatures do indicate warming in these regions, in better agreement with GCM reconstructions from increased CO_2 forcing. As in the study noted above, climate models cannot produce a response to increased CO_2 with large high latitude warming and yet minimal tropical temperature change unless strong increases in ocean heat transport also occur (Rind and Chandler, 1991).

The substantial high latitude response is shown by both marine and terrestrial paleo-data, and it may indicate that high latitudes are more sensitive to increased CO_2 than model simulations suggest for the 21st century. Alternatively, it may be the result of increased ocean heat transports due to either an enhanced thermohaline circulation (Raymo et al., 1989; Rind and Chandler, 1991), or increased flow of surface ocean currents due to greater wind stresses (Ravelo, 1997; Haywood et al., 2000), or associated with the reduced extent of land and sea ice (Jansen et al., 2000; Knies et al., 2002; Haywood et al., 2005). Currently available proxy data are equivocal concerning a possible thermohaline increase for either transient or equilibrium climate states during the Pliocene. Data are just beginning to emerge that describes the deep ocean state during the Pliocene (Cronin et al., 2005). An increase would, however, contrast with the North Atlantic deep-water production decreases that are found in several coupled model simulations for the 21st century. The transient response in those models tends to favor reduced deep-water formation and ocean transports as climate warms. Understanding the climate distribution and forcing for the Pliocene period may help improve our predictions of the likely response to increased CO_2 in the future, including the ultimate role of the ocean circulation in a globally warmer world.

6.3.3 What Does the Record of the Paleocene-Eocene Thermal Maximum Tell Us?

Approximately 55 million years ago, an abrupt warming (in this case occurring on the order of ten thousand years) by several degrees C is indicated by changes in ^{18}O isotope and Mg/Ca records (Kennett and Stott, 1991; Zachos et al., 2003; Tripati and Elderfield, 2004). The warmth lasted approximately 100,000 years. Evidence for shifts in global precipitation patterns is present in a variety of fossil records including vegetation (Wing et al., 2005). The climate anomaly, along with an accompanying carbon isotope excursion, occurred at the boundary between the Paleocene-Eocene epochs, and is therefore often referred to as the Paleocene-Eocene Thermal Maximum (PETM). The thermal maximum clearly stands out in high-resolution records of that time (Figure 6.2). At the same time, ^{13}C isotopes in marine and continental records show that a large mass of carbon with low ^{13}C concentration must have been released into the atmosphere and ocean. The mass of carbon was sufficiently large to lower the pH of the ocean and drive widespread dissolution of seafloor carbonates (Zachos et al., 2005). Possible sources for this carbon could have been methane from decomposition of clathrates on the sea floor, CO_2 from volcanic activity, or oxidation of organic rich sediments (Dickens et al., 1997; Kurtz et al., 2003; Svensen and al., 2004). The PETM, which altered ecosystems world-wide (Koch et al., 1992; Bowen et al., 2002; Bralower, 2002; Crouch et al., 2003; Thomas, 2003; Bowen et al., 2004; Harrington et al., 2004), is being intensively studied as it has some similarity with the ongoing rapid release of carbon into the atmosphere by humans. The estimated magnitude of carbon release for this time period is on the order of 1–2 x 10^{18}g of carbon (Dickens et al., 1997), a similar magnitude to that associated with greenhouse gas releases during the coming century. Moreover, the period of recovery through natural carbon sequestration processes, ~100,000 years, is similar to that forecast for the future. Although there is still too much uncertainty in the data to derive a quantitative estimate of climate sensitivity from the PETM, the event is an excellent example of massive carbon release and related extreme climatic warming.

[INSERT FIGURE 6.2 HERE]

6.4 Glacial-Interglacial Variability and Dynamics

6.4.1 Climate Forcings and Responses Over Glacial-Interglacial Cycles

Paleoclimatic records document a sequence of glacial-interglacial cycles covering the last 650,000 years in ice cores (Figure 6.3), and several million years in deep oceanic sediments (Lisiecki and Raymo, 2005) and loess (Ding et al., 2002). The last 450,000 years, which are the best documented, are characterized by 100 ka glacial-interglacial cycles of very large amplitude, as well as large climate changes at other orbital frequencies (Hays et al., 1976) (Box 6.1), and at millennial time scales (McManus et al., 2002; North Greenland Ice Core Project, 2004). Long glacial periods are interrupted by shorter interglacial warm periods lasting for 10 to 30 ka. There is clear evidence for interglacial periods prior to 450,000 years, but these were apparently colder than the typical interglacials of the latest Quaternary (EPICA community members, 2004). We are now living in the Holocene period, the latest of these interglacials.

[INSERT FIGURE 6.3 HERE]

The ice core record indicates that greenhouse gases co-varied with Antarctic temperature over glacial-interglacial cycles, suggesting a close link between natural atmospheric greenhouse gas variations and temperature. CO_2 variations over the last 420,000 years broadly followed Antarctic temperature, typically with a time lag of several centuries to a millennium (Mudelsee, 2001). The sequence of climatic forcings and responses during deglaciations (transitions from full glacial conditions to warm interglacials) are well documented. High resolution ice core records of temperature proxies and CO_2 during deglaciation indicates that Antarctic temperature starts to rise several hundred years before CO_2 (Monnin et al., 2001; Caillon et al., 2003). During the last deglaciation, and likely also the three previous ones, the onset of warming at both high southern and northern latitudes preceded by several thousand years the first signals of significant sea level increase resulting from the melting of the northern ice sheets linked with the rapid warming at high northern (Petit et al., 1999; Shackleton, 2000; Pépin et al., 2001). Current data are not accurate enough to identify whether warming started earlier in the Southern or Northern Hemisphere, but a major deglacial feature is the difference between North and South in terms of the magnitude and timing of strong reversals in the warming trend, which are out of phase between the hemispheres, and often much more pronounced in the Northern Hemisphere (Blunier and Brook, 2001).

Greenhouse gas (especially CO_2) feedbacks contributed largely to the global radiative perturbation corresponding to the transitions from glacial to interglacial modes (see Section 6.4.1.2). The relationship between Antarctic temperature and CO_2 did not change significantly during the past 650,000 years, indicating a rather stable coupling between climate and the carbon cycle during the late Pleistocene (Siegenthaler et al., 2005b). The rate of change in atmospheric CO_2 varied considerably over time. For example, different phases in the CO_2 increase from ~185 ppm at the Last Glacial Maximum to ~265 ppm in the early Holocene can be distinguished (Stenni et al., 2001) (Figure 6.4).

6.4.1.1 How do glacial-interglacial variations in the greenhouse gases carbon dioxide, methane and nitrous oxide compare with the Industrial Era greenhouse gas increase?

The present atmospheric concentrations of CO_2, CH_4, and N_2O are higher than ever measured in the ice core record, spanning the past 650,000 years (Figure 6.3 and 6.4). The concentrations of the three greenhouse gases were fluctuating within 4% for CO_2 and N_2O and within 7 % for CH_4 over the past millennium prior to the Industrial Era, and also varied within a restricted range over the late Quaternary. Within the 200 years, this natural range has been exceeded by at least 25% for CO_2, 120% for CH_4 and 9 % for N_2O. All three records show effects of the large and increasing growth in anthropogenic emissions during the Industrial Era.

[INSERT FIGURE 6.4 HERE]

Variations in atmospheric CO_2 dominate the radiative forcing by all three gases (Figure 6.4). The Industrial Era increase in CO_2, and in the radiative forcing (Chapter 2) by all three gases, is similar in magnitude to the increase over the transitions from glacial to interglacial periods, but occurred one to two orders of magnitude faster (Stocker and Monnin, 2003). There is no indication in the ice core record that an increase comparable in magnitude and rate to the Industrial Era increase has occurred in the past 650,000 years. The ice core records show that during the Industrial Era, average rate of increase in the radiative forcing from CO_2, CH_4 and N_2O is larger than at any time during the past 20,000 years (Figure 6.4). The smoothing of the atmospheric signal (Schwander et al., 1993; Spahni et al., 2003) is small at Law Dome, a high-accumulation site in Antarctica, and decadal-scale rates of changes can be computed from the Law Dome record spanning the past two millennia (Etheridge et al., 1996; MacFarling Meure, 2004; Ferretti et al., 2005). The decadal-scale averaged rate of change in atmospheric CO_2 is at least seven times faster at present than at any time during the past two millennia before the Industrial Era. The average rate of increase in atmospheric CH_4 peaked around 1980, when it was almost eight times higher than at any time during the past two millennia before the Industrial Era, and the rate for N_2O is at least three times higher than during the previous two millennia. Correspondingly, the present average rate in cumulative radiative forcing by all three greenhouse gases is at least six times faster at present than at any time during the period 0 to 1800 AD (Figure 6.4d).

Box 6.1: Orbital Forcing

It is well known from astronomical calculations (Berger, 1978) that periodic changes in parameters of the orbit of the Earth around the Sun modify the seasonal and latitudinal distribution of incoming solar radiation at the top of the atmosphere (hereafter called "insolation"). Past and future changes in insolation can be calculated over several millions of years with a high degree of confidence (Berger and Loutre, 1991).

The obliquity (tilt) of the Earth axis varies between 22.05 to 24.50° from –800 kyr to + 200 kyr with two neighbouring quasi-periodicities around 41 kyr. Changes in obliquity modulate seasonal contrasts as well as annual mean insolation changes with opposite effects in low versus high latitudes (and therefore no effect on global average of insolation). Local annual mean insolation changes remain below 6 W/m² (Box 6.1, Figure 1).

[INSERT BOX 6.1, FIGURE 1 HERE]

The eccentricity of the Earth's orbit around the Sun has longer quasi-periodicities at 400 and around 100 kyr, and varies between values of ~0.002 and 0.050 during the time period from –800 to +200 kyr. Changes in eccentricity alone have limited impacts on insolation due to changes in Sun-Earth distance. However, changes in eccentricity interact with seasonal effects induced by obliquity and climatic precession. Due to the precession of the equinoxes and the longitude of perihelion, periodic shifts in the position of solstices and equinoxes on the orbit occur and modulate the seasonal cycle of insolation with periodicities of ~19 and ~23 kyr. As a result, changes in the position and duration of the seasons on the orbit strongly modulate the latitudinal and seasonal distribution of insolation. Seasonal changes of insolation are much larger than annual mean changes and can reach 60 W/m² (Box 6.1, Figure 1). During periods of low eccentricity, such as ~400 kyr ago and during the next 100 kyr, seasonal insolation changes induced by precession are less strong than during periods of larger eccentricity (Box 6.1, Figure 1). High-frequency variations of orbital variations appear to be associated with very small orders of magnitude of insolation changes (Bertrand et al., 2002a). Due to the time constants of the orbital parameters of the Earth, orbital forcing alone cannot account for climate changes occurring on time scales shorter than a thousand years.

The Milankovitch theory proposed that ice ages were triggered by changes in 65°N summer insolation minima, enabling winter snowfall to persist all year trough and therefore accumulate to build northern hemisphere glacial ice sheets. Typically, the onset of the last ice age, ~116 kyr ago, corresponds to a 65°N mid-June insolation decrease of ~110 W/m² compared to today. Studies on the link between orbital parameters and past climate changes include spectral analysis of orbital periodicities identified in paleoclimatic records; precise dating of specific climatic transitions; modelling of the climate response to orbital forcings including climatic and biogeochemical feedbacks Current studies point out to other aspects of the orbital forcing than the 65°N summer insolation changes to account for paleoclimatic changes including monsoon responses. Sections 6.4 and 6.5 describe some aspects of the state-of-the-art understanding of the relationships between orbital forcing, climate feedbacks and past climate changes.

Box 6.2: What Caused the Low Atmospheric CO_2 Concentrations During Glacial Times?

Ice core records show that atmospheric CO_2 varied in the range of 180 to 300 ppm over the glacial-interglacial cycles of the last 650 thousand years (Figure 6.3) (Petit et al., 1999; Siegenthaler et al., 2005b). The quantitative and mechanistic explanation of these CO_2 variations remains one of the big unsolved questions in climate research. Processes in the atmosphere, ocean, marine sediments, on land, and the dynamics of sea ice and ice sheets must be considered. A number of hypotheses for the low glacial CO_2 concentrations have emerged over the past 20 years and a rich body of literature is available (Webb et al., 1997; Broecker and Henderson, 1998; Archer et al., 2000; Sigman and Boyle, 2000; Kohfeld et al., 2005). Many processes have been identified that could potentially regulate atmospheric CO_2 on glacial-interglacial time scales. However, the existing proxy data with which to test hypothesis are relatively scarce, uncertain, and their interpretation is partly conflicting.

Most explanations propose changes in oceanic processes as the cause for low glacial CO_2. The ocean is by far the largest of the relatively fast (<1000 yr) exchanging carbon reservoirs, and terrestrial changes cannot explain the low glacial values because terrestrial storage was also low at the Last Glacial Maximum (see Section 6.4.1). On glacial-interglacial time scales, atmospheric CO_2 is mainly governed by the interplay between ocean circulation, marine biological activity, ocean-sediment interactions, seawater carbonate chemistry, and air-sea exchange. Upon dissolution in seawater, CO_2 maintains an acid/base equilibrium with bicarbonate and carbonate ions that depends on the acid-titrating capacity of seawater, i.e., alkalinity. Globally, atmospheric CO_2 would be higher in an ocean without biological activity. CO_2 is more soluble in colder than in warmer waters; therefore changes in surface and deep ocean temperature have the potential to alter atmospheric CO_2. Most hypotheses focus on the Southern Ocean, where a large fraction of the cold deep-water masses of the world ocean are currently formed, and large amounts of biological nutrients (phosphate and nitrate) upwelled to the surface remain unused. A strong argument for the importance of Southern Hemisphere processes is the co-evolution of Antarctic temperature and atmospheric CO_2.

One family of hypotheses of low glacial CO_2 values invokes an increase or redistribution in the ocean alkalinity as a primary cause. Potential mechanisms are (i) the increase of $CaCO_3$ weathering on land, (ii) a decrease of coral reef growth in the shallow ocean, or (iii) a change in the export ratio of $CaCO_3$ and organic material to the deep ocean. These mechanisms require large changes in the deposition pattern of $CaCO_3$ to explain the full amplitude of the glacial-interglacial CO_2 difference through a mechanism called carbonate compensation (Archer et al., 2000). The available sediment data does not support a dominant role for carbonate compensation in explaining low glacial CO_2 levels. Furthermore, carbonate compensation may only explain slow CO_2 variation, as its typical time scale is multi-millennial.

Another family of hypotheses invokes changes in the sinking of marine plankton. Possible mechanisms include (iv) fertilization of phytoplankton growth in the Southern Ocean by increased deposition of iron-containing dust from the atmosphere after being lofted from colder, drier continental areas, and a subsequent redistribution of limiting nutrients, (v) an increase in the whole ocean nutrient content, e.g., through input of material exposed on shelves or nitrogen fixation, and (vi) an increase in the ratio between carbon and other nutrients assimilated in organic material, resulting in a higher carbon export per unit of limiting nutrient exported. As with the first family of hypotheses, this family of mechanisms also suffers from the inability to account for the full amplitude of the reconstructed CO_2 variations when constrained by the available information. For example, periods of enhanced biological production and increased dustiness (iron supply) are coincident with 20 to 50 ppm changes (Figure 6.7). Consistently, model simulations suggest a limited role for iron in regulating atmospheric CO_2 concentration (Bopp et al., 2002).

Physical processes also likely contributed to the observed CO_2 variations. Possible mechanisms include (vii) changes in ocean temperature (and salinity), (viii) suppression of air-sea gas exchange by sea ice, and (ix) increased stratification in the Southern Ocean. The combined changes in temperature and salinity increased the solubility of CO_2, causing a depletion in atmospheric CO_2 of perhaps 30 ppm. Simulations with general circulation ocean models do not fully support the gas exchange-sea ice hypothesis. One explanation (ix) conceived in the 1980s invokes more stratification, less upwelling of carbon and nutrient-rich waters to the surface of the Southern Ocean, and increased carbon storage at depth during glacial times. The stratification may have caused a depletion of nutrients and carbon at the surface, but proxy evidence for surface nutrient utilization is controversial. Qualitatively, the slow ventilation is consistent with very saline and very cold deep waters reconstructed for the last glacial maximum (Adkinson et al., 2002) and low glacial stable carbon isotope ratios ($^{13}C/^{12}C$) in the deep South Atlantic.

In conclusion, the explanation of glacial-interglacial CO_2 variations remains a difficult attribution problem. It appears likely that a range of mechanisms have acted in concert (Köhler et al., in press). The challenge is not only to explain the amplitude of glacial-interglacial CO_2 variations, but also the complex temporal evolution of atmospheric CO_2 in a way that is consistent with the underlying changes in climate.

6.4.1.2 What do the Last Glacial Maximum and the last deglaciation tell us?

Past glacial cold periods, sometimes referred to as "ice ages", provide a means for evaluating our understanding and modeling of the response of the climate system to large radiative perturbations. The most recent glacial period started ~116 kyr ago, in response to orbital forcing, with the growth of ice sheets and fall of sea level culminating in the Last Glacial Maximum (LGM), around 21 kyr ago. The Last Glacial Maximum, and the subsequent deglaciation has been widely studied because the radiative forcings, boundary conditions and climate response are relatively well known.

Climate models indicate that the changes from glacial to interglacial conditions during the last deglaciation, which occurred between 20 and 10 ka ago, can be consistently explained by the orbital forcing working in concert with observed changes in greenhouse trace gases, northern ice sheet albedo and to a lesser extent, dust and vegetation albedo. Feedbacks in the atmosphere and on land amplified the response of the climate system to the orbital forcing (Box 6.1). Concentrations of well-mixed greenhouse gases at LGM were reduced relative to preindustrial values, amounting to a global radiative perturbation of –2.8 W m^{-2}, approximately equal to, but opposite from, the radiative forcing of these gases for year 2000 relative to 1750 (see Chapter 2). Land ice covered large parts of North America and Europe at LGM, lowering sea level and exposing new land. The radiative perturbation of the ice sheets and lowered sea level, specified as a boundary condition for LGM simulations, was –3.2 W m^{-2}, but with a large uncertainty associated with the coverage and height of LGM continental ice (Mangerud et al., 2002; Peltier, 2004; Toracinta et al., 2004) and the parameterization of ice albedo in climate models (Taylor et al., 2000). Vegetation was altered, with tundra expanded over the northern continents and tropical rain forest reduced (Prentice et al., 2000), and atmospheric aerosols (dust primarily), itself a consequence of reduced vegetation cover (Mahowald et al., 1999), were increased (Kohfeld and Harrison, 2001). These land surface feedbacks are treated as specified conditions in many LGM simulations and each contribute about –1 W m^{-2} of radiative perturbation (Claquin et al., 2003; Crucifix and Hewitt, 2005). Changes in biogeochemical cycles thus played an important role and contributed, through changes in greenhouse gas concentration, dust loading and vegetation cover, more than half of the know radiative forcing during the LGM. Overall, the radiative perturbation for the changed greenhouse gas concentrations and land surface is approximately –6 to –11 W m^{-2} for LGM (Figure 6.5).

[INSERT FIGURE 6.5 HERE]

Our understanding of the magnitude of tropical cooling over land at LGM has improved since the TAR with more records, as well as better dating and interpretation of the climate signal associated with snowline elevation and vegetation change. Reconstructions of terrestrial climate show strong spatial differentiation, regionally and with elevation. Pollen records with their extensive spatial coverage indicate that tropical lowlands were on average 2–3°C cooler than present, with strong cooling (5–6°C) in Central and northern South America and weak cooling (<2°C) in the western Pacific Rim (Farrera et al., 1999). Tropical highland cooling estimates derived from snowline and pollen-based inferences show similar spatial variations of cooling although involving substantial uncertainties from dating and mapping, multiple climatic causes of treeline and snowline changes during glacial periods (Porter, 2001; Kageyama et al., 2005), and temporal asynchroneity between different regions of the tropics (Smith et al., 2005). Still, these new studies give a much richer regional picture of cooling of tropical land, and stress the need to use more than a few widely-scattered proxy records as a measure of low-latitude climate sensitivity (Harrison, 2005).

The CLIMAP reconstruction in the early 1980's indicated ~3°C cooling in the tropical Atlantic, and little or no cooling in the tropical Pacific. More pronounced tropical cooling for the LGM tropical oceans has been proposed since, including 4–5°C based on coral skeleton records from off Barbados (Guilderson et al., 1994) and up to 6°C in the cold tongue off western South America based on foraminiferal assemblages (Mix et al., 1999). New data syntheses from multiple proxy types using carefully defined chronostratigraphies and new calibration datasets are now available from the GLAMAP and MARGO projects, although with caveats including selective species dissolution, dating precision, non-analogue situations, and environmental preferences of the organisms (Sarnthein et al., 2003b; Kucera et al., 2005); and references therein). These recent reconstructions confirmed moderate cooling, generally 0–3.5°C, of tropical SST at LGM, although with significant regional variation and greater cooling in eastern boundary currents and equatorial upwelling regions. Estimates of cooling show notable differences among the different proxies. Notable is that faunal-based proxies argued for an intensification of the SST gradient across the equatorial Pacific, with relevance to ENSO, in contrast to Mg/Ca-based SST estimates (Rosenthal and Broccoli, 2004).

These ocean proxy syntheses projects also indicated colder glacial winter North Atlantic with more extensive sea ice than present, whereas summer sea ice only covered the glacial Arctic Ocean and Fram Strait with the northern North Atlantic and Nordic Seas largely ice-free and more meridional ocean surface circulation in the eastern parts of the Nordic Seas (Sarnthein et al., 2003a; deVernal et al., 2005; Meland et al., 2005). Sea ice around Antarctica at LGM also displayed a large expansion of winter sea ice and substantial seasonal variation (Gersonde et al., 2005). Over middle and high latitude northern continents, strong reduction in temperatures produced southward displacement and major reduction in forest area (Bigelow and al., 2003), expansion of permafrost limits over NW Europe (Renssen and Vandenberghe, 2003), fragmentation of temperate forests (Prentice et al., 2000; Williams et al., 2000), and predominance of steppe-tundra in Western Europe (Peyron et al., 2005). Polar ice core temperature reconstructions indicated strong cooling at high latitudes, ~9°C in Antarctica (Stenni et al., 2001) and ~21°C in Greenland (Dahl-Jensen et al., 1998).

The strength and depth extent of the LGM Atlantic overturning circulation have been examined through the application of a variety of new marine proxy indicators (Rutberg et al., 2000; Duplessy et al., 2002; Marchitto et al., 2002; McManus et al., 2004). These tracers indicate that the boundary between North Atlantic Deep Water (NADW) and Antarctic Bottom Water (AABW) was much shallower during LGM, with a reinforced pycnocline between intermediate and particularly cold and salty deep water (Adkins et al. 2002).

In summary, significant progress has been made in our understanding of the regional changes at LGM with the development of new proxies, many new records, improved understanding of the relationship of the various proxies to climate variables, and syntheses of proxy records into reconstructions with stricter dating and common calibrations.

6.4.1.3 How realistic are results from climate model simulations of the Last Glacial Maximum?

Model intercomparisons from the first phase of the Paleoclimate Modeling Intercomparison Project (PMIP-1), using atmospheric models (either with prescribed SST or with simple slab ocean models), were featured in the IPCC TAR. We now have five simulations of LGM from the second phase (PMIP-2) using AOGCMs, though only a few regional comparisons have been completed in time for the AR4. The radiative perturbation for the PMIP-2 LGM simulations available for this assessment, which do not yet include the effects of vegetation or aerosol changes, is –4 to –7 W m^{-2}. These simulations allow an assessment of a subset of the models presented in Chapters 8 and 10 to very different conditions than present-day.

The PMIP-2 multi-model LGM SST change shows modest cooling (1–2°C) in the tropics, and greatest cooling at mid to high latitudes in association with increases in sea ice and shifts in the Kuroshio and Gulf Stream currents (Figure 6.5). The PMIP-2 modeled strengthening of the SST meridional gradient in the LGM North Atlantic and cooling and expanded sea ice agrees with proxy indicators (Kageyama et al., 2005). Polar amplification of global cooling, as recorded in ice cores, is also realistically simulated for Antarctica, but the strong LGM cooling over Greenland is underestimated (Masson-Delmotte et al., in press).

The PMIP-2 models give a range of tropical ocean cooling between 15°S–15°N of 1.7–2.3°C. Models have indicated that this tropical cooling can be explained by the reduced glacial greenhouse gas concentrations, both directly affecting the tropical radiative forcing (Shin et al., 2003; Otto-Bliesner et al., in press-b) and indirectly, through LGM cooling in the Southern Ocean by the positive sea-ice-albedo feedback contributing to enhanced ocean ventilation of the tropical thermocline and the intermediate waters (Liu et al., 2002). Regional variations of simulated tropical cooling are much smaller than indicated by MARGO data, partly related to models at current resolutions being unable to simulate the intensity of coastal upwelling and eastern boundary currents. Simulated cooling in the Indian Ocean, a region influenced by radiative forcing and with important teleconnections to Africa and the North Atlantic at present-day, compares favourably to the MARGO results (Barrows and Juggins, 2005).

Considering changes in vegetation appears to improve the realism of simulations of the Last Glacial Maximum (LGM), and also points to important climate-vegetation feedbacks. The biome distribution simulated with dynamic global vegetation models reproduce the broad features observed in paleodata (Crucifix and Hewitt, 2005). For example, extension of the tundra in Asia during the LGM contributes to the local surface cooling, while the tropics warm where tropical forest is replaced by savannah (Wyputta and McAvaney, 2001). Feedbacks between climate and vegetation occur locally, with a decrease in the tree fraction in central Africa reducing precipitation, and remotely with cooling in Siberia (tundra replacing trees) and Tibet (bare soil replacing grasslands) altering (diminishing) the Asian summer monsoon. The physiological effect of CO_2 concentration on vegetation needs to be included to properly represent changes in global forest (Harrison and Prentice, 2003), as well as to widen the climatic range where grasses and shrubs dominate.

In summary, the PMIP-2 LGM simulations confirm that current AOGCMs are able to simulate the broad-scale spatial patterns of regional climate change recorded by paleodata to the radiative forcing and land surface changes of the LGM, thus adequately representing the feedbacks that determine the climate sensitivity of this past climate state. PMIP-2 simulations of the glacial-interglacial changes in greenhouse gas forcing and ice sheet conditions give a radiative perturbation in reference to preindustrial of –4.1 to –7.2 W m^{-2} and mean global temperature change of –3.5 to –5.2°C, similar to the range reported in the TAR for PMIP-1 (IPCC, 2001). The climate sensitivity inferred from the PMIP-2 LGM simulations is 2.3 to 3.7°C for CO_2 doubling (see Chapter 9, Section 9.6.2).

6.4.1.4 How realistic are simulations of terrestrial carbon storage at the Last Glacial Maximum?

There is evidence that terrestrial carbon storage was reduced during the LGM compared to today. Mass balance calculations based on ^{13}C measurements on shells of benthic foraminifera yield a reduction in the terrestrial biosphere carbon inventory (soil and living vegetation) of about 300 to 700 GtC (Shackleton, 1977; Bird et al., 1994) compared to the preindustrial inventory of about 3000 GtC. Estimates of terrestrial carbon storage based on ecosystem reconstructions suggest a larger difference (e.g., Crowley, 1995), however, these are very approximate due to large gaps in the data considered, and assumptions about the average carbon density of different forests. Simulations with carbon cycle models yield a reduction in global carbon stocks of 600 to 1000 GtC at the LGM compared to pre-industrial time (Francois et al., 1998; Beerling, 1999; Francois et al., 1999; Liu et al., 2002; Kaplan et al., 2003; Kaplan et al., 2002; Joos et al., 2004). The majority of this simulated difference is due to reduced simulated growth resulting from lower atmospheric CO_2. A major regulating role for CO_2 is consistent with the model-data analysis of (Bond et al., 2003) who suggest that low atmospheric CO_2 could have been a significant factor in the reduction of trees during glacial times, because of their slower regrowth after disturbances such as fire. In summary, results of terrestrial models, also used to project future CO_2 concentrations, are broadly compatible with the range of reconstructed differences in glacial-interglacial carbon storage on land.

6.4.1.5 How long did the previous interglacials last?

The four interglacials of the last 450 kyr preceding the Holocene (marine isotope stages 5, 7, 9 and 11) were all different in multiple aspects, including duration (Figure 6.3). The shortest (Stage 7) lasted a few thousands years, and the longest (Stage 11; ~420 to 395 kyr ago) lasted almost 30 kyr. Evidence for an unusually long Stage 11 has been recently reinforced by new ice core and marine sediment data. The EPICA Dome C Antarctic ice core record suggests that Antarctic temperature remained approximately as warm as the Holocene for 28 kyr (EPICA community members, 2004). A new stack of 57 globally-distributed benthic $\delta^{18}O$ records presents age estimates at Stage 11 nearly identical to those provided by the EPICA results (Lisiecki and Raymo, 2005).

It has been suggested that Stage 11 was an extraordinary long interglacial period because of its low eccentricity dampening the effect of climatic precession on insolation (Box 6.1) (Berger and Loutre, 2003). But the weak orbital forcing allows other candidate forcings, such as CO_2, to play an important climatic role. The EPICA Dome C and the recently revisited Vostok records offers a CO_2 record covering the complete Stage 11 warm period, and this record shows CO_2 concentrations similar to pre-industrial Holocene values over all of Stage 11 (Raynaud et al., 2005). Thus, both the orbital forcing and the CO_2 feedback were providing favourable conditions for an unusually long interglacial. Moreover, the length of Stage 11 has been simulated by conceptual models of the Quaternary climate, based on threshold mechanisms (Paillard, 1998). For Stage 11, these conceptual models show that the deglaciation is triggered by the insolation maximum at ~427 kyr, but that the next insolation minimum is not sufficiently low to start another glaciation. The interglacial thus lasts an additional precessional cycle, yielding a total duration of 28 kyr.

The long duration of Stage 11 results from the interplay between orbital forcing and the effects of elevated CO_2 (Loutre, 2003). In terms of climate forcings and responses, Stage 11 appears quite similar to the elapsed part of the Holocene, as well as the next tens of thousands of years, in terms of orbital conditions. Because of this, attempts have been made to estimate the length of the Holocene interglacial if it were free of anthropogenic perturbation. Different results are obtained depending on how the proxy record is aligned with the climatic precession and eccentricity (Ruddiman, 2005) or with their transitions and obliquity (Augustin et al., 2004).

6.4.1.6 How much did the Earth warm during the previous interglacial?

Globally, there was less glacial ice on Earth during the Last Interglacial (LIG, ~129–116 kyr ago) than now. This suggests significant meltback of the Greenland and possibly Antarctica ice sheets (see Section 6.4.3). The climate of the LIG has been inferred to be warmer than present (Kukla and al., 2002), although the evidence is regional and not neccessarily synchronous globally. For the first half of this interglacial (~129–123 kyr ago), orbital forcing (Box 6.1) produced a Northern Hemisphere summer insolation maximum. Proxy data indicated warmer-than-present coastal waters in the Pacific, Atlantic, and Indian Oceans and in the Mediterranean Sea, greatly reduced sea ice in the coastal waters around Alaska, and extension of boreal forest into areas now occupied by tundra in interior Alaska and Siberia (Brigham-Grette and Hopkins, 1995; Lozhkin and Anderson, 1995; Muhs et al., 2001). Ice core data indicate a large response over Greenland and Antarctica with temperatures 4–5°C warmer than present at ~129–125 kyr ago (North Greenland Ice Core Project, 2004). Paleofauna evidence from New Zealand also indicates LIG warmth although during the late LIG consistent with the latitudinal dependence of orbital forcing (Marra, 2003).

When forced with orbital forcing of ~129–125 kyr ago (Box 6.1), with more than 10% more summer insolation in the NH than today, AOGCMs produce a summer Arctic warming of up to 5°C, with greatest warming over Eurasia, and the oceans in the Baffin Island/northern Greenland region associated with sea ice retreat (Figure 6.6) (Montoya et al., 2000; Kaspar et al., 2005; Otto-Bliesner et al., in press-b; Otto-Bliesner et al., in press-a). Simulations match proxy reconstructions of the maximum summer warmth (CAPE Last Interglacial Project Members, 2005; Kaspar and Cubasch (in press)) although may still underestimate warmth because vegetation feedbacks are not included in current simulations. Simulated global temperature change is less than 1°C.

[INSERT FIGURE 6.6 HERE]

6.4.1.7 What do we know about the mechanisms of transitions into ice ages?

Successful simulation of glacial inception has been a key target for models simulating climate change. The Milankovitch theory proposed that ice ages were triggered by changes in 65°N summer insolation minima, enabling winter snowfall to persist all year and accumulate to build Northern Hemisphere glacial ice sheets. (Box 6.1). Continental ice sheet growth and associated sea level lowering took place at about 120 ka BP (Waelbroeck et al., 2002) when the summer incoming solar radiation in NH at high latitudes reached minimum values. The inception took place while the continental ice volume was minimal and stable, and low and mid latitudes of the North Atlantic continuously warm (Cortijo et al., 1999; Goni et al., 1999; McManus et al., 2002; Risebrobakken et al., 2005). When forced with orbital insolation changes only, past model studies have failed to find the proper magnitude of response to allow for perennial snow cover. Recent modeling results including additional factors have been more promising. These include vegetation feedbacks (Crucifix and Loutre, 2002; Meissner et al., 2003), increased sea ice (Jackson and Broccoli, 2003), a coupled dynamical ice sheet model (Pollard and Thompson, 1997), increased northward atmospheric moisture transport from warm low-to-mid latitude oceans as suggested by paleodata (Khodri et al., 2003; Khodri et al., 2005), or increased Atlantic MOC allowing for increased snowfall (Wang and Mysak, 2002; Otterå et al., 2004). EMICs that include models for continental ice simulate the rapid growth of the ice sheets after inception, with increased Atlantic MOC allowing for increased snowfall, and increasing ice sheet altitude and extent important, though the modeled ice volume-equivalent drop in sea level found in records is not well reproduced (Wang and Mysak, 2002; Otterå et al., 2004) (Kageyama et al., 2004; Calov et al., 2005).

6.4.1.8 When will the current interglacial end?

There is no evidence of mechanisms which could mitigate the current global warming by a natural cooling trend. Only a strong reduction in summer insolation at high northern latitudes, along with associated feedbacks, can end the current interglacial. Given that current low orbital eccentricity will persist over the next tens of thousand years, the effects of precession are minimized, and extreme cold-northern-summer orbital configurations like that of the last glacial initiation at 116 kyr ago will not take place (Box 6.1). Under a natural CO_2 regime (i.e., with the global temperature-CO_2 correlation continuing as in the Vostok and EPICA Dome C ice-cores), the next glacial period would not be expected to start within the next 30 kyr (Loutre and Berger, 2000; Berger and Loutre, 2002; Augustin et al., 2004). Sustained high atmospheric greenhouse concentrations, comparable to a mid-range CO_2 stabilization scenario, may lead to a complete melting of the Greenland ice cap (Church et al., 2001) and further delay the onset of the next glacial period (Loutre and Berger, 2000; Archer and Ganopolski, 2005).

6.4.2 Abrupt Climatic Changes in the Glacial-Interglacial Record

6.4.2.1 What is the evidence for past abrupt climate changes?

Abrupt climate changes have been variously defined either simply as large changes within less than 30 years (Clark et al., 2002), or in a physical sense, as a threshold transition or a response that is fast compared to forcing (Rahmstorf, 2001; Alley et al., 2003), or duration, of the subsequent climatic regime. (Overpeck and Trenberth, 2004) note that all abrupt change need not be externally forced. Numerous terrestrial, ice, and oceanic climatic records show that large, widespread, abrupt climate changes have occurred repeatedly throughout the past glacial interval (see review by Rahmstorf, 2002). High-latitude records show that ice-age abrupt temperature events were larger and more widespread than those of the Holocene. The most dramatic of these abrupt climate changes are the Dansgaard-Oeschger (DO) events, characterised by a warming in Greenland by 8 to 16ºC within a few decades (see Severinghaus and Brook, 1999; Masson-Delmotte et al., 2005b for a review) followed by much slower cooling over centuries. Another type of abrupt change is the Heinrich event; characteristic of these is a large discharge of icebergs into the northern Atlantic leaving diagnostic drop-stones in the ocean sediments (Hemming, 2004). In the North Atlantic, Heinrich events are accompanied by a strong lowering of sea surface salinity (Bond et al., 1993), as well as a sea surface cooling on a century time-scale; the cold periods lasted hundreds to thousands of years, and the warming that ended them took place within decades (Figure 6.7; (Cortijo et al., 1997; Voelker, 2002). At the end of the last glacial, as the climate warmed and ice sheets melted, climate went through a number of abrupt cold phases, notably the Younger Dryas and the 8.2 kyr event.

[INSERT FIGURE 6.7 HERE]

The repercussions of these abrupt climate changes were global, although out-of-phase responses in the two hemispheres (Blunier et al., 1998). Landais et al. (2006) suggest that they were not primarily changes in global mean temperature. The highest amplitude of the changes, in terms of temperature, appears centred around the North Atlantic. Strong changes are found in the global methane concentration (on the order of 100–150 ppbv), which may point to changes in the extent or productivity of tropical wetlands (see Chappellaz et al., 1993; Brook et al., 2000 for a review; Masson-Delmotte et al., 2005b), and in the Asian monsoon (Wang et al., 2001). The Northern Hemisphere cold phases were linked with a reduced northward flow of warm waters in the Nordic Seas (fig. 6.7), southward shift of the inter-tropical convergence zone (ITCZ) and thus the location of the tropical rainfall belts (Peterson et al., 2000; Lea et al., 2003). Cold, dry, and windy conditions with low methane and high dust aerosol concentrations generally occurred together in the Northern Hemisphere cold events. The accompanying changes in atmospheric CO_2 content were relatively small (up to 20 ppm; Figure 6.7) and parallel to the Antarctic counterparts of Greenland DO events. The record in N_2O is less complete and shows an increase of ~50 ppbv and a decrease of ~30 ppbv during warm and cold periods respectively (Flückiger et al., 2004).

A southward shift of the boreal treeline and other rapid vegetation responses were associated with past cold events (Peteet, 1995; Shuman et al., 2002; Williams et al., 2002). Decadal-scale changes in vegetation have been recorded in annually-laminated sequences at the beginning and the end of the Younger Dryas and the 8.2 ka event (Birks and Ammann, 2000; Tinner and Lotter, 2001; Veski et al., 2004). Marine pollen records with a typical sampling resolution of 200 years provide unequivocal evidence of the immediate response of vegetation in Southern Europe to the climate fluctuations during glacial times (Sànchez Goñi et al., 2002; Tzedakis, 2005). The same holds true for the vegetation response in Northern South America during the last deglaciation (Hughen et al., 2004).

6.4.2.2 What do we know about the mechanism of these abrupt changes?

There is solid evidence now from sediment data for a link between these glacial-age abrupt changes in surface climate and ocean circulation changes (Clark et al., 2002). Proxy data show that the South Atlantic cooled when the north warmed, and vice versa (Voelker, 2002), a (lagged) see-saw of northern and southern hemisphere temperatures which indicates an ocean heat transport change (Broecker, 1998; Stocker, 1998). During DO-event warming, salinity in the Irminger Sea increased strongly (Elliot et al., 1998; Kreveld et al., 2000), and nortward flow of temeparate waters increased in the Nordic Seas (Dokken and Jansen, 1999), indicative of saline Atlantic waters advancing northward. Abrupt changes in deep water properties of the Atlantic have been documented from both proxy data reconstructing the ventilation of the deep water masses (e.g., ^{13}C, ^{231}Pa/^{230}Th) and kinematic proxies that reconstruct changes in the overturning rate and flow speed of the deep waters (Vidal et al., 1998; Dokken and Jansen, 1999; McManus et al., 2004; Gherardi et al., 2005). Despite this evidence many features of the abrupt changes are still not well constrained due to a lack of precise temporal control of the sequencing and phasing of events between the surface, the deep ocean and ice sheets.

Heinrich events are thought to have been caused by ice-sheet instability (Macayeal, 1993). Iceberg discharge would have provided a large freshwater forcing to the Atlantic, which can be estimated from changes in the oxygen isotope ^{18}O. These yield a volume of freshwater addition typically corresponding to a few (up to 15) meters of global sea-level rise occurring over several centuries (100–2,000 years), i.e., a flux of the order of 0.1 Sv (Hemming, 2004). For Heinrich event 4, Roche et al. (2004) have been able to constrain the freshwater amount to 2 (±1) meters of sea level equivalent provided by the Laurentide ice sheet, and the duration of the event to 250 (±150) years.

Freshwater influx is the likely cause for the cold events at the end of the last ice age (i.e., the Younger Dryas and the 8.2 kyr event). Rather than sliding ice, it is the inflow of meltwater from melting ice due to the climatic warming at this time which could have interfered with the meridional overturning circulation and heat transport in the Atlantic – a discharge into the Arctic Ocean of the order 0.1 Sv may have triggered the Younger Dryas (Tarasov and Peltier, 2005), while the 8.2 kyr event was probably linked one or more inflows ranging up to 7×10^{13} m^3 (i.e., up to 19 cm of sea level) within a few years (Clarke et al., 2004). This is an important difference relative to the DO events, for which no large forcing of the ocean is known; model simulations suggest that small forcing may be sufficient if the ocean circulation was close to a threshold (Ganopolski and Rahmstorf, 2001). The exact cause and nature of these ocean circulation changes, however, is not universally agreed. Some authors have argued that some of the abrupt climate shifts discussed could have been triggered from the tropics (e.g. Clement and Cane, 1999), but a more specific and quantitative explanation for D/O events building on this idea is yet to emerge.

CO_2 changes during the glacial Antarctic warm events, linked to changes in North Atlantic Deep Water (Knutti et al., 2004), were small (less than 20 ppm, Figure 6.7). Consistently, a relatively small positive feedback between atmospheric CO_2 and changes in the rate of North Atlantic Deep Water formation are found in paleo and global warming simulations (Joos et al., 1999; Marchal et al., 1999). Thus, paleodata and available model simulations agree that possible future changes in the North Atlantic Deep Water formation rate would have only modest effects on atmospheric CO_2. This finding does not, however, preclude the possibility that circulation changes in other ocean regions, in particular in the Southern Ocean, could have a larger impact on atmospheric CO_2 (Greenblatt and Sarmiento, 2004).

6.4.2.3 Can climate models simulate these abrupt changes?

Modeling the ice sheet instabilities that are the likely cause of Heinrich events is a difficult problem where the physics is not sufficiently understood, although recent results show some promise (Calov et al., 2002). Many model studies have been performed in which an influx of freshwater from an ice sheet instability (Heinrich event) or a meltwater release (8.2 kyr event see Section 6.5.2) has been assumed and prescribed, and its effects on ocean circulation and climate have been simulated. These experiments suggest that freshwater input of the order of magnitude deduced from paleoclimatic data could indeed have caused NADW formation to shut down, and that this is a physically viable explanation for many of the climatic repercussions found in the data: e.g., the high-latitude northern cooling, the shift in the ITCZ and the hemispheric see-saw (Vellinga and Wood, 2002; Dahl et al., 2005; Zhang and Delworth, 2005). The phase relation between Greenland and Antarctic temperature has been explained by a reduction in the North Atlantic Deep Water formation rate and oceanic heat transport into the North Atlantic region, producing cooling in the North Atlantic and a lagged warming in the southern hemisphere (Ganopolski and Rahmstorf, 2001; Stocker and Johnsen, 2003). In freshwater simulations where the North Atlantic meridional overturning circulation is forced to collapse, the consequences also include an increase in nutrient-rich water in the deep Atlantic Ocean, higher $^{231}Pa/^{230}Th$ ratios in North Atlantic sediments (Marchal et al., 2000), a retreat of the northern treeline (Scholze et al., 2003; Higgins, 2004; Köhler et al., in press), a small (10 ppm) temporary increase in atmospheric CO_2 in response to a reorganization of the marine carbon cycle (Marchal et al., 1999), and CO_2 changes of a few ppm due to carbon stock changes in the land biosphere (Köhler et al., in press). A 10 ppb reduction in atmospheric N_2O is found in one ocean-atmosphere model (Goldstein et al., 2003), suggesting that a large part of the observed N_2O variation is of terrestrial origin. In summary, model simulations broadly reproduce the observed variations during abrupt events of this type.

DO events appear to be associated with latitudinal shifts in oceanic convection between the Nordic Seas and the open mid-latitude Atlantic (Alley and Clark, 1999). Models suggest that the temperature evolution in Greenland, the see-saw response in the South Atlantic, the observed Irminger Sea salinity changes and other observed features of the events may be explained by such a mechanism (Ganopolski and Rahmstorf, 2001), although it remains unclear what the trigger of these ocean circulation changes was. Alley et al. (2001) show evidence for a stochastic resonance process at work in the timing of these events, which means that a regular cycle together with random "noise" could have triggered them. This can be reproduced in models (e.g., the above), as long as a threshold mechanism is involved in causing the events.

Some authors have argued that climate models tend to underestimate the size and extent of past abrupt climate changes (Alley et al., 2003), and hence may underestimate the risk of future ones. However, such a general conclusion is probably too simple, and a case-by-case evaluation is required to understand which effects may be misinterpreted in the paleoclimatic record and which mechanisms may be underestimated in current models. This issue is important for an assessment of risks for the future: the expected rapid warming in the coming centuries could approach the amount of warming at the end of the last glacial, and would occur at a much faster rate. Hence, meltwater input from ice sheets could again become an important factor influencing the ocean circulation, as for the Younger Dryas and 8.2 kyr events. A melting of the Greenland Ice Sheet (equivalent to 7 m of global sea level) over 1,000 years would contribute an average freshwater flux of 0.1 Sv; this is a comparable magnitude to the estimated freshwater fluxes associated with past abrupt climate events. Most climate models used for future scenarios have thus far not included meltwater runoff from melting ice sheets. Inter-comparison experiments subjecting different models to freshwater influx have revealed that while responses are qualitatively similar, the amount of freshwater needed for a shutdown of the Atlantic circulation can differ greatly between models; the reasons for this model-dependency have not yet been understood (Rahmstorf et al., 2005; Stouffer et al., in press). At present knowledge, future abrupt climate changes due to ocean circulation changes cannot be ruled out.

6.4.3 Sea Level Variations Over the Last Glacial-Interglacial Cycle

6.4.3.1 What is the influence of past ice volume change on modern sea level change

Paleo-records of sea level history provide a crucial basis on which to understand the background variations upon which the sea level rise related to modern processes is superimposed. Even if no anthropogenic effect were currently operating in the climate system, measurable and significant changes of relative sea level (RSL) would still be occurring, in response to the planet's memory of the last deglaciation. Indeed, glacial isostatic adjustment restores gravitational equilibrium by movements of the Earth's crust and water in the ocean basins. Models of isostatic adjustment make it possible to isolate such long term effects, estimated to be –0.28 mm yr^{-1} (Peltier, 1996) to –0.36 mm yr^{-1} (Peltier, 2004), and to rule out a significant contribution of Holocene melting of Antarctic ice to the present-day sea level rise (Peltier and Solheim, 2002). These results are based upon the recently released ICE-5G(VM2) model (Peltier, 2004), and imply that the impact of modern climate change on sea level measurements by the Topex/Poseidon system is larger by this same amount that would be expected from uncorrected T/P measurements.

By employing the same theory to predict the impact upon Earth's rotational state due to both the Late Pleistocene glacial cycle and the influence of present day melting of the great polar ice sheets on Greenland and Antarctica, it has also proven possible to estimate the extent to which these ice sheets may have been losing mass over the past century. In Peltier (1998), such analysis led to an upper bound estimate of 0.5 mm per year for the sea level equivalent rate of mass loss from the polar ice sheets. This suggests the plausibility of the notion that polar ice sheet melting may provide the required closure of the global sea level rise budget (see Chapters 4 and 5).

6.4.3.2 *What was the magnitude of glacial-interglacial sea level change?*

Model based paleo-sea level analysis also helps to refine estimates of the eustatic (globally averaged) rise of sea level that occurred during the most recent glacial-interglacial transition from LGM to Holocene. The extended coral based relative sea level curve from the island of Barbados in the Caribbean Sea (Fairbanks, 1989; Peltier and Fairbanks, accepted) is especially important, as the relative sea level history from this site has been shown to provide a good approximation to the "ice equivalent" eustatic curve itself (Peltier and Solheim, 2002). The fit of the prediction of the ICE-5G(VM2) model to the Fairbanks data set Figure 6.8b constrains the net "ice equivalent" eustatic rise subsequent to the LGM to a value of 118.7 m, very close to the value of approximately 120 m conventionally inferred (e.g., Shackleton, 2000) on the basis of deep sea oxygen isotopic information (Figure 6.8). Waelbroeck et al. (2002) produced a sea level reconstruction based on coral evidence and deep sea O-isotopes corrected for the influence of bottom water temperature variations for the entire last glacial interglacial, which scales with the Barbados estimate (Figure 6.8a).

[INSERT FIGURE 6.8 HERE]

The ice equivalent eustatic sea level curve of Lambeck and Chappell (2001) based upon data from a variety of different sources, including the Barbados coral record, measurements from the Sunda Shelf of Indonesia (Hanebuth et al., 2000), and observations from the J. Bonaparte Gulf of northern Australia (Yokoyama et al., 2000), gives an ice equivalent eustatic sea level history that conflicts somewhat with that based upon the extended Barbados record (Figure 6.8). First, the depth of the low stand of the sea at LGM is approximately 140m below present sea level rather than approximately 120m required by the Barbados data set. Second, the Barbados data appear to rule out the possibility of the sharp rise of sea level at 19 ka that was hypothesized by Yokoyama et al. (2000). The disagreement between these interpretations of the depth of the LGM low stand may be connected to a flaw in the original analysis procedure (Yokoyama et al., 2001).

The record of eustatic sea level change can be extended into the time of the Eemian interglacial at ~125,000 years before present. Direct sea level measurements based upon coastal sedimentary deposits and tropical coral sequences have clearly established that eustatic sea level was higher than present during this last interglacial by approximately 4–6m (e.g., Rostami et al., 2000; Muhs et al., 2002). Ice cores in the western Arctic indicate that the Greenland Summit region remained ice-covered in the LIG, while southern Greenland and the Canadian Arctic became ice-free (Koerner, 1989; North Greenland Ice Core Project, 2004; Raynaud et al., 2005). Greenland ice sheet models forced with ice core-derived temperature histories (Cuffey and Marshall, 2000; Tarasov and Peltier, 2003; Lhomme et al., 2005b) and temperatures and precipitation produced by an AOGCM (Otto-Bliesner et al., in press-a) simulated the minimal LIG GIS as a steeply-sided ice sheet in central and northern Greenland (Figure 6.6). This ice sheet, combined with the change in other Arctic ice fields, likely generated 2–3.5 m of early LIG sea level rise over several millennia (Figure 6.6). The simulated contribution of Greenland to this sea level rise was likely driven by 2-4°C summer warming in Greenland (see Section 6.4.1). The evidence that sea level was 4–6 m above present implies there must also have been a contribution from Antarctica (Scherer et al., 1998; Overpeck et al., in press).

6.4.3.3 *What is the significance of higher than present sea levels during the last interglacial period?*

(Overpeck et al., in press) argue that since the circum-Arctic LIG warming is very similar to that expected in a future doubled CO_2 climate, we must also expect significant retreat of the GIS to occur under this future condition. Since not all of the LIG increment of sea level appears to be explained by the melt-back of the GIS, however, the Antarctic Ice Sheet, most likely the West Antarctic Ice Sheet (WAIS) must also have contributed (see also Scherer et al., 1998; Domack et al., 2005; Oppenheimer and Alley, 2005). That this may already be occurring is suggested by the previously discussed analysis of the Earth rotation data.

6.4.3.4 *What is the long-term contribution of polar ice sheet meltwater to the observed modern sea level rise?*

Holocene sea-level observations and models can be used to assess whether or not a significant part of the observed 2 mm/yr sea-level rise during the 20th century could be explained by long-term effect of the last deglaciation on polar ice sheets. From post TAR estimates from geological observations of sea level from 16 equatorialPacific Islands (Peltier, 2002; Peltier et al., 2002) and the tectonically stable Australian margin (Lambeck, 2002) it appears likely that over the past 2000 years prior to the 20th century sea level rise was zero and at most 0–0.2 mm yr^{-1}.

6.5 The Current Interglacial

A variety of proxy records provide detailed temporal and spatial information concerning climate change during the current interglacial, the Holocene, a *ca* 11,600-year long period of increasingly intense anthropogenic modifications of the local (e.g., land use) to global (e.g., atmospheric composition) environment. The well-dated reconstructions of the past 2000 years are covered in Section 6.6. In the context of both climate forcing and response, the Holocene is far better documented in terms of spatial coverage, dating and temporal resolution than previous interglacials. The evidence is clear that significant changes in climate forcing during the Holocene induced significant and complex climate responses, including long-term and abrupt changes in temperature, precipitation, monsoon strength and ENSO. For selected periods such as the mid-Holocene, *ca* 6 ka, intensive efforts have been dedicated to the synthesis of paleoclimatic observations and modeling intercomparisons. Such extensive data coverage provides a sound basis to evaluate the capacity of climate models to capture the response of the climate system to the orbital forcing.

6.5.1 Climate Forcing and Response During the Current Interglacial

6.5.1.1 What were the main climate forcings during the Holocene?

During the current interglacial, changes in the Earth's orbit modulated the latitudinal and seasonal distribution of insolation (Box 6.1). Ongoing efforts to quantify Holocene changes in stratospheric aerosol content recorded in the chemical composition of ice cores from both poles (Zielinski, 2000; Castellano et al., 2005) confirm that volcanic forcing amplitude and occurrence varied significantly during the Holocene (see also Section 6.5). Fluctuations of cosmogenic isotopes (ice core ^{10}Be and tree ring residual ^{14}C) have been used as proxies for Holocene changes in solar activity (e.g., Bond et al., 2001), but substantial work remains to be done to disentangle solar from non-solar influences on these proxies over the full Holocene (Muscheler et al., accepted). Residual continental ice sheets formed during the last ice age were retreating during the first half of the current interglacial period (Figure 6.8). The associated ice sheet albedo is thought to have locally modulated the regional climate response to the orbital forcing (e.g., Davis et al., 2003).

The evolution of atmospheric trace gases during the Holocene is well known from ice core analyses (Figure 6.4). A first decrease in atmospheric CO_2 of about 7 ppmv from 11 to 8 ka is followed by a 20 ppmv CO_2 increase until the onset of the industrial revolution (Monnin et al., 2004). Atmospheric methane decreased from a Northern Hemisphere value of ~730 ppbv around 10 ka to about 580 ppb around 6 ka, and increased again slowly to 730 ppbv at preindustrial times (Chappellaz et al., 1997; Flückiger et al., 2002). Atmospheric N_2O largely followed the evolution of atmospheric CO_2 and shows an early Holocene decrease of about 10 ppb and an increase of the same magnitude between 8 and 2 ka (Flückiger et al., 2002). Implied radiative forcing changes from Holocene greenhouse gas variations are 0.4 W m^{-2} (CO_2) and 0.1 W m^{-2} (N_2O and CH_4), relative to preindustrial.

6.5.1.2 Why did Holocene atmospheric greenhouse gas concentrations vary before the industrial period?

Recent transient carbon cycle-climate model simulations with a predictive global vegetation model have attributed the early Holocene CO_2 decrease to forest regrowth in areas of the waning Laurentide ice sheet, partly counteracted by ocean sediment carbonate compensation (Joos et al., 2004). Carbonate compensation of terrestrial carbon uptake during the glacial-interglacial transition and the early Holocene, as well as coral reef build-up during the Holocene, have likely contributed to the subsequent CO_2 rise (Broecker and Clark, 2003; Ridgwell et al., 2003; Joos et al., 2004), whereas recent carbon isotope data (Eyer, 2004) and model results (Brovkin et al., 2002; Kaplan et al., 2002; Joos et al., 2004) suggest that the terrestrial carbon inventory has been rather stable over the past 7000 years preceeding the industrialisation. Such natural mechanisms cannot account for the much more significant industrial trace gas increases; atmospheric CO_2 would be expected to remain well below 290 ppm in the absence of anthropogenic emissions (Gerber et al., 2003).

It has been hypothesized, based on Vostok ice core CO_2 data (Petit et al., 1999), that atmospheric CO_2 would have dropped naturally by 20 ppm during the Holocene (in contrast with the observed 20 ppm increase), just as it did during the previous three glacial-interglacial cycles, if human activities had not caused a release of terrestrial carbon and methane during the Holocene (Ruddiman, 2003; Ruddiman et al., 2005); this hypothesis also suggests that incipient late Holocene high-latitude glaciation was prevented by these pre-Industrial greenhouse gas emissions. However, this hypothesis is in conflict with several, independent lines of evidence, including the lack of orbital similarity of the three previous interglacials with the Holocene (see Box 6.1 and Section 6.3.1). This hypothesis requires much larger changes in the Holocene atmospheric stable carbon isotope ratio ($^{13}C/^{12}C$) than found in ice cores (Eyer, 2004) as well as a carbon release by anthropogenic land use that is larger than estimated by comparing carbon storage for natural vegetation and present day land cover (Joos et al., 2004).

6.5.1.3 Was any part of the current interglacial period warmer than the late 20th century?

The temperature evolution over the Holocene has been established for many different regions but often with proxy records more sensitive to specific seasons (see Section 6.1). In the North Atlantic and adjacent Arctic, there was a tendency for temperature maxima to occur earlier and over shorter periods with increasing latitude, pointing to the direct influence of the summer insolation maximum on sea ice extent (Koc and Jansen 1994; Kim et al., 2004). Climate reconstructions in the mid-northern latitudes exhibit a long-term decline in SST from the warmer early- to mid-Holocene to the cooler late-Holocene pre-industrial period (Johnsen et al., 2001; Marchal et al., 2002; Andersen et al., 2004; Kim et al., 2004), most likely in response to annual mean and summer orbital forcings at these latitudes. Near ice sheet remnants in northern Europe or western North America, peak warmth is locally delayed, probably as a result of the interplay between ice elevation, albedo, atmospheric and oceanic heat transport and orbital forcing (MacDonald et al., 2000; Kaufman et al., 2004). The warmest period in northern Europe and western north America occurs from 7 to 5 ka (Davis et al., 2003; Kaufman et al., 2004). During this mid-Holocene period, global pollen-based reconstructions (Prentice, 1998; Prentice et al., 2000) show a widespread northward expansion of northern temperate forest (Bigelow et al., 2003; Kaplan et al., 2003), as well as substantial glacier retreat (see Box 6.3). Other early warm periods are identified in the equatorial west Pacific (Stott et al 2004), China (He et al., 2004), New Zealand (Williams et al, 2004), south Africa (Holmgren et al, 2003) and Antarctica (Masson et al., 2000). At high southern latitudes, the early warm period cannot be explained by local summer insolation changes (see Box 6.1), suggesting that large-scale reorganisation of latitudinal heat transport may have been responsible. In contrast, tropical temperature reconstructions, only available from marine records, show that tropical Atlantic, Pacific, Indian Ocean SSTs exhibit a progressive warming from the beginning of the current interglacial onwards (Rimbu et al., 2004; Stott et al., 2004), possibly a reflection of annual mean insolation change (Figure 6.5). When considering the periods of largest temperature changes (Figure 6.9), paleoclimatic records of the Holocene provide no conclusive evidence for globally synchronous warm periods, especially because the temperature trends appear distinct in the low versus mid- and high-latitudes during the Holocene (Lorentz et al, 2006).

[INSERT FIGURE 6.9 HERE]

When forced by mid-Holocene orbital parameters, state-of-the-art coupled climate models capture observed regional temperature and precipitation changes, whereas simulated global mean temperatures remain essentially unchanged, just as expected from the seasonality of the orbital forcing (see Box 6.1) (Y. Wang et al., 2005a). It is obvious that there were places, seasons and periods in the Holocene where local temperature was likely as warm as or warmer than at the end of the 20th century. However, these warm periods were not of global scale, nor consistent through seasons, in contrast to the observed post-industrial warming. Due to different regional temperature responses from the tropics to high latitudes, as well as between hemispheres, commonly used concepts such as “mid-Holocene thermal optimum,” “Altithermal,” etc. are not globally relevant and should only be applied in a well-articulated regional context.

Box 6.3: Holocene Glacier Variability

The near global retreat of mountain glaciers is among the most visible evidence for 20th/21st centuries climate change (see Chapter 4), and the question arises as to the significance of this current retreat within a longer time perspective. The climatic conditions that cause an advance, or a retreat, may be different for glaciers located in different climate regimes (see Chapter 4). This distinction is crucial if reconstructions of past glacier activity are to be understood properly.

Records of Holocene glacier fluctuations provide a necessary backdrop for evaluating the current global retreat. However, in most mountain regions records documenting past glacier variations exist as discontinuous low resolution series (see Box 6.3, Figure 1), whereas continuous records providing the most coherent information on the whole Holocene are available so far only in Scandinavia (e.g., Nesje, 2005) (see Box 6.3, Figure 1).

[INSERT BOX 6.3, FIGURE 1 HERE]

What do glaciers tell us about climate change during the Holocene?

Most archives from the Northern Hemisphere and the tropics show small or absent glaciers between 9.0 and 6.0 ka, whereas during the second half of the Holocene glaciers reformed and expanded. This tendency is primarily related to changes in summer and winter insolation due to the configuration of orbital parameters (see Box 6.1). Long-term changes in solar insolation, however, cannot explain the shorter, decadal-scale, regionally diverse glacier responses, driven by complex and poorly understood causes. On these shorter timescales, climate phenomenon such as the North-Atlantic Oscillation (NAO) and El Niño - Southern Oscillation (ENSO) impacted glaciers mass balance, explaining some of the discrepancies found between regions. This is exemplified in the anti-phasing between decadal glacier mass balance variations from the Alps and Scandinavia in 20th century (Six, 2001).

Comparing the ongoing retreat of glaciers with the reconstruction of glacier variations during the Holocene, we cannot identify an analogous period with a globally homogenous trend of retreating glaciers over centennial and shorter timescales in the past.

6.5.1.4 What are the links between orbital forcing and mid-Holocene monsoon intensification?

Lake levels and vegetation changes reconstructed in the early to mid Holocene in North Africa indicate large precipitation increases in North Africa (Jolly et al, 1998). Simulating this intensification of African monsoon is widely used as a benchmark for climate models. When forced by mid-Holocene insolation resulting from changes in the Earth's orbit (see Box 6.1), but fixed present-day vegetation and ocean temperatures, atmospheric models do not produce precipitation changes far enough and intense enough in the Sahara (Joussaume 1999, Coe and Harrison, 2002). Model characteristics together with the mean tropical temperature of the control simulation are a primary reason for the differences between different models results (Braconnot et al. 2002). New coupled ocean-atmosphere simulations show that the ocean feedback strengthens the inland monsoon flow, and that the results are in better agreement with pollen and lake reconstructions (Braconnot et al 2004, Zhao et al. 2005). As already noted in the TAR, the vegetation feedback plays a major role in the enhancement of the African monsoon (e.g., Claussen and Gayler 1997, de Noblet et al. 2000); when combined, vegetation and ocean feedbacks produce nonlinear interactions resulting in simulated precipitation in closer agreement with data (Braconnot et al., 2000). However, it was recently shown that soil moisture changes may counteract some of these effects (Levis et al. 2004), suggesting that modelling improvements are still required to properly capture the monsoon changes in Africa. Ocean feedbacks are also invoked to explain the strong intensification of the north Australian monsoon, in simulations that are consistent with observations (Liu et al. 2004). Finally, two models have been used to investigate the mechanism involved in the enhancement of monsoon over southwest America (Harrison et al. 2003). They showed that the American monsoon increase was primarily due to continental warming, although the ocean feedback reinforced the process, and that the drying in midcontinent was dynamically linked to the monsoon enhancement. There is less consensus between the various simulations for the Asian monsoons (Liu et al 2004.). Transient simulations of Holocene climate performed with intermediate complexity climate models have further shown that land-surface feedbacks may be involved in abrupt monsoon fluctuations (see Section 6.5.2).

6.5.1.5 What are the links between orbital forcing and mid-Holocene climate in the middle and high latitudes?

Terrestrial records of the mid-Holocene indicate an expansion of forest at the expense of tundra at mid- to high-latitudes of the Northern Hemisphere (Prentice et al., 2000). Since the IPCC TAR, coupled atmosphere-ocean models, including the recent PMIP-2 simulations, have investigated the response of the climate system to orbital forcing for 6 ka BP during the mid-Holocene (Table 6.1). Fully coupled atmosphere-ocean-vegetation models do produce the northward shift in the position of the northern limit of boreal forest, in response to simulated summer warming, and the northward expansion of temperate forest belts in North America, in response to simulated winter warming (Wohlfahrt et al., 2004). At high latitudes the vegetation and ocean feedbacks enhance the warming in spring and autumn, respectively. Models do capture qualitatively the reconstructed mid-continental drying in North America and Eurasia (Wohlfahrt et al., 2004).

Ocean changes simulated for this period are generally small and difficult to quantify from data due to uncertainties in the way proxy methods respond to the seasonality and stratification of the surface waters (Waelbroeck et al., 2005). Simulations with atmosphere and slab ocean models indicate that a change in the mean tropical Pacific SSTs in the mid-Holocene to more La-Niña-like conditions can explain North American drought conditions at mid-Holocene (Shin et al., 2005). Based on proxies of SST in the North Atlantic, it has been suggested that trends from early to late Holocene are consistent with a shift from a more meridional regime over northern Europe to a positive NAO-like mean state in the early to mid Holocene (Rimbu et al., 2004). Results from PMIP-2 models find that six of nine models support a positive NAO-like atmospheric circulation in the mean state for the mid-Holocene as compared to pre-industrial (Gladstone et al.,2005).

6.5.1.6 Are there long-term modes of climate variability identified during the Holocene that could be involved in the observed current warming?

An increasing number of Holocene proxy records are of sufficiently high resolution to describe the climate variability on centennial to millennial time scales, and to identify possible natural quasi-periodic modes of climate variability at these time scales (Haug et al., 2001; Gupta et al., 2003). Although earlier studies suggested that Holocene millennial variability could display similar frequency characteristics as the glacial variability in the North Atlantic (Bond et al., 1997), this assumption is increasingly being questioned (Risebrobakken et al., 2003; Schulz et al., 2004; Moros et al., in press). The suggested synchroneity of tropical and North Atlantic centennial to millennial variability (de Menocal et al., 2000; Mayewski et al., 2004; Y. Wang et al., 2005b) is also not common to the full globe, as revealed by millennial scale variability in the southern hemisphere (Masson et al., 2000; Holmgren et al., 2003). In several regions, such as Alaska, Svalbard, and parts of North American Cordillera, the glacial advances of the last thousand years were the most extensive of the Holocene, whereas in other regions, especially in the Southern Hemisphere, previous advances were larger (Grove, 2004; Box 6.3).

Based on the correlation between changes in cosmogenic isotopes (^{10}Be or ^{14}C) – assumed to relate to solar activity changes- and climate proxy records, some authors argue that solar activity may be the driver for centennial to millennial variability (Karlen and Kuylenstierna, 1996; Bond et al., 2001; Fleitmann et al., 2003; Y. Wang et al., 2005b). The possible importance of (forced or unforced) modes of variability within the climate system, for instance related to the deep ocean circulation, has also been highlighted (Bianchi and McCave, 1999; Duplessy et al., 2001; Marchal et al., 2002; Oppo et al., 2003). However, in many records, there is no apparent consistent pacing at specific centennial to millennial frequencies through the Holocene period, but rather shifts between different frequencies (Moros et al., in press). The current lack of consistency between various data sets makes it difficult, based on current knowledge, to attribute the century and longer time scale large-scale climate variations to solar activity, episodes of intense volcanism, or variability internal to the climate system.

6.5.2 Abrupt Climate Change During the Current Interglacial

6.5.2.1 What do abrupt changes in oceanic and atmospheric circulation at mid- and high-latitudes tell us?

At the beginning of the Holocene, approximately 11,600 years ago, significant residual continental ice cover still existed in the Northern Hemisphere. Significant volumes of fresh water were also impounded in pro-glacial lakes adjacent to the remnants of this ice. In particular, the residual ice cover over the North American continent, together with adjacent pro-glacial Lake Agassiz to the southwest, is believed to have been responsible for the occurrence of the "8.2 kyr event" that was recognized as a prominent feature in the Summit, Greenland ice cores and other records (Alley et al., 1997). This event is believed to have occurred as a consequence of an "outburst flood" during which Lake Agassiz drained 1.6 Sv in 1-2 years into Hudson Bay (Renssen et al., 2001; Nesje et al., 2004). The 8.2 kyr event is recorded as a brief adjustment of the Atlantic meridional overturning circulation (Bianchi and McCave, 1999; Risebrobakken et al., 2003; McManus et al., 2004), as well as a 2°C to 6°C cooling of the North Atlantic region identified in Greenland, Europe and North America (Klitgaard-Kristensen et al., 1998; von Grafenstein et al., 1998; Barber et al., 1999; Nesje et al., 2000; McDermott et al., 2001). There was an associated decrease in precipitation or runoff, taking 30–40 years to reach a minimum, in Northern South America (Hughen et al., 1996). A large decrease in methane (several tens of ppb) (Spahni et al., 2003) reveals the widespread consequences of the abrupt 8.2 kyr event associated with large scale atmospheric circulation change recorded from the Arctic to the tropics (Stager and Mayewski, 1997; Haug et al., 2001; Fleitmann et al., 2003).

Intense modelling efforts have been targeted to assess the vulnerability of the ocean and atmospheric circulation to a well-constrained freshwater release. Simulations conducted with intermediate complexity climate models (see Alley and Agustsdottir, 2005 for a review) point to changes in north Atlantic deep water formation and shifts in the ITCZ associated with equilibrium states of the models (Bauer et al., 2004), and to responses to the freshwater forcing depending on the specific model's high frequency variability (Renssen et al., 2002). Ensemble simulations conducted with a coupled climate model equipped with the explicit modelling of a variety of proxies (LeGrande et al 2006) showed consistency between the model response to the freshwater forcing and the available proxy records.

The end of the first half of the Holocene – between ca. 5 and 4 ka – is punctuated by rapid events at various latitudes, such as an abrupt increase in northern hemisphere sea-ice cover (Jennings et al., 2001), decrease in Greenland deuterium excess, reflecting a change in the hydrological cycle (Masson-Delmotte et al., 2005a), abrupt cooling events in European climate (Seppa and Birks, 2001; Lauritzen, 2003), widespread North American drought for centuries (Booth et al., 2005), and changes in South American climate (Marchant and Hooghiemstra, 2004). The processes behind these observed abrupt shifts are not well understood, in part because of the difficulty to assess if the abrupt changes recorded in some continental proxy records are due to the recording process in the proxy or to an abrupt change in climate. As these particular events take place at the end of a local warm period caused by orbital forcing (see Box 6.1 and Section 6.5.1), these observations suggest that under gradual climate forcings (e.g., orbital) the climate system can change abruptly.

6.5.2.2 What is the significance of abrupt changes in monsoons?

In the tropics, precipitation-sensitive records and models indicate that summer monsoons in Africa, India and southeast Asia were enhanced in the early- to mid-Holocene due to orbital forcing, a resulting increase in land-sea temperature gradients, and displacement of the intertropical convergence zone. All high resolution precipitation-sensitive records reveal that the local transitions from wetter conditions in the early Holocene to drier modern conditions occurred in one or more steps (Guo et al., 2000; Fleitmann et al., 2003; Morrill et al., 2003; Y. Wang et al., 2005a). In the early Holocene, large increases in African monsoon precipitation and/or wetter conditions over the Mediterranean are associated with dramatic changes in Mediterranean Sea ventilation, as evidenced by sapropel layers (Ariztegui, 2000).

Transient simulations of the Holocene have been performed with models of intermediate complexity, although usually after the final disappearance of ice sheets, and forced by orbital parameters (Box 6.1). These models have pointed to the operation of mechanisms that can generate rapid events in response to orbital forcing, such as changes in African monsoon intensity due to nonlinear interactions between vegetation and monsoon dynamics (Claussen et al., 1999; Renssen et al., 2003).

6.5.3 How and Why has ENSO Changed Over the Present Interglacial?

Paleoclimate records clearly indicate fundamental changes in ENSO during the Holocene; model simulations suggest that these changes resulted from altered radiative forcing and background climate states. Data from diverse sources (corals, archaeological middens, and lake and ocean sediments) indicate that the early-mid Holocene experienced weak ENSO variability, with a transition to a stronger modern regime occurring in the past few thousand years (Shulmeister and Lees, 1995; Gagan et al., 1998; Rodbell et al., 1999; Tudhope et al., 2001; Moy et al., 2002). Most data sources are discontinuous, providing only snapshots of mean conditions or interannual variability, and making it difficult to precisely characterize the rate and timing of the transition to the modern regime. Fossil coral records from New Guinea indicate clearly that interannual variability was weaker between about 7.7–5.4 ka than it was at 2.7–1.7 ka (Tudhope et al., 2001; McGregor and Gagan, 2004). A continuous lake record from Ecuador, which tracks the rainstorms characteristic of strong El Niño events, notes a stepped increase in the frequency of such events at around 7000 and at 5000 years ago (Moy et al., 2002).

Paleoclimate simulations using models of varying complexity support a mechanism by which orbital forcing leads to a weakening of ENSO variability. A simple model of the coupled Pacific ocean-atmosphere, forced with orbital insolation variations, suggests that seasonal changes in insolation can produce systematic changes in ENSO behavior. Key elements of the Holocene ENSO response are the Bjerknes feedback mechanism (Bjerknes, 1969) and ocean dynamical thermostat (Clement et al., 1996; Clement et al., 2000; Cane, 2005). These studies indicate a progressive, somewhat irregular, increase in both event frequency and amplitude throughout the Holocene. Coupled general circulation models also reproduce the intensification of ENSO over the Holocene, although with some disagreement as to the magnitude of change. Both model results and data syntheses suggest that before the mid-Holocene, the tropical Pacific exhibited a more La Niña-like background state (Clement et al., 2000; Liu et al., 2000; Kitoh and Murakami, 2002; Otto-Bliesner et al., 2003; Liu, 2004). In paleoclimate simulations with general circulation models, ENSO teleconnections robust in the modern system show signs of weakening under mid-Holocene orbital forcing (Otto-Bliesner, 1999; Otto-Bliesner et al., 2003).

6.6 The Last 2000 Years

6.6.1 Northern Hemisphere Temperature Variability

6.6.1.1 What do reconstructions based on paleoclimatic proxies tell us?

Figure 6.10 shows the various instrumental and proxy-climate evidence of the variations in average large-scale surface temperatures over the last 1300 years. Figure 6.10a shows two instrumental compilations representing the mean annual surface temperature of the Northern Hemisphere since 1850, one based on land data only, and one using land and surface ocean data combined (see Chapter 3). The uncertainties associated with one of these series are also shown (30-year smoothed combined land and marine). These arise primarily from the incomplete spatial coverage of instrumentation through time (Jones et al., 1997) and whereas these uncertainties are larger in the 19th compared to the 20th century, the prominence of the recent warming, especially in the last two to three decades of the record, is clearly apparent in this 150-year context. The land-only record shows similar variability, although the rate of warming is greater than in the combined record after about 1980. The land-only series can be extended back beyond the 19th century, and is shown plotted from 1781 onwards. The early section is based on a much sparser network of available station data, with at least 23 European stations, but only one North American stations, spanning the first two decades, and the first Asian station beginning only in the 1820s. Four European records (Central England, De Bilt, Berlin and Uppsala) provide an even longer, though regionally-restricted, indication of the context for the warming observed in the last ~20–30 years, which is even greater in this area than is observed over the Northern Hemisphere land as a whole.

[INSERT FIGURE 6.10 HERE]

[INSERT TABLE 6.1 HERE]

The instrumental temperature data that exist before 1850, although increasingly biased towards Europe in earlier periods, show that the warming observed after 1980 is unprecedented compared to the levels measured in the previous 280 years, even allowing for the greater variance expected in an average of so few early data compared to the much greater number in the 20th century. Recent analyses of instrumental, documentary and proxy climate records, focusing on European temperatures, have also pointed to the unprecedented warmth of the 20th century and shown that the extreme summer of 2003 was very likely warmer than any that has occurred in at least 500 years (Luterbacher et al., 2004; Guiot et al., 2005). (See Chapter 3, Box 3.6.5).

If the behaviour of recent temperature change is to be understood, and the mechanisms and causes correctly attributed, parallel efforts are needed to reconstruct the longer and more-widespread pre-instrumental history of climate variability, as well as the detailed changes in various factors that might influence climate (Bradley et al., 2003b; Jones and Mann, 2004).

The TAR discussed various attempts to use proxy data to reconstruct changes in the average temperature of the Northern Hemisphere for the period after A.D. 1000, but focused on three reconstructions, all with yearly resolution. The first (Mann et al., 1999) represents mean annual temperatures, and is based on a range of proxy types, including data extracted from tree rings, ice cores and documentary sources; this reconstruction also incorporates a number of instrumental (temperature and precipitation) records from the 18th century onwards. For 900 years, this series exhibits multi-decadal fluctuations with amplitudes up to 0.3°C superimposed on a negative trend of 0.15°C, followed by an abrupt warming (~0.4°C) matching that observed in the instrumental data during the first half of the 20th century. Of the other two reconstructions, one (Jones et al., 1998) was based on a very much smaller number of proxies, whereas the other (Briffa et al., 2001) was based solely on tree-ring density series from an expansive area of the extra-tropics, but reached back only to AD 1400. These two reconstructions emphasise warm season rather than annual temperatures, with a geographical focus on extra-tropical land areas. They indicate a greater range of variability on centennial timescales prior to the 20th century, and also suggest slightly cooler conditions during the 17th century than those portrayed in the Mann et al. (1998; 1999) series.

Following the emphasis placed on it in the TAR, the “hockey stick” reconstruction of Mann et al. (1999) has been the subject of several critical studies. Soon and Baliunas (2003) challenged the conclusion that the 20th century was the warmest on a hemispheric average scale. They surveyed regionally diverse proxy climate data, noting evidence for relatively warm (or cold), or alternatively dry (or wet) conditions occurring at any time within pre-defined periods assumed to bracket the Medieval Warm Period (Little Ice Age). Their qualitative approach precluded any quantitative summary of the evidence at precise times, limiting the value of their review as a basis for comparison of the relative magnitude of mean Hemispheric 20th-century warmth (Mann and Jones, 2003; Osborn and Briffa, 2006).

Box 6.4: Hemispheric Temperatures in the “Medieval Warm Period”

At least as early as the beginning of the 20th century, different authors were already examining the evidence for climate changes during the last two millennia, particularly in relation to North America, Scandinavia and Eastern Europe (Brooks, 1922) . With regard to Iceland and Greenland, (Pettersson, 1914) cites evidence for considerable areas of Iceland being cultivated in the 10th century. At the same time, Norse settlers colonized areas of Greenland, while a general absence of sea ice allowed regular voyages at latitudes far to the north of what was possible in the colder 14th century. Brooks (1922) describes how, after some amelioration in the 15th and 16th centuries, conditions worsened considerably in the 17th century; in Iceland previously cultivated land was covered by ice. Hence, at least for the area of the northern North Atlantic, a picture was already emerging of generally warmer conditions around the centuries leading up to the end of the 1st millennium, but framed largely by comparison with strong evidence of much cooler conditions in later centuries, particularly the 17th century.

Lamb (1965) seems to have been the first to coin the phrase “Medieval Warm Epoch” or “Little Optimum” to describe the totality of multiple strands of evidence principally drawn from western Europe, for a period of widespread and generally warmer temperatures which he put at between AD 1000 to 1200 (Lamb, 1982). It is important to note that Lamb also considered the warmest conditions to have occurred at different times in different areas: between 950 to 1200 in European Russia and Greenland, but somewhat later, between 1150 to 1300 (though with notable warmth also in the later 900s) in most of Europe (Lamb, 1977).

Much of the evidence used by Lamb was drawn from a very diverse mixture of sources such as historical anecdotes, evidence of vegetation changes, or records of the cultivation of cereals and vines. He also drew inferences from very preliminary analyses of some Greenland ice core data and European tree-ring records. Much of this evidence is difficult to interpret in terms of accurate quantitative temperature influences. Much is not precisely dated, or results from physical or biological systems that involve complex lags between forcing and response, as is the case for vegetation and glacier changes. Lamb’s analyses also predate any formal statistical calibration of much of the evidence he considered. Largely on the basis of summer temperature inferences, he concluded that “High Medieval” temperatures were probably 1.0°C to 2.0°C above early 20th century levels at various European locations (Lamb, 1977; Bradley et al., 2003a).

A later study, based on examination of more quantitative evidence, in which efforts were made to control for accurate dating and specific temperature response, concluded that it was not possible to say anything other than “… in some areas of the Globe, for some part of the year, relatively warm conditions may have prevailed” (Hughes and Diaz, 1994).

In medieval times, as now, climate was unlikely to have changed in the same direction, or by the same magnitude, everywhere (Box 6.4, Figure 1). At some times, some regions may have experienced even warmer conditions than those that prevailed throughout the 20th century (e.g., see Bradley et al., 2003a). Regionally restricted evidence by itself, especially when the dating is imprecise, is of little practical relevance to the question of whether climate in medieval times was globally as warm or warmer than today. Local climate variations can be dominated by internal climate variability, often the result of the redistribution of heat by regional climate processes. Only very large-scale climate averages can be expected to reflect global forcings over recent millennia (Mann and Jones, 2003; Goosse et al., 2005a). To define medieval warmth in a way that has more relevance for exploring the causes of recent large-scale warming, widespread and continuous paleoclimatic evidence must be assimilated in a homogeneous way and scaled against recent measured temperatures to allow a meaningful quantitative comparison against 20th century warmth (Figure 6.10).

[INSERT BOX 6.4, FIGURE 1 HERE]

A number of studies that have attempted to produce very large spatial scale reconstructions have come to the same conclusion: that medieval warmth was complex in terms of its precise timing and regional expression (Crowley and Lowery, 2000; Folland et al., 2001; Esper et al., 2002; Bradley et al., 2003b; Jones and Mann, 2004; D'Arrigo et al., 2006).

The uncertainty associated with present paleoclimate estimates of Northern Hemispheric mean temperatures are significant, especially for the period prior to 1600 when data are scarce (Mann et al., 1999; Briffa and Osborn, 2002; Cook et al., 2004a). However, Figure 6.10 shows that the warmest period prior to the 20th century, very likely occurred between 950 and 1100, but temperatures were between 0.1°C and 0.2°C below the 1961–1990 mean and noticeably below the warmth shown by instrumental data after 1980.

In order to reduce the uncertainty, further work is necessary to update existing records and produce many more paleoclimate series with much wider geographic coverage. There are far from sufficient data to make any meaningful estimates of global medieval warmth (Figure 6.11). There are very few long records with high temporal resolution data from the oceans, the tropics or the Southern Hemisphere.

The evidence currently available indicates that Northern Hemisphere mean temperatures during Medieval times (950–1100) were indeed warm in a 2000-year context and even warmer in relation to the less sparse but still limited evidence of widespread average cool conditions in the 17th century (Osborn and Briffa, 2006). However, the evidence is not sufficient to support a conclusion that hemispheric mean temperatures were as warm, or the extent of warm regions as expansive, as those in the 20th century as a whole, during any period in medieval times (Jones et al., 2001; Bradley et al., 2003b; Bradley et al., 2003a; Osborn and Briffa, 2006).

McIntyre and McKitrick (2003) reported that they were unable to replicate the results of Mann et al. (1998). Wahl and Ammann (accepted) demonstrated that this was due to the omission by McIntyre and McKitrick of several proxy series used by Mann et al. (1998). Wahl and Ammann (accepted) were able to reproduce the original reconstruction closely when all records were included. McIntyre and McKitrick (2005) raised further concerns about the details of the Mann et al. (1998) method, principally relating to the independent verification of the reconstruction against 19th century instrumental temperature data and to the extraction of the dominant modes of variability present in a network of western North American tree-ring chronologies, using Principal Components Analysis. The latter may have some foundation, but it is unclear whether it has a marked impact upon the final reconstruction (Von Storch et al., 2004; Huybers, 2005; McIntyre and McKitrick, 2005). However, subsequent work using different methods to those of Mann et al. (1998, 1999), also provides evidence of rapid 20th century warming compared to reconstructed temperatures in the preceding millennium.

Since the TAR, a number of additional proxy data syntheses based on annually or near-annually resolved data, variously representing mean Northern Hemisphere temperature changes over the last one or two thousand years, have been published (Esper et al., 2002; Crowley et al., 2003; Mann and Jones, 2003; Cook et al., 2004a; Moberg et al., 2005; Rutherford et al., 2005; D'Arrigo et al., 2006). These are shown, plotted from AD 700 in Figure 6.10b, along with the three series from the TAR. As with the original TAR series, these new records are not entirely independent reconstructions inasmuch as there are some predictors (most often tree-ring data) that are common between them, but, in general, they represent some expansion in the length and geographical coverage of the previously available data (Figures 6.10 and 6.11).

[INSERT FIGURE 6.11 HERE]

Briffa (2000) produced an extended history of interannual tree-ring growth incorporating records from sites across northern Fennoscandia and northern Siberia, using a statistical technique to construct the tree-ring chronologies that is capable of preserving multi-centennial timescale variability. Although ostensibly representative of northern Eurasian summer conditions, these data were later scaled using simple linear regression against a mean Northern Hemisphere land series to provide estimates of summer temperature over the past 2000 years (Briffa et al., 2004).

Esper et al. (2002) took tree-ring data from 14 sites from Eurasia and North America, and applied a variant of the same statistical technique designed to produce ring-width chronologies in which evidence of long-timescale climate forcing is better represented compared with earlier tree-ring processing methods. The resulting series were averaged, smoothed and then scaled so that the multi-decadal variance matched that in the Mann et al. (1998) reconstruction over the period 1900–1977. This produced a reconstruction with markedly cooler temperatures during the 12th to the end of the 14th century than are apparent in any other series. The relative amplitude of this reconstruction is reduced somewhat when recalibrated directly against smoothed instrumental temperatures (Cook et al., 2004a) or by using annually-resolved temperature data (Briffa and Osborn, 2002), but even then, this reconstruction remains at the coldest end of the range defined by all currently available reconstructions.

Mann and Jones (2003) selected only eight normalised series (all screened for temperature sensitivity) to represent annual mean Northern Hemisphere temperature change over the last 1800 years, though the majority of these eight represent integrations of multiple proxy site records or reconstructions, including some oxygen isotope records from ice cores and documentary information as well tree-ring records The average of these decadally-smoothed series was scaled so that its mean and standard deviation matched those of the Northern Hemisphere decadal mean land and marine record, over the period 1856–1980.

Moberg et al. (2005) used a mixture of tree-ring and other proxy-based climate reconstructions to represent short- and longer-timescale changes, respectively, across the Northern Hemisphere. Seven tree-ring series provided information on timescales below 80 years, while eleven far-less-accurately dated records (including ice melt series, lake diatoms and pollen data, chemistry of marine shells and Foraminifera, and one borehole temperature record from the Greenland icecap) were combined and scaled to match the mean and standard deviation of the instrumental record between 1856 and 1979. This reconstruction displays the warmest temperatures of any reconstruction during the 10th and early 11th centuries, although still below the level of warmth observed since 1980.

Many of the individual annually-resolved proxy series used in the various reconstruction studies cited above have been combined in a new reconstruction (only back to AD 1400) based on a climate field reconstruction technique (Rutherford et al., 2005). This study also involved a methodological exploration of the sensitivity of the results to the precise specification of the predictor set, as well as the predictand target region and seasonal window. It concluded that the reconstructions were reasonably robust to differences in the choice of proxy data and statistical reconstruction technique.

D'Arrigo et al. (2006) used only tree-ring data, but these include a substantial number not used in other reconstructions, particularly in northern North America. Their reconstruction, similar to that of Esper et al., (2002), displays a large amplitude of change during the past 1000 years, associated with notably cool excursions during most of the 9th, 13th and 14th centuries, clearly below those of most other reconstructions.

Hegerl et al., (in press), used a mixture of 14 regional series, of which only three were not made up from tree-ring data (a Greenland ice oxygen isotope record and two composite series, from China and Europe, including a mixture of instrumental, documentary and other data). Many of these are common to the earlier reconstructions. However, these series were combined and scaled using a regression approach (total least squares) intended to prevent the loss of low-frequency variance inherent in other regression approaches. The reconstruction produced lies close to the centre of the range defined by the other reconstructions.

Various statistical methods are used to convert the various sets of original paleoclimatic proxies into the different estimates of mean Northern Hemisphere temperatures shown in Figure 6.10 (see discussions in Jones and Mann, 2004; Rutherford et al., 2005). These range from simple averaging of regional data, and scaling of the resulting series so that its mean and standard deviation match those of the observed record over some period of overlap (Jones et al., 1998; Crowley and Lowery, 2000), to complex climate field reconstruction, where large scale modes of spatial climate variability are linked to patterns of variability in the proxy network, via a multivariate transfer function that explicitly provides estimates of the spatio-temporal changes in past temperatures, and from which large-scale average temperature changes are derived by averaging the climate estimates across the required region (Mann et al., 1998; Rutherford et al., 2003; Rutherford et al., 2005). Other reconstructions can be considered to represent what are essentially intermediate applications of these two approaches, in that they involve regionalisation of much of the data prior to the use of a statistical transfer function, and so involve fewer, but potentially more robust, regional predictors (Briffa et al., 2001; Mann and Jones, 2003). Some of these studies explicitly or implicitly reconstruct tropical temperatures based on data largely from the extra-tropics, and assume stability in the patterns of climate association between these regions. This assumption has been questioned on the basis of both observational and model simulated data suggesting that tropical to extra-tropical climate variability can be decoupled (Rind et al., 2005), and also that extra-tropical teleconnections associated with ENSO may also vary through time (see Section 6.5.6).

Oerlemans (2005) constructed a temperature history for the globe based on 169 glacier-length records. He used simplified glacier dynamics that incorporate specific response time and climate sensitivity estimates for each glacier. The reconstruction suggests that moderate global warming occurred after the middle of the 19th century, with about 0.6°C warming by the middle of the 20th century. Following a 25-year cooling, temperatures rose again after 1970, though much regional and high-frequency variability is superimposed on this overall interpretation. However, this approach does not allow for changing glacier sensitivity over time, which may limit the information before 1900. Analyses of glacier mass balances, volume changes, and length variations along with temperature records in the western European Alps (Vincent et al., 2005) indicate that between 1760 and 1830, glacier advance was driven by precipitation that was 25% above the 20th century average, while there was little difference in average temperatures. Glacier retreat after 1830 was related to reduced winter precipitation and the influence of summer warming only became effective at the beginning of the 20th century. In southern Norway, early 18th century glacier advances can be attributed to increased winter precipitation rather than cold temperatures (Nesje and Dahl, 2003).

Changes in proxy records, either physical (such as the isotopic composition of various elements in ice) or biological (such as the width of a tree ring or the chemical composition of a growth band in coral), do not respond precisely or solely to changes in any specific climate parameter (such as mean temperature or total rainfall), or to the changes in that parameter as measured over a specific “season” (such as June-August or January-December). For this reason, the proxies must be ‘calibrated’ empirically, by comparing their measured variability over a number of years with available instrumental records to identify some optimal climate association, and to quantify the statistical uncertainty associated with scaling proxies to represent this specific climate parameter. All reconstructions, therefore, involve a degree of compromise with regard to the specific choice of ‘target’ or dependent variable. Differences between the temperature reconstructions shown in Figure 6.10b are to some extent related to this, as well as to the choice of different predictor series (including differences in the way these have been processed). The use of different statistical scaling approaches (including whether the data are smoothed prior to scaling, and differences in the period over which this scaling is carried out) also influences the apparent spread between the various reconstructions. Discussions of these issues can also be found in Harris and Chapman, (2001); Beltrami, (2002); Briffa and Osborn, (2002); Trenberth and Otto-Bliesner, (2003); Zorita et al., (2003); Jones and Mann, (2004); Esper et al., (2002); (Esper et al., 2005); Pollack and Smerdon, (2004); and Rutherford et al., (2005).

The considerable uncertainty associated with individual reconstructions (on the order of ±0.5°C two-standard-error limits on the multi-decadal timescale), is shown in several publications, calculated on the basis of analyses of regression residuals (Mann et al., 1998; Briffa et al., 2001; Jones et al., 2001; Mann and Jones, 2003; Rutherford et al., 2005). In virtually all cases, these are likely to be minimum uncertainties because they do not take into account other sources of uncertainty in the predictor series themselves (Briffa and Osborn, 1999; Esper et al., 2002; Bradley et al., 2003b; Osborn and Briffa, 2006)

Figure 6.10b illustrates how, when viewed together, the currently available reconstructions indicate generally greater variability in centennial time scale trends over the last 1000 years than was apparent in the TAR. It should be stressed that each of the reconstructions included in Figure 6.10b is shown scaled as it was originally published, despite the fact that some represent seasonal and others mean annual temperatures. Except for the borehole curve (Pollack and Smerdon, 2004) and the interpretation of glacier length changes (Oerlemans, 2005), they were originally also calibrated against different instrumental data, using a variety of statistical scaling approaches. For all these reasons, these reconstructions would be expected to show some variation in relative amplitude.

Figure 6.10c is a schematic representation of the most likely course of hemispheric-mean temperature change during the last 1300 years based on all of the reconstructions shown in Figure 6.10b, and taking into account their associated statistical uncertainty. The envelopes that enclose the two standard error confidence limits bracketing each reconstruction have been overlain (with greater emphasis placed on the area within the 1 standard error limits) to show where there is most agreement between the various reconstructions. The result is a picture of relatively cool conditions in the 17th and early 19th centuries and warmth in the 11th and early 15th centuries, but the warmest conditions are apparent in the 20th century. Given that the confidence levels surrounding all of the reconstructions are wide, virtually all reconstructions are effectively encompassed within the uncertainty previously indicated in the TAR. The major differences between the various proxy reconstructions relate to the magnitude of past cool excursions, principally during the 12th to 14th and 17th to 19th centuries. Several reconstructions exhibit a short-lived maximum just prior to AD 1000 but only one, that of Moberg et al. (2005), during the early decades of both the 11th and 12th centuries (990–1050 and 1080–1120), indicates persistent hemispheric-scale conditions that were as warm as those in the 1940s and 50s. The long-timescale variability in this reconstruction is determined by low-resolution proxy records which cannot be rigorously calibrated against recent instrumental temperature data (Mann et al., 2005a). None of the reconstructions in Fig. 6.10 shows pre-20th century temperatures reaching the levels seen in the instrumental temperature record for the last two decades of the 20th century.

It is important to recognise that in the Northern Hemisphere as a whole there are relatively few long and well-dated climate proxies, particularly for the period prior to the 17th century (Figure 6.11). Those that do exist are concentrated in extra-tropical, terrestrial locations, and many have greatest sensitivity to summer rather than winter (or annual) conditions. Changes in seasonality probably limit the conclusions that can be drawn regarding annual temperatures derived from predominantly summer-sensitive proxies (Jones et al., 2003). There are very few strongly temperature-sensitive proxies from tropical latitudes. Stable isotope data from high-elevation ice cores provide long records and have been interpreted in terms of past temperature variability (Thompson, 2000), but recent calibration and modelling studies, in South America and southern Tibet (Hoffmann et al., 2003; Vuille and Werner, 2005; Vuille et al., 2005), indicate a dominant sensitivity to precipitation changes, at least on seasonal to decadal timescales, in these regions. Very rapid and apparently unprecedented melting of tropical ice caps has been observed in recent decades (Thompson et al., 2000; Thompson, 2001) (see Box 6.3), possibly associated with enhanced warming at high elevations (Gaffen et al., 2000), but other factors besides temperature can strongly influence tropical glacier mass balance (see Chapter 3). Coral oxygen isotopes and Sr/Ca ratios primarily reflect SSTs, though they are also influenced by salinity changes associated with precipitation variability. Unfortunately, these records are invariably short, on the order of centuries at best, and can be associated with age uncertainties of 1 or 2%. Virtually all coral records currently available from the tropical Indo-Pacific indicate unusual warmth in the 20th century (Cole, 2003), and in the tropical Indian ocean many records show a trend towards isotopically warmer conditions (Charles et al., 1997; Kuhnert et al., 1999; Cole et al., 2000). In most multi-centennial length coral series, the late 20th century is warmer than any time in the last 100–300 years.

Recent work using pseudo-proxy networks extracted from GCM simulations of global climate during the last millennium indicate that a number of the NH temperature reconstructions may not fully represent variance on time scales longer than those represented in the calibration period (Burger and Cubasch, 2005; von Storch and Zorita, 2005; Burger et al., 2006). If true, this would represent a bias, as distinct from the random error represented by published reconstruction uncertainty ranges. At present, the extent of any such biases, in specific reconstructions and as indicated by pseudo proxy studies, is uncertain. It is certainly model dependent (with regard to the choice of statistical regression model and to the choice of climate model simulation used to provide the pseudo proxies). It is not likely that any bias would be as large as the factor of 2 suggested by von Storch et al., (2004) with regard to the reconstruction by Mann et al., (1998), as discussed by Burger and Cubash (2005) and Wahl and Ritson (accepted). However, the bias will depend on the degree to which past climate departs from the range of temperatures encompassed within the calibration period data (Mann et al., 2005a; Osborn and Briffa, 2006) and on the proportions of temperature variability occurring on short and long time scales (Osborn and Briffa, 2004). In any case, this bias would act to damp the amplitude of reconstructed departures that are further from the calibration period mean, so that in the reconstructions depicted in Figures 6.10b,c (except those of Pollack and Smerdon (2004) and Oerlemans (2005), which did not require calibration in the same sense, and Hegerl et al. (in press), which is based on total least squares regression), temperatures during cooler periods may have been colder than estimated, while periods with comparable temperatures would be largely unbiased. As only one reconstruction (Moberg et al., 2005) shows an early period that is noticeably warmer than the mean for the calibration period, the possibility of a bias does not affect the general conclusion about the relative warmth of the twentieth century based on these data.

The weight of current multi-proxy evidence, therefore, suggests greater 20th century warmth in comparison with temperature levels of the previous 400 years, than was shown in the TAR. On the evidence of the few new reconstructions that reach back across most, or all, of the last two millennia, it is likely that the 20th century was the warmest in at least the past 1300 years.

6.6.1.2 What do large-scale temperature histories from ground surface temperature measurements tell us?

Hemispheric or global ground surface temperature (GST) histories reconstructed from measurements of subsurface temperatures in continental boreholes have been presented by several geothermal research groups (Huang et al., 2000; Harris and Chapman, 2001; Beltrami, 2002; Beltrami and Bourlon, 2004; Pollack and Smerdon, 2004) see Pollack and Huang, (2000) for a review of this methodology). These borehole reconstructions have been derived using the contents of a publicly-available database of borehole temperatures and climate reconstructions (Huang and Pollack, 1998) that in 2004 included 695 sites in the Northern Hemisphere and 166 in the Southern Hemisphere (Figure 6.11). Because the solid Earth acts as a low-pass filter on downward-propagating temperature signals, borehole reconstructions lack annual resolution; accordingly they typically portray only multi-decadal to centennial changes. These geothermal reconstructions provide independent estimates of surface temperature history with which to compare other multiproxy reconstructions. Figure 6.10b shows a reconstruction of average Northern Hemisphere GST by Pollack and Smerdon (2004). This reconstruction, very similar to that presented by Huang et al. (2000), shows an overall warming of the ground surface of about 1.0 ºC over the past five centuries. The two standard error uncertainties for their series (not shown here) are 0.20 (in 1500), 0.10 (1800) and 0.04 (1900) ºC. These are errors associated with various scales of areal weighting and consequent suppression of site-specific noise through aggregation (Pollack and Smerdon, 2004). The reconstruction is similar to the cooler multiproxy reconstructions in the 16th and 17th centuries but sits in the middle of the multiproxy range in the 19th and early 20th centuries. A geospatial analysis of the Huang et al. (2000) results by Mann et al.(2003) (see correction by Rutherford and Mann, 2004) argued for significantly less overall warming, a conclusion contested by Pollack and Smerdon (2004). Geothermal reconstructions yield somewhat muted estimates of the 20th-century trend, because about half of the borehole sites at the time of measurement had not yet been exposed to the significant warming of the last two decades of the 20th century.

The assumption that the reconstructed GST history is a good representation of the SAT history has been examined both with observational data and model studies. SAT and GST observations display differences at daily and seasonal time-scales, and indicate that the coupling of SAT and GST over a single year is complex (Sokratov and Barry, 2002; Stieglitz et al., 2003; Bartlett et al., 2004; Smerdon et al., in press). The mean annual GST differs from the mean annual SAT in regions where there is snow cover and/or seasonal freezing and thawing (Gosnold et al., 1997; Smerdon et al., 2004), as well as in regions without those effects (Smerdon et al., in press). Observational time-series of ground temperatures are not long enough to establish whether the mean annual differences are stable over long time-scales. The long-term coupling between SAT and GST has been addressed by simulating both air and soil temperatures in global three-dimensional coupled climate models. Mann and Schmidt (2003), in a 50-year experiment using the GISS Model E suggested that GST reconstructions may be biased by seasonal influences and snow cover variability, an interpretation contested by Chapman et al (2004). Thousand year simulations by Gonzalez-Rouco et al.

(2003; 2006) using the ECHO-G model suggest that seasonal differences in coupling are of little significance over long time-scales. They also indicate that deep soil temperature is a good proxy for the annual SAT on continents and that the spatial array of borehole locations is adequate to reconstruct the Northern Hemisphere mean SAT. Neither of these climate models included time-varying vegetation cover.

6.6.2 Southern Hemisphere Temperature Variability

There are markedly fewer well-dated proxy records for the SH compared to the NH (Figure 6.11), and consequently little evidence of how large-scale average surface temperatures have changed over the past few thousand years. Mann and Jones (2003) used only three series to represent annual mean Southern Hemisphere temperature change over the last 1500 years. A weighted combination of the individual standardized series was scaled to match (at decadal timescales) the mean and the standard deviation of Southern Hemisphere annual mean land-and-marine temperatures over the period 1856–1980. The recent proxy-based temperature estimates, up to the end of the reconstruction in 1980, do not capture the full magnitude of the warming seen in the instrumental temperature record. Earlier periods, around AD 700 and 1000, are reconstructed as warmer than the estimated level in the 20th century, and may have been as warm as the measured values in the last 20 years. The paucity of Southern Hemisphere proxy data also means that uncertainties associated with hemispheric temperature estimates are much greater than for the Northern Hemisphere, and it is more appropriate at this time to consider the evidence in terms of limited regional indicators of temperature change (Figure 6.12).

[INSERT FIGURE 6.12 HERE]

The long-term oscillations in warm-season temperatures shown in a tree-ring reconstruction for Tasmania (Cook et al., 2000) suggest that the last 30 years was the warmest multi-decadal period in the last 1000 years but only by a marginal degree. Conditions were generally warm over a longer period from 1300 to 1500 (Figure 6.12). Another tree-ring reconstruction, of austral summer temperatures based on data from South Island, New Zealand, spans the past 1100 years and is the longest yet produced for the region (Cook et al., 2002b). Disturbance at the site from which the trees were sampled restricts the calibration of this record to the 70 years up until 1950, but both tree-rings and instrumental data indicate that the 20th century was not anomalously warm when compared to several warm periods reconstructed in the last 1000 years (around the mid 12th and early 13th centuries and at around 1500).

Tree-ring based temperature reconstructions across the Southern Andes (37–55°S) of South America indicate that the annual temperatures during the 20th century have been anomalously warm in the context of the past four centuries (Figure 6.12). The mean annual temperatures for northern and southern Patagonia during the interval 1900–1990 are 0.53°C and 0.86°C above the 1640–1899 means, respectively. In Southern Patagonia, the year 1998 was the warmest of the past four centuries (Villalba et al., 2003). The rate of temperature increase from 1850 to 1920 was the highest over the past 360 years.

Figure 6.12 also shows the evidence of ground surface temperature changes over the last 500 years, provided by regionally aggregated borehole temperature inversions (Figure 6.11), from southern Africa (92 records) and Australia (57 records). Within the limitations of their resolvable temporal resolution, these both indicate unusually warm conditions prevailing in the 20th century (Pollack and Smerdon, 2004). The instrumental records for these areas show warmer conditions that post-date the time when the boreholes were logged; thus, the most recent warming is no registered in the borehole curves.

Taken together, the very sparse evidence for Southern Hemisphere temperatures prior to the period of instrumental records indicates that warming is occurring in some regions. However, more proxy data are required to verify the apparent warm trend.

6.6.3 Paleoclimate Model-Data Comparisons

A range of increasingly complex climate models have been used to simulate Northern Hemisphere temperatures over the last 500 to 1000 years using both natural and anthropogenic forcings (Figure 6.13). These models include an energy balance formulation (Crowley et al., 2003), two- and three- dimensional, reduced complexity models (Bertrand et al., 2002b; Bauer et al., 2003; Gerber et al., 2003), and three fully coupled ocean-atmosphere general circulation models (Ammann et al., 2003; Von Storch et al., 2004; Tett et al., accepted).

Comparison and evaluation of the output from paleoclimate simulations is complicated by their use of different historical forcings, as well as by the way indirect evidence of the history of various forcings is translated into geographically and seasonally specific radiative inputs within the models. Some factors, such as orbital variations of the Earth in relation to the Sun can be calculated accurately (e.g., Berger, 1977; Bradley et al., 2003b), and also directly implemented in terms of regional and seasonal insolation. For the last 2000 years, although this forcing is incorporated in most models, its impact on climate can be neglected compared to the other forcings (Bertrand et al., 2002b).

[INSERT FIGURE 6.13 HERE]

[INSERT TABLE 6.2 HERE]

[INSERT TABLE 6.3 HERE]

Over recent millennia, the analysis of the gas bubbles in high-deposition-rate ice cores provides good evidence of greenhouse gas changes at near decadal resolution (Figure 6.4). Other factors, such as land-use changes (Ramankutty and Foley, 1999), and the concentrations and distribution of tropospheric aerosols and ozone, are not as well known (Mickley et al., 2001). However, because of their magnitude, uncertainties in the history of solar irradiance and volcanic effects are more significant for the preindustrial period.

6.6.3.1 Solar forcing

The direct measurement of solar irradiance by satellite began less than 30 years ago, and over this period only very small changes are apparent (0.1% between the peak and trough of recent sunspot cycles which equates to only ~0.2 W m^{-2} change in radiative forcing; Fröhlich and Lean (2004); see also Chapter 2). Earlier extensions of irradiance change used in most model simulations are estimated by assuming a direct correlation with evidence of changing sunspot numbers and cosmogenic isotope production as recorded in ice cores (^{10}Be) and tree rings (^{14}C) (Lean et al., 1995; Crowley, 2000).

There is general agreement in the evolution of the different proxy records of solar activity such as cosmogenic isotopes, sunspot numbers or aurora observations, and the annually-resolved records clearly depict the well-known 11-year solar cycle (Muscheler et al., accepted). For example, paleoclimatic ^{10}Be and ^{14}C values are higher during times of low or absent sunspot numbers. During these periods, their production is high as the shielding of the Earth's atmosphere from cosmic rays provided by the Sun's open magnetic field is weak (Beer et al., 1998). However, the relationship between the isotopic records indicative of the Sun's open magnetic field, sunspot numbers, and the Sun's closed magnetic field or energy output is not fully understood (Wang and Sheeley, 2003).

The cosmogenic isotope records have been scaled linearly to estimate solar energy output (Bard et al., 2000) in many climate simulations. More recent studies utilize physics-based models to estimate solar activity from the production rate of cosmogenic isotopes taking into account non-linearities between isotope production and the Sun's open magnetic flux and variations in the geomagnetic field (Solanki et al., 2004; Muscheler et al., 2005). Following this approach, Solanki et al. (2004) suggest that the current level of solar activity has been without precedent over the last 8000 years. An even more recent analysis linking the isotope proxy records to instrumental data identifies, for the last millennium, three periods (AD 1777–1795, 1599–1605, 1137–1146) when solar activity was as high, or higher, than in the satellite era (Muscheler et al., 2005).

The magnitude of the long-term trend in solar irradiance remains uncertain. A reassessment of the stellar data (Hall and Lockwood, 2004) has been unable to confirm or refute the analysis by (Baliunas and Jastrow, 1990) that implied significant long-term solar irradiance changes, and also underpinned some of the earlier reconstructions (see Chapter 2). Several new studies (Lean et al., 2002; Foster, 2004; Foukal et al., 2004; Y.M. Wang et al., 2005) suggest that long-term irradiance changes were notably less than in earlier reconstructions (Hoyt and Schatten, 1993; Lean et al., 1995; Lockwood and Stamper, 1999; Bard et al., 2000; Fligge and Solanki, 2000; Lean, 2000) that were employed in a number of IPCC TAR climate change simulations and in many of the simulations shown in Figure 6.13d.

In the previous reconstructions, the seventeenth century "Maunder Minimum" total irradiance was 0.15% to 0.65% (irradiance change: ~2.0 to 8.7 W m^{-2}; radiative forcing: ~0.36 to 1.55 W m^{-2}) below the present-day mean (Figure 6.13b). Most of the recent studies (with the exception of Solanki and Krivova, 2003) calculate a reduction of only around 0.1% (irradiance change on the order of –1 W m^{-2}, radiative forcing of –0.2 W m^{-2}) (see Chapter 2). Following these results the magnitude of the radiative forcing used in Chapter 9 for the Maunder Minimum period is relatively small (–0.2 W m^{-2} relative to today).

6.6.3.2 Volcanic forcing

There is also uncertainty in the estimates of volcanic forcing during recent millennia because of the necessity to infer atmospheric optical depth changes (including geographic details as well as temporal accuracy and persistence), where there is only indirect evidence in the form of levels of acidity and sulfate measured in ice cores (Figure 6.14). All of the volcanic histories used in current model-based paleoclimate simulations are based on analyses of polar ice cores containing minor dating uncertainty and obvious geographical bias.

The considerable difficulties in calculating hemispheric and regional volcanic forcing changes (Robock and Free, 1995; Robertson et al., 2001; Crowley et al., 2003) result from sensitivity to the choice of which ice cores are considered, assumptions as to the extent of stratosphere penetration by eruption products, and the radiative properties of different volcanic aerosols and their residence time in the stratosphere. Even after producing some record of volcanic activity, there are major differences in the way models implement this. Some use a direct reduction in global radiative forcing with no altitudinal or spatial discrimination, while other models prescribe geographical changes in radiative forcing (Crowley et al., 2003; Von Storch et al., 2004; Goosse et al., 2005a). Models with more sophisticated radiative schemes are able to incorporate prescribed aerosol optical depth changes, and also interactively calculate the perturbed (long and short wave) radiation budgets (Tett et al., accepted). The effective level of (prescribed or diagnosed) volcanic forcing therefore varies considerably between the simulations (Figure 6.13a).

6.6.3.3 Industrial Era sulfate aerosols

Ice core data from Greenland and the middle latitudes of the Northern Hemisphere (Fischer et al., 1998; Bigler et al., 2002; Mieding, 2005) provide evidence of the rapid increase in sulfur dioxide emissions, above the pre-industrial background, during the modern Industrial Era as well as a very recent decline in emissions (Figure 6.14). The changes of the sulfate concentrations in these NH ice cores parallels the evolution of sulfur dioxide emissions estimated for North America, Europe and the Northern Hemisphere (Stern, 2005). Sulfate aerosol deposition did not change in ice cores from Antarctica, remote from anthropogenic sulfur dioxide sources. The records are indicative of the regional-to-hemispheric scale atmospheric burden of sulfate aerosols. Tropospheric sulfate aerosol loading varies regionally as aerosols have a typical lifetime of weeks in the troposphere. In recent years, sulfur dioxide emissions and sulfate aerosol loading shows a decrease, in response to emission control measures implemented as a result of the concern about the health impact of air pollution.

In general, tropospheric sulfate aerosols exert a negative forcing (cause cooling), and their increase over the Industrial Era has offset part of the positive forcing by greenhouse gases and certain heat absorbing aerosols (see Chapter 2). The cooling effect of tropospheric sulfate is reducing with recent diminishing emissions of sulfur dioxide.

6.6.3.4 Comparing Simulations of Northern Hemisphere Mean Temperatures with Paleoclimatic Observations

Various simulations of Northern Hemisphere (mean land and marine) surface temperatures produced by a range of climate models, and the forcings that were used to drive them, are shown in Figure 6.13. Despite differences in the detail and implementation of the different forcing histories, there is generally good qualitative agreement between the simulations as regards the major features: warmth during much of the 12th through 14th centuries, with lower temperatures being sustained during the 17th, mid 15th and early 19th centuries, and the subsequent sharp rise to unprecedented levels of warmth at the end of the 20th century. The spread of this multi-model ensemble is constrained to be small during the 1500–1899 reference period (selected following Osborn et al. (in press)), but the model spread also remains small back to 1000, with the exception of the ECHO-G simulation (Von Storch et al., 2004). The implications of the greater model spread in the rates of warming after 1840 will be clear only after determining the extent to which it can be attributed to differences in prescribed forcings and individual model sensitivities (Goosse et al., 2005b). The ECHO-G simulation (dotted red line in Figure 6.11d) is atypical compared to the ensemble as a whole, being notably warmer in the pre-1300 and post-1900 periods. Osborn et al. (in press) show that these anomalies are likely the result of a large initial disequilibrium and the lack of anthropogenic tropospheric aerosols in that simulation (see Figure 6.13c). One other simulation (Gonzalez-Rouco et al., 2006) also exhibits greater early 20th-century warming in comparison to the other simulations but, similarly, does not include troposheric aerosols among the forcings. All of these simulations, therefore, appear to be consistent with the available evidence from reconstructions of past Northern Hemisphere temperatures, for which the evidence (taken from Figure 6.10c) is shown by the grey shading underlying the simulations in Figure 6.13d.

It is important to note that many of the simulated temperature variations during the pre-industrial time period shown in Figure 6.13 have been driven by assumed solar forcing, the magnitude of which is currently in doubt. Therefore, although the data and simulations appear consistent at this hemispheric scale, they are not a powerful test of the models because of the large uncertainty in both the reconstructed Northern Hemisphere changes and the total radiative forcing. The influence on simulated NH surface temperature, of solar irradiance variability and anthropogenic forcings, is further illustrated in Figure 6.13e. A range of Earth System Models of Intermediate Complexity (EMICSs: Petoukhov et al., 2000; Plattner et al., 2001; Montoya et al., 2005) were forced with two different reconstructions of solar irradiance (Bard et al., 2000; Y.M. Wang et al., 2005) to compare the influence of large versus small changes in the long-term strength of solar irradiance over the last 1000 years.

Radiative forcing related to explosive volcanism (Crowley, 2000), atmospheric CO_2 and other anthropogenic agents (Joos et al., 2001) were identically prescribed within each model simulation. Additional simulations, in which anthropogenic forcings were not included, enable a comparison to be made between 'natural' versus 'all' (i.e., natural plus anthropogenic) forcings on the evolution of hemispheric temperatures before and during the 20th century.

The alternative solar irradiance histories used in the simulations differ in their low-frequency amplitudes by a factor of about 3. The 'high-amplitude' case (strong solar irradiance forcing) corresponds roughly with the level of irradiance change assumed in many of the simulations shown in Figure 6.13b, whereas the 'low-amplitude' case (weaker solar irradiance forcing) is representative of the more recent reconstructions of solar irradiance changes (as discussed in Section 6.6.3). The high-amplitude forcing history is based on an ice-core record of ^{10}Be scaled to give an average reduction in solar irradiance of 0.25% during the Maunder Minimum, as compared to today (Bard et al., 2000). The low-amplitude history is estimated using sunspot data and a model of the Sun's closed magnetic flux for the period from 1610 to the present (Y.M. Wang et al., 2005), with an earlier extension based on the Bard et al. (2000) record scaled to a Maunder Minimum reduction of 0.08% compared to today. The low-frequency evolution of the two reconstructions is very similar even though they are based on completely independent sources of observational data (sunspots versus cosmogenic isotopes) and are produced differently (simple linear scaling versus modelled Sun's magnetic flux) after 1610.

The EMIC simulations shown in Figure 6.13e, like those in Figure 6.13d, fall within the range of proxy-based Northern Hemispheric temperature reconstructions shown in Figure 6.11c and are compatible with reconstructed and observed 20th century warming only when anthropogenic forcings are incorporated. The standard deviation of multi-decadal variability in NH surface air temperature is greater by 0.04 to 0.07°C for the stronger solar forcing (Bard25) compared to the weaker solar forcing (Bard08-WLS).

The uncertainty associated with the proxy-based temperature reconstructions and climate sensitivity of the models is too large to establish which of the two solar irradiance histories is the most likely, on the basis of these simulations.

However, in the simulations that do not include anthropogenic forcing, NH temperatures reach a peak in the middle of the 20th century, and decrease afterwards, for both the strong and weak solar irradiance cases. This suggests that the contribution of natural forcing to observed 20th century warming is small and that solar and volcanic forcings are not responsible for the degree of warmth that occurred in the second half of the 20th century, consistent with the evidence of earlier work based on simple and more complex climate models

(Crowley and Lowery, 2000; Bertrand et al., 2002b; Gerber et al., 2003; Tett et al., accepted; Hegerl et al., in press) (see also Chapter 9).

An overall conclusion can be drawn from the available instrumental and proxy evidence for the history of hemispheric average temperature change over the last 500 to 2000 years, as well as the modeling studies exploring the possible roles of various causal factors: that is, greenhouse gases must be included among the forcings in order to simulate hemispheric mean temperatures that are compatible with the evidence of unusual warmth observed in the second half of the 20th century.

6.6.4 Consistency Between the Temperature, Greenhouse Gas, and Forcing Records and Compatibility of Coupled Carbon Cycle – Climate Models with the Proxy Records

It is difficult to constrain the climate sensitivity from the proxy records of the last millennium (see Chapter 9). As noted above, the evidence for hemispheric temperature change as interpreted from the different proxy records, and for atmospheric trace greenhouse gases, inferred solar forcing, and reconstructed volcanic forcing, is to varying degrees uncertain. The available temperature reconstructions suggest that decadally-averaged Northern Hemisphere temperatures varied within 1°C or less during the two millennia preceding the 20th century (Figure 6.10), but the magnitude of the reconstructed low-frequency variations differs by up to about a factor of two for different reconstructions. The reconstructions of natural forcings (solar and volcanic) are uncertain for this period. If they produced substantial negative energy balances (reduced solar, increased volcanic activity), then low-to-medium estimates of climate sensitivity are compatible with the reconstructed temperature variations (Figure 6.10); however, if solar and volcanic forcing varied only weakly, then moderate-to-high climate sensitivity would be consistent with the temperature reconstructions, especially those showing larger cooling (see also Chapter 9), assuming that the sensitivity of the climate system to solar irradiance changes and explosive volcanism is not different than for changes in greenhouse gases or other forcing agents.

The greenhouse gas record provides indirect evidence for a limited range of low-frequency, hemispheric-scale climate variations over the last two millennia prior to the period of industrialisation (AD 1–1750). The greenhouse gas histories of CO_2, CH_4, and N_2O, show only small changes over this time period (MacFarling Meure, 2004; Siegenthaler et al., 2005a) (Figure 6.4), although, there is evidence from the ice core record (Figures 6.3 and 6.7) and from models that greenhouse gas concentrations react sensitively to climatic changes.

The sensitivity of atmospheric CO_2 to climatic changes as simulated by coupled carbon cycle-climate models is broadly consistent with the ice core CO_2 record and the amplitudes of the preindustrial, decadal-scale Northern Hemisphere temperature changes in the proxy-based reconstructions (Joos and Prentice, 2004). The CO_2-climate sensitivity can be formally defined as the change in atmospheric CO_2 relative to a nominal change in NH temperature in units of ppm/°C. Its strength depends on several factors, including the change in solubility of CO_2 in seawater, and the responses of productivity and heterotrophic respiration on land to temperature and precipitation. The sensitivity was estimated for modest (NH temperature change $<\sim 1$°C) temperature variations from simulations with the Bern Carbon Cycle-Climate model driven with solar and volcanic forcing over the last millennium (Gerber et al., 2003) and from simulations with the range of models participating in the coupled carbon cycle-climate model intercomparison project (C4MIP) over the industrial period (Friedlingstein et al., in press). The range of the CO_2-climate sensitivity is 4 to 16 ppm/°C for the ten models participating in the C4MIP intercomparison (evaluated as the difference in atmospheric CO_2 for the 1990 decade between a simulation with, and without, climate change, divided by the increase in NH temperature from the 1860 decade to the 1990 decade). This is comparable to a range of 10 to 17 ppm/°C obtained for CO_2 variations in the range of 6 to 10 ppm (Etheridge et al., 1996; MacFarling Meure, 2004; Siegenthaler et al., 2005a) and assuming that (decadally-averaged) NH temperature varied within 0.6°C.

6.6.5 Regional Variability in Quantities Other than Temperature

6.6.5.1 Changes in the El Niño-Southern Oscillation (ENSO) system

Considerable interest in the El Niño-Southern Oscillation (ENSO) system has encouraged numerous attempts at its paleoclimatic reconstruction. These include a boreal winter (December-February) reconstruction of the

Southern Oscillation Index (SOI) based on ENSO-sensitive tree ring indicators (Stahle et al., 1998), two multiproxy reconstructions of annual and October-March Niño-3 index (average SST anomalies over 5°N–5°S, 150°W–90°W (Mann et al., 2005b; Mann et al., 2005a), and a tropical coral-based Niño 3.4 SST reconstruction (Evans et al., 2002). Fossil coral records from Palmyra Island in the tropical Pacific also provide 30–150-year windows of ENSO variability within the last 1100 years (Cobb et al., 2003). Finally, a new 600-yr reconstruction of December–February Niño-3 SST has recently been developed (D'Arrigo et al., 2005), which is considerably longer than previous series. These reconstructions share significant common variance (typically more than 30% during their respective cross-validation periods), suggesting a relatively consistent history of El Niño in past centuries (Jones and Mann, 2004). In most coral records from western Pacific and the Indian Oceans, late 20th-century warmth is unprecedented over the past 100–300 years (Cole, 2003). In addition, reconstructions of extratropical temperatures and atmospheric circulation features (e.g., the North Pacific Index) correlate significantly with tropical estimates, supporting evidence for tropical/high-latitude Pacific links during the past 3–4 centuries (Evans et al., 2002; Linsley et al., 2004; D'Arrigo et al., 2006).

Several coral and tree-ring studies indicate that interannual ENSO weakened during the cooler and drier late 19th century (i.e., in the central Pacific), while decadal variability intensified, suggesting that the frequency-domain characteristics of ENSO are sensitive to background conditions (Urban et al., 2000). The superposition of the late 20th-century warming trend on interannual variability has led to increasingly warm/wet ENSO events in the central Pacific during recent decades.

ENSO may have responded to radiative forcing induced by solar and volcanic variations over the past millennium (Adams et al., 2003; Mann et al., 2005b). Model simulations support a statistically significant response of ENSO to radiative changes such that during higher radiative inputs, La Niña-like conditions result from an intensified zonal SST gradient that drives stronger trade winds, and vice versa (Mann et al., 2005b). Comparing data and model results over the past millennium suggests that warmer background conditions are associated with higher variability (Cane, 2005). Numerical experiments suggest that the dynamics of ENSO may have played an important role in the climatic response to past changes in radiative forcing (Mann et al., 2005a). Indeed, the low-frequency changes in both amplitude of variability and mean state indicated by ENSO reconstructions from Palmyra corals (Cobb et al., 2003) were found to correspond well with the model responses to changes in tropical volcanic radiative forcing over the past 1000 years, with solar forcing playing a secondary role.

Proxy records suggest that ENSO's global climate imprint evolves over time, complicating predictions. Comparisons of ENSO and drought indices clearly show changes in the linkage between ENSO and U.S. moisture balance over the past 150 years. Significant ENSO-drought correlations occur consistently in the southwest U.S., but the strength of moisture penetration into the continent varies substantially over time (Cole and Cook, 1998; Cook et al., 2000). Comparing reconstructed Niño 3 SST with global temperature patterns suggests that some features are robust through time, such as the warming in the eastern tropical Pacific and western coasts of North and South America, whereas teleconnections into North America, the Atlantic and Eurasia are variable (Mann et al., 2000). The spatial correlation pattern for the period 1801–1850 provides striking evidence of nonstationarity in ENSO teleconnections, showing a distinct absence of the typical pattern of tropical Pacific warming (Mann et al., 2000).

6.6.5.2 *The record of past Atlantic variability*

Climate variations over the North Atlantic are related to changes in the North Atlantic Oscillation (NAO; (Hurrell, 1995) and the Atlantic Multidecadal Oscillation (Delworth and Mann, 2000; Sutton and Hodson, 2005). From 1980 to 1995, the NAO tended to remain in one extreme phase and accounted for a substantial part of the wintertime warming over Europe and northern Eurasia. The North Atlantic region has a unique combination of long instrumental observations, many documentary records and multiple sources of proxy records. However, it still remains difficult to document past variations in the dominant modes of climate variability in the region, including NAO, due to problems of establishing proxies for atmospheric pressure, as well as the lack of stationarity in the NAO frequency and in storm tracks. Several reconstructions of NAO have been proposed (Cook et al., 2002a; Cullen et al., 2002; Luterbacher et al., 2002). Although the reconstructions differ in many aspects, there is a general tendency for more negative NAO during the 17th and 18th centuries than in the 20th century, thus indicating that the colder mean climate was characterized by a less zonal atmospheric pattern than in the 20th century. The coldest reconstructed European winter in

1708/1709, and the strong warming trend between 1684 and 1738 (+0.32°C per decade), have been related to a negative NAO index and the NAO response to increasing radiative forcing, respectively (Luterbacher et al., 2004). Some spatially-resolved simulations employing GCMs indicate that solar and volcanic forcings lead to continental warming associated with a shift toward a high NAO index (Shindell et al., 2001; Shindell et al., 2003; Shindell et al., 2004; Stendel et al., 2006). Increased solar irradiance at the end of the 17th century and through the first half of the 18th century might have induced such a shift toward a high NAO index (Luterbacher et al., 2004).
It is well known that NAO exerts a dominant influence on wintertime temperature and precipitation over Europe, but the strength of the relationship can change over time and region (Jones et al., 2003). The strong trend towards a more positive NAO in the early part of the 18th century in the (Luterbacher et al., 2002) NAO-reconstruction appears connected with positive winter precipitation anomalies over NW Europe and marked expansions of maritime glaciers in a manner similar to the effect of positive winter precipitation anomalies over the recent decades for the same glaciers (Nesje and Dahl, 2003).

6.6.5.3 Asian monsoon variability

In China, in a region dominated by the East Asian Monsoon, it appears that 15 severe (3 years or longer) droughts have occurred over the last 1000 years, and for poorly understood reasons (Zhang, 2005). These paleodroughts were generally more severe than droughts in the same region within the last 50 years. Another intriguing finding is that the South Asian (Indian) monsoon has, in the drier areas of its influence, recently reversed its millennia-long orbitally-driven low-frequency trend toward less rainfall. This recent reversal in monsoon rainfall also appears to coincide with a synchronous increase in inferred monsoon winds over the western Arabian Sea (Anderson et al., 2002), a change that could be related to increased summer heating over and around the Tibetan Plateau (Brauning and Mantwill, 2004; Morrill et al., 2006).

6.6.5.4 Northern and eastern Africa hydrologic variability

Lake sediment and historical documentary evidence indicates that northern Africa and the Sahel region have for a long time experienced substantial droughts lasting from decades to centuries (Kadomura, 1992; Verschuren, 2001; Russell et al., 2003; Stager et al., 2003; Nguetsop et al., 2004; Brooks et al., 2005; Stager et al., 2005). Although there have been attempts to link these dry periods to solar variations, the evidence is not conclusive (Stager et al., 2005), particularly given that the relationship between hypothesized solar proxies and variation in total solar irradiance remains unclear (see Section 6.6.3). The paleoclimate record indicates that persistent droughts have been a common feature of climate in northern and eastern Africa. However, it has not been demonstrated that these droughts can be simulated with coupled ocean-atmosphere models.

6.6.5.5 The record of North American hydrologic variability and change

Multiple proxies, including tree-rings, sediments, historical documents, and lake sediment records make it clear that the past 2000 years included periods with more frequent, longer and/or geographically more extensive drought in North America (Stahle and Cleaveland, 1992; Stahle et al., 1998; Woodhouse and Overpeck, 1998; Forman et al., 2001; Cook et al., 2004b; Hodell et al., 2005; MacDonald and Case, 2005). Past droughts, including decadal-length “megadrought” (Woodhouse and Overpeck, 1998) are most likely due to extended periods of anomalous SST (Hoerling and Kumar, 2003; Schubert et al., 2004; MacDonald and Case, 2005; Seager et al., 2005) but still remain difficult to simulate with coupled ocean-atmosphere models. Thus, the paleoclimatic record suggests that multi-year, decadal, and even century-scale drier periods are likely to remain a feature of future North American climate, particularly in the area to the west of the Mississippi River.

There is some evidence that North American drought was more regionally extensive, severe and frequent during past intervals that were characterized by warmer than average Northern Hemisphere summer temperatures (e.g., during medieval times and the mid-Holocene (Forman et al., 2001; Cook et al., 2004b)).

There is evidence that changes in the North American hydrologic regime can occur abruptly relative to the rate of change in climate forcing and duration of the subsequent climate regime. Abrupt shifts in drought frequency and duration have been found in paleohydrologic records from western North America (Cumming et al., 2002; Laird et al., 2003; Cook et al., 2004b). Similarly, the Upper Mississippi River basin and elsewhere have seen abrupt shifts in the frequency and size of the largest flood events (Knox, 2000). Recent investigations of past large-hurricane activity in the southeast United States suggests that changes in the frequency of large hurricanes can shift abruptly in response to more gradual forcing (Liu, 2004). Although the paleoclimatic record indicates that hydrologic shifts in drought, floods and tropical storms have occurred abruptly (i.e., within years), this past abrupt change has not been simulated with coupled atmosphere ocean models.

6.7 Robust Findings and Key Uncertainties

Observations of Changes in Climate	
Robust Findings	***Key Uncertainties***
Post-industrial levels of atmospheric carbon dioxide and methane have risen far above the natural variability found in the longest (up to 650,000 years) ice-core records. The present average rate of increase in radiative forcing from carbon dioxide, methane and nitrous oxide is larger than at any time during the past 20,000 years. Global sea level rise due to primarily to ice sheet retreat likely exceeded 4 m the last time the Arctic was 3 to 4°C warmer than present. A number of abrupt climate events of the past are very likely linked to changes in the Atlantic Ocean circulation and had global implications. There is no evidence for a natural interglacial climate cycle that could explain recent global warming, or that the current warming will be mitigated by a natural cooling trend. Biogeochemical and biogeophysical feedbacks have amplified climatic changes in the past and are likely to do so in the future. It is very likely that average Northern Hemisphere temperatures during the second half of the 20th century were warmer than any other 50-year period in the last 500 years; it is also likely that this was the warmest 50-period in the past 1300 years. Droughts lasting decades to centuries are a recurrent feature of climate in North America and northern Africa under a wide range of climate forcing. Models are capable of simulating climate and vegetation change for past periods of very different forcings and climate.	A comprehensive mechanistic explanation of the observed glacial-interglacial variations in climate and greenhouse gases remains to be articulated. The mechanisms of abrupt climate change (for example, in ocean circulation and drought frequency) are not well understood, nor are the key climate thresholds that, when crossed, could trigger an acceleration in regional climate change. The ability of climate models to simulate realistic abrupt change in ocean circulation, drought frequency, flood frequency, El Niño-Southern Oscillation behaviour, and monsoon strength is uncertain. The rates and processes by which ice sheets disintegrated in the past are not well known. Knowledge of climate variability over the last 1000 years in the Southern Hemisphere and tropics is severely limited by the lack of paleoclimatic records. The differing amplitudes observed in available millennial-length Northern Hemisphere temperature reconstructions, and the relation of these differences to choice of proxy data and statistical calibration methods, needs to be reconciled. The lack of extensive networks of proxy data that run right up to the present day means that we are not able to measure how well they respond to the rapid global warming observed in the last 20 years. This also restricts our ability to investigate whether other environmental changes are biasing the climate response of proxies in recent decades.

References

Adams, J.B., M.E. Mann, and C.M. Ammann, 2003: Proxy evidence for an El Nino-like response to volcanic forcing. *Nature,* 426(6964), 274-278.

Adkins, J. F., K. McIntyre, et al. (2002). "The salinity, temperature, and δ^{18}O of the glacial deep ocean." Science 298: 1769-1773.

Adkinson, J.F., K. McIntyre, and S.D. P, 2002: The salinity, temperature, and delta O-18 of the glacial deep ocean. *Science,* 298, 1769-1773.

Alley, R. B. and A. M. Agustsdottir (2005). "The 8k event: cause and consequences of a major Holocene abrupt climate change." Quaternary Science Reviews 24: 1123-1149.

Alley, R.B., and P.U. Clark, 1999: The deglaciation of the northern hemisphere: A global perspective. *Annual Review of Earth and Planetary Sciences,* 27, 149-182.

Alley, R.B., J. Marotzke, W.D. Nordhaus, J.T. Overpeck, D.M. Peteet, R.A. Pielke, R.T. Pierrehumbert, P.B. Rhines, T.F. Stocker, L.D. Talley, and J.M. Wallace, 2003: Abrupt climate change. *Science,* 299(5615), 2005-2010.

Alley, R.B., P.A. Mayewski, T. Sowers, M. Stuiver, K.C. Taylor, and P.U. Clark, 1997: Holocene climatic instability : A large, widespread event 8200 years ago. *Geology,* 25, 483-486.

Alley, R.B., S. Anandakrishnan, and P. Jung, 2001: Stochastic resonance in the North Atlantic. *Paleoceanography,* 16, 190-198.

Alverson, K.D., R.S. Bradley, and T.F. Pedersen, 2003: *Paleoclimate, Global Change and the Future.* Global Change - The IGBP Series, 221 pp.

Ammann, C.M., G.A. Meehl, W.M. Washington, and C.S. Zender, 2003: A monthly and latitudinally varying volcanic forcing dataset in simulations of 20th century climate. *Geophysical Research Letters,* 30(12), art. no.-1657.

Andersen, C., N. Koç, A. Jennings, and J.T. Andrews, 2004: Non uniform response of the major surface currents in the Nordic Seas to insolation forcing : implications for the Holocene climate variability. *Paleoceanography,* 19, 1-16.

Anderson, D.M., J.T. Overpeck, and A.K. Gupta, 2002: Increase in the Asian southwest monsoon during the past four centuries. *Science,* 297(5581), 596-599.

Archer, D., and A. Ganopolski, 2005: A movable trigger: Fossil fuel CO2 and the onset of the next glaciation. *Geochemistry Geophysics Geosystems,* 6, Q05003.

Archer, D.A., A. Winguth, D. Lea, and N. Mahowald, 2000: What caused the glacial/interglacial atmospheric pCO_2 cycles? *Reviews of Geophysics,* 12, 159-189.

Ariztegui, D., Asioli A., Lowe J.J., Trincardi F., Vigliotti L., Tamburini F., Chondrogianni C., Accorsi C.A., Mazzanti M.B., Mercuri A.M., Van der Kaars S., McKenzie J.A., Oldfield F., 2000: Paleoclimate and the formation of sapropel S1: inferences from Late Quaternary lacustrine and marine sequences in the central Mediterranean region. *Palaeogeography, Palaeoclimatology, Palaeoecology,* 158, 215-240.

Augustin, L., C. Barbante, P.R.F. Barnes, J.M. Barnola, M. Bigler, E. Castellano, O. Cattani, J. Chappellaz, D. DahlJensen, B. Delmonte, G. Dreyfus, G. Durand, S. Falourd, H. Fischer, J. Fluckiger, M.E. Hansson, P. Huybrechts, R. Jugie, S.J. Johnsen, J. Jouzel, P. Kaufmann, J. Kipfstuhl, F. Lambert, V.Y. Lipenkov, G.V.C. Littot, A. Longinelli, R. Lorrain, V. Maggi, V. Masson-Delmotte, H. Miller, R. Mulvaney, J. Oerlemans, H. Oerter, G. Orombelli, F. Parrenin, D.A. Peel, J.R. Petit, D. Raynaud, C. Ritz, U. Ruth, J. Schwander, U. Siegenthaler, R. Souchez, B. Stauffer, J.P. Steffensen, B. Stenni, T.F. Stocker, I.E. Tabacco, R. Udisti, R.S.W. van de Wal, M. van den Broeke, J. Weiss, F. Wilhelms, J.G. Winther, E.W. Wolff, and M. Zucchelli, 2004: Eight glacial cycles from an Antarctic ice core. *Nature,* 429(6992), 623-628.

Bakke, J., S.O. Dahl, and A. Nesje, 2005c: Lateglacial and early Holocene palaeoclimatic reconstruction based on glacier fluctuations and equilibrium-line altitudes at northern Folgefonna, Hardanger, western Norway. *Journal of Quaternary Science,* 20(2), 179–198.

Bakke, J., S.O. Dahl, O. Paasche, R. Lovlie, and A. Nesje, 2005a: Glacier fluctuations, equilibrium-line altitudes and palaeoclimate in Lyngen, northern Norway, during the Lateglacial and Holocene. *Holocene,* 15(4), 518-540.

Baliunas, S., and R. Jastrow, 1990: Evidence for long-term brightness changes of solar-type stars. *Nature,* 348, 520-522,

Bao, Y., A. Brauning, and S. Yafeng, 2003: Late Holocene temperature fluctuations on the Tibetan Plateau. *Quaternary Science Reviews,* 22(21), 2335-2344(10).

Barber, D.C., A. Dyke, C. Hillaire-Marcel, A.E. Jennings, J.T. Andrews, M.W. Kerwin, G. Bilodeau, R. McNeely, J. Southon, and M.D. Morehead, 1999: Forcing of the cold event of 8,200 years ago by catastrophic drainage of Laurentide lakes. *Nature,* 400, 344-347.
Bard, E., G. Raisbeck, F. Yiou, and J. Jouzel, 2000: Solar irradiance during the last millennium based on cosmogenic nucleides. *Tellus,* 52B, 985-992.
Barrows, T.T., and S. Juggins, 2005: Sea-surface temperatures around the Australian margin and Indian Ocean during the Last Glacial Maximum. *Quaternary Science Reviews,* 24, 1017-1047.
Bartlett, M.G., D.S. Chapman, and R.N. Harris, 2004: Snow and the ground temperature record of climate change. *Journal of Geophysical Research- Earth Surface* 109 (F4): Art. No. F04008, doi:10.1029/2004JF000224.
Battle, M., M. Bender, T. Sowers, P.P. Tans, J.H. Butler, J.W. Elkins, J.T. Ellis, T. Conway, N. Zhang, P. Lang, and A.D. Clarke, 1996: Atmospheric gas concentrations over the past century measured in air from firn at the South Pole. *Nature,* 383(6597), 231-235.
Bauer, E., A. Ganopolski, and M. Montoya, 2004: Simulation of the cold climate event 8200 years ago by meltwater outburst from Lake Agassiz. *Paleoceanography,* 19, Art PA3014.
Bauer, E., M. Claussen, V. Brovkin, and A. Huenerbein, 2003: Assessing climate forcings of the Earth system for the past millennium. *Geophysical Research Letters,* 30(6), art. no.-1276.
Beer, J., S. Tobias, and N. Weiss, 1998: An active sun throughout the Maunder Minimum. *Solar Physics,* 181(1), 237-249.
Beerling, D.J., 1999: New estimates of carbon transfer to terrestrial ecosystems between the last glacial maximum and the Holocene. *Terra Nova,* 11(4), 162-167.
Beltrami, H., 2002: Paleoclimate: Earth's long-term memory. *Science,* 297(5579), 206-207.
Beltrami, H., and E. Bourlon, 2004: Ground warming patterns in the Northern Hemisphere during the last five centuries. *Earth and Planetary Science Letters,* 227(3-4), 169-177.
Berger, A., 1977: Long-Term Variations of Earths Orbital Elements. *Celestial Mechanics,* 15(1), 53-74.
Berger, A., 1978: Long-term variation of caloric solar radiation resulting from the Earth's orbital elements. *Quaternary Research,* 9, 139-167.
Berger, A., and M.F. Loutre, 2003: Climate 400,000 years ago, a key to the future? In: *Earth's Climate and orbital Eccentricity* [A.W. Droxler, R.Z. Poore, and L.H. Burckle (eds.)]. American Geophysical Union, Washington DC, pp. 17-26.
Berger, A.L., and M.F. Loutre, 1991: Insolation values for the climate of the last 10 million years. *Quaternary Science Reviews,* 10, 297-317.
Berger, A.L., and M.F. Loutre, 2002: An exceptionally long interglacial ahead? *Science,* 297, 1287-1288.
Berggren, W.A., D.V. Kent, C.C.I. Swisher, and M.P. Aubry, 1995: *Geochronology, Time Scales and Global Stratigraphic Correlation* Special Publication [W.A. Berggren (ed). Vol. 54. Society for Sedimentary Geology, Tulsa, 386 pp.
Berner, R.A., and Z. Kothavala, 2001: GEOCARB III: A revised model of atmospheric CO2 over phanerozoic time. *American Journal of Science,* 301(2), 182-204.
Bertrand, C., M.F. Loutre, and A. Berger, 2002a: High frequency variations of the Earth"s orbital parameters and climate change. *Geophysical Research Letters,* 29, doi:10.1029/2002GL015622.
Bertrand, C., M.F. Loutre, M. Crucifix, and A. Berger, 2002b: Climate of the last millennium: a sensitivity study. *Tellus Series a-Dynamic Meteorology and Oceanography,* 54(3), 221-244.
Bianchi, G., and I.N. McCave, 1999: Holocene periodicity in north Atlantic climate and deep ocean flow south of Iceland. *Nature,* 397, 515-518.
Bigelow, N., Brubaker LB, Edwards ME, Harrison SP, Prentice IC, Anderson PM, Andreev AA, Bartlein PJ, Christensen TR, Cramer W, Kaplan JO, Lozhkin AV, Matveyeva NV, Murray DF, McGuire AD, Razzhivin VY, Ritchie JC, Smith B, Walker DA, Gajewski K, Wolf V, Holmqvist BH, Igarashi Y, Kremenetskii K, Paus A, Pisaric MFJ, and V. VS, 2003: Climate change and Arctic ecosystems: 1. Vegetation changes north of 55 degrees N between the last glacial maximum, mid-Holocene, and present. *J. Geophys. Res.,* 108. doi:10.1029/2002JD002558.
Bigelow, N.H., et al., 2003: Climate change and Arctic ecosystems: 1. Vegetation changes north of 55 N between the last glacial maximum, mid-Holocene, and present. *Journal of Geophysical Research,* 108, 8170, doi:10.1029/2002JD002558.
Bigler, M., D. Wagenbach, H. Fischer, J. Kipfstuhl, H. Millar, S. Sommer, and B. Stauffer, 2002: Sulphate record from a northeast Greenland ice core over the last 1200 years based on continuous flow analysis. In: *Annals of Glaciology*. Vol. 35, pp. 250-256.

Billups, K., J.E.T. Channell, and J. Zachos, 2002: Late Oligocene to early Miocene geochronology and paleoceanography from the subantarctic South Atlantic. *Paleoceanography,* 17(1), *Art. No. 1004, 10.1029/2000PA000568.*
Bird, M.I., J. Lloyd, and G.D. Farquhar, 1994: Terrestrial Carbon Storage At The Lgm. *Nature,* 371(6498), 566-566.
Birks, H.H., and B. Ammann, 2000: Two terrestrial records of rapid climatic change during the glacial-Holocene transition (14,000-9,000 calender years B.P.) from Europe. *Proceedings of the National Academy of Science,* 97, 1390-1394.
Bjerknes, J., 1969: Atmospheric Teleconnections From Equatorial Pacific. *Monthly Weather Review,* 97(3), 163–172
Blunier, T., and E.J. Brook, 2001: Timing of millennial-scale climate change in Antarctica and Greenland during the last glacial period. *Science,* 291, 109-112.
Blunier, T., J. Chappellaz, J. Schwander, A. Dällenbach, B. Stauffer, T.F. Stocker, D. Raynaud, J. Jouzel, H.B. Clausen, C.U. Hammer, and J.S. Johnsen, 1998: Asynchrony of Antarctic and Greenland climate climate change during the last glacial period. *Nature,* 394, 739-743.
Blunier, T., J. Chappellaz, J. Schwander, B. Stauffer, and D. Raynaud, 1995: Variations in Atmospheric Methane Concentration During the Holocene Epoch. *Nature,* 374(6517), 46-49.
Blunier, T., J.A. Chappellaz, J. Schwander, J.M. Barnola, T. Desperts, B. Stauffer, and D. Raynaud, 1993: Atmospheric Methane, Record from a Greenland Ice Core over the Last 1000 Year. *Geophysical Research Letters,* 20(20), 2219-2222.
Bohaty, S.M., and J.C. Zachos, 2003: Significant Southern Ocean warming event in the late middle Eocene. *Geology,* 31(11), 1017-1020.
Bond, G., B. Kromer, J. Beer, R. Muscheler, M.N. Evans, W. Showers, S. Hoffmann, R. Lotti-Bond, I. Hajdas, and G. Bonani, 2001: Persistent solar influence on north Atlantic climate during the Holocene. *Science,* 294, 2130-2136.
Bond, G., W. Showers, M. Cheseby, R. Lotti, P. Almasi, P. deMenocal, P. Priore, H. Cullen, I. Hajdas, and G. Bonami, 1997: A pervasive millennial-scale cycle in the north atlantic Holocene and glacial climates. *Science,* 278, 1257-1266.
Bond, G., W.S. Broecker, S. Johnsen, J. McManus, L. Labeyrie, J. Jouzel, and G. Bonani, 1993: Correlations between climate records from North Atlantic sediments and Greenland ice. *Nature,* 365, 143-147.
Bond, W.J., G.F. Midgley, and F.I. Woodward, 2003: The importance of low atmospheric CO2 and fire in promoting the spread of grasslands and savannas. *Global Change Biology,* 9(7), 973-982.
Booth, R.K., S.T. Jackson, S.L. Forman, J.E. Kutzbach, E.A. Bettis, J. Kreig, and D.K. Wright, 2005: A severe centennial-scale drought in mid-continental North America 4200 years ago and apparent global linkages. *Holocene,* 15, 321-328.
Bopp, L., K.E. Kohlfeld, C. Le Quéré, and O. O. Aumont, 2002: Dust impact on marine biota and atmospheric CO_2 in glacial periods. *Geochimica Et Cosmochimica Acta 66 (15A): A91-A91 Suppl. 1, AUG 2002.*
Bowen, G.J., D.J. Beerling, P.L. Koch, J.C. Zachos, and T. Quattlebaum, 2004: A humid climate state during the Palaeocene/Eocene thermal maximum. *Nature,* 432(7016), 495-499.
Bowen, G.J., W.C. Clyde, P.L. Koch, S.Y. Ting, J. Alroy, T. Tsubamoto, Y.Q. Wang, and Y. Wang, 2002: Mammalian dispersal at the Paleocene/Eocene boundary. *Science,* 295(5562), 2062-2065.
Braconnot, P., S.P. Harrison, S. Joussaume, C.D. Hewitt, A. Kitoch, J.E. Kutzbach, Z. Liu, B. Otto-Bliesner, J. Syktus, and S.L. Weber, 2004: Evaluation of PMIP coupled ocean-atmosphere simulations of the Mid-Holocene. Past Climate Variability through Europe and Africa, Volume 6, R.W. Battarbee, F. Gasse, and C.E. Stickley (eds), Springer, Dordrecht, The Netherlands, 515-534.
Braconnot, P., M. F. Loutre, et al. (2002). "How the simulated change in monsoon at 6 ka BP is related to the simulation of the modern climate: results from the Paleoclimate Modeling Intercomparison Project." Climate Dynamics 19(2): 107-121.
Braconnot, P., O. Marti, S. Joussaume, and Y. Leclaninche (2000). Ocean feedbacks in response to 6 kyr insolation. Journal of Climate, 13, 1537-1553.
Bradley, R.S., 1999: Climatic variability in sixteenth-century Europe and its social dimension - Preface. *Climatic Change,* 43(1), 1-2.
Bradley, R.S., K.R. Briffa, J. Cole, and T.J. Osborn, 2003b: The climate of the last millennium. In: *Paleoclimate, Global Change and the Future* [K.D. Alverson, R.S. Bradley, and T.F. Pedersen (eds.)]. Springer, Berlin, pp. 105-141.
Bradley, R.S., M.K. Hughes, and H.F. Diaz, 2003a: Climate in Medieval time. *Science,* 302(5644), 404-405.

Bralower, T.J., 2002: Evidence of surface water oligotrophy during the Paleocene-Eocene thermal maximum: Nannofossil assemblage data from Ocean Drilling Program Site 690, Maud Rise, Weddell Sea (vol 17, pg 1023, 2002). *Paleoceanography,* 17(4).
Brauning, A., and B. Mantwill, 2004: Summer temperature and summer monsoon history on the Tibetan plateau during the last 400 years recorded by tree rings. *Geophysical Research Letters,* 31(24).
Briffa, K.R., 2000: Annual climate variability in the Holocene: interpreting the message of ancient trees. *Quaternary Science Reviews,* 19(1-5), 87-105.
Briffa, K.R., and T.J. Osborn, 1999: Perspectives: Climate warming - Seeing the wood from the trees. *Science,* 284(5416), 926-927.
Briffa, K.R., and T.J. Osborn, 2002: Paleoclimate - Blowing hot and cold. *Science,* 295(5563), 2227-2228.
Briffa, K.R., T.J. Osborn, and F.H. Schweingruber, 2004: Large-scale temperature inferences from tree rings: a review. *Global and Planetary Change,* 40(1-2), 11-26.
Briffa, K.R., T.J. Osborn, F.H. Schweingruber, I.C. Harris, P.D. Jones, S.G. Shiyatov, and E.A. Vaganov, 2001: Low-frequency temperature variations from a northern tree ring density network. *Journal of Geophysical Research-Atmospheres,* 106(D3), 2929-2941.
Brigham-Grette, J., and D.M. Hopkins, 1995: Emergent-marine record and paleoclimate of the last interglaciation along the northwest Alaskan coast. *Quarternary Research,* 43, 154-173.
Broecker, W., 1998: Paleocean circulation during the last deglaciation: a bipolar seesaw? *Paleoceanography,* 13, 119-121.
Broecker, W.S., and E. Clark, 2003: Holocene atmospheric CO2 increase as viewed from the seafloor. *Glob. Biogeochem. Cycles,* 17(2), *doi:10.1029/2002GB001985*.
Broecker, W.S., and G.M. Henderson, 1998: The sequence of events surrounding Termination II and their implications for the cause of glacial-interglacial CO2 changes. *Paleoceanography,* 13, 352-364.
Brook, E.J., S. Harder, J. Severinghaus, E.J. Steig, and C.M. Sucher, 2000: On the origin and timing of rapid changes in atmospheric methane during the last glacial period. *Global Biogeochemical Cycles,* 14(2), 559-572.
Brooks, C.E.P. (1922) The Evolution of Climate. [Preface by Simpson, G.C.] Benn Brothers, London. pp. 173.
Brooks, K., C.A. Scholz, J.W. King, J. Peck, J.T. Overpeck, J.M. Russell, and P.Y.O. Amoako, 2005: Late-Quaternary lowstands of lake Bosumtwi, Ghana: evidence from high-resolution seismic-reflection and sediment-core data. *Palaeogeography Palaeoclimatology Palaeoecology,* 216(3-4), 235-249.
Brovkin, V., J. Bendtsen, M. Claussen, i.A. Ganopolsk, C. Kubatzki, V. Petoukhov, and A. Andreev, 2002: Carbon cycle, vegetation and climate dynamics in the Holocene: Experiments with the CLIMBER-2 model. *Glob. Biogeochem. Cycles,* 16, 1139, doi: 10.1029/2001GB001662.
Burger, G., and U. Cubasch, 2005: Are multiproxy climate reconstructions robust? *Geophysical Research Letters,* 32(23), 10.1029/2005GL024155.
Burger, G., I. Fast, and U. Cubasch, 2006: Climate reconstruction by regression - 32 variations on a theme. *Tellus Series a-Dynamic Meteorology and Oceanography,* 58(2), 227-235.
Caillon, N., J.P. Severinghaus, J. Jouzel, J.-M. Barnola, J. Kang, and V.Y. Lipenkov, 2003: Timing of Atmospheric CO2 and Antarctic Temperature Changes Across Termination III. *Science,* 299, 1728-1731.
Calov, R., A. Ganopolski, V. Petoukhov, and M. Claussen, 2002: Large-scale instabilities of the Laurentide ice sheet simulated in a fully coupled climate-system model. *Geophysical Research Letters,* 29, 2216.
Calov, R., A. Ganopolski, V. Petoukhov, M. Claussen, V. Brovkin, and C. Kubatzki, 2005: Transient simulation of the last glacial inception. Part II: sensitivity and feedback analysis. *Climate Dynamics,* 24, 563-576.
Cane, M.A., 2005: The evolution of El Nino, past and future. *Earth and Planetary Science Letters,* 230(3-4), 227-240.
CAPE Last Interglacial Project Members, in press: Last Interglacial Arctic warmth confirms polar amplification of climate change. *Quaternary Science Reviews,*. In press..
Castellano, E., S. Becagli, M. Hansson, M. Hutterli, J.R. Petit, M.R. Rampino, M. Severi, J.P. Steffensen, R. Traversi, and R. Udisti, 2005: Holocene volcanic history as recorded in the sulfate stratigraphy of the European Project for Ice Coring in Antarctica Dome C (EDC96) ice core. *J. Geophys. Res.,* 110, Art. No. D06114.
Cerling, T.E., 1991: Carbon dioxide in the atmosphere: Evidence from Cenozoic and Mesozoic paleosols. *Am. J. Sci.,* 291, 377-400.

Chandler, M.A., D. Rind, and R.S. Thompson 1994. Joint investigations of the middle Pliocene climate II: GISS GCM Northern Hemisphere results. *Global Planet. Change* **9**, 197-219.
Chapman, D.S., M.G. Bartlett, and R.N. Harris, 2004: Comment on "Ground vs. surface air temperature trends: Implications for borehole surface temperature reconstructions" by M. E. Mann and G. Schmidt. *Geophysical Research Letters,* 31(7), art. no.-L07205.
Chappellaz, J., T. Blunier, S. Kints, A. Dällenbach, J.M. Barnola, J. Schwander, D. Raynaud, and B. Stauffer, 1997: Changes in the atmospheric CH4 gradient between Greenland and Antarctica during the Holocene. *Journal of Geophysical Research-Atmospheres,* 102(D13), 15987-15997.
Chappellaz, J.A., I.Y. Fung, and A.M. Thompson, 1993: The Atmospheric Ch4 Increase Since The Last Glacial Maximum. *Tellus Series B-Chemical And Physical Meteorology,* 45(3), 228-241.
Charles, C.D., D.E. Hunter, and R.G. Fairbanks, 1997: Interaction between the ENSO and the Asian monsoon in a coral record of tropical climate. *Science,* 277(5328), 925-928.
Church, J.A., J.M. Gregory, P. Huybrechts, M. Kuhn, K. Lambeck, M.T. Nhuan, D. Qin, and P.L. Woodworth, 2001: *Changes in Sea Level.* 3, Cambridge, 639-693 pp.
Claquin, T., C. Roelandt, K.E. Kohfeld, S.P. Harrison, I. Tegen, I.C. Prentice, Y. Balkanski, G. Bergametti, M. Hansson, N. Mahowald, H. Rodhe, and M. Schulz, 2003: Radiative forcing of climate by ice-age atmospheric dust. *Climate Dynamics,* 20, 193-202.
Clark, P.U., N.G. Pisias, T.F. Stocker, and A.J. Weaver, 2002: The role of the thermohaline circulation in abrupt climate change. *Nature,* 415, 863-869.
Clarke, G.K.C., D.W. Leverington, J.T. Teller, and A.S. Dyke, 2004: Paleohydraulics of the last outburst flood from glacial Lake Agassiz and the 8200 BP cold event. *Quaternary Science Reviews,* 23, 389–407.
Claussen, M. and Gayler , V., 1997: The greening of Sahara during the mid-Holocene: results of an interactive atmosphere - biome model. Global Ecology and Biogeography Letters, 6, 369-377.
Claussen, M., C. Kubatzki, V. Brovkin, A. Ganopolski, P. Hoelzmann, and H.J. Pachur, 1999: Simulation of an abrupt change in Saharan vegetation in the mid-Holocene. *Geophysical Research Letters,* 26(14), 2037-2040.
Claussen, M., L.A. Mysak, A.J. Weaver, M. Crucifix, T. Fichefet, M.F. Loutre, S.L. Weber, J. Alcamo, V.A. Alexeev, A. Berger, R. Calov, A. Ganopolski, H. Goosse, G. Lohmann, F. Lunkeit, Mokhov, II, V. Petoukhov, P. Stone, and Z. Wang, 2002: Earth system models of intermediate complexity: closing the gap in the spectrum of climate system models. *Climate Dynamics,* 18(7), 579-586.
Clement, A.C., and M.A. Cane, 1999: A role for the tropical Pacific coupled ocean-atmosphere system on Milankovitch and millennial timescales. Part I: A modeling study of tropical Pacific variability. In: *Mechanisms of global climate change at millennial time scales* [P.U. Clark, R.S. Webb, and L.D. Keigwin (eds.)]. AGU, Washington, pp. 363-371.
Clement, A.C., R. Seager, and M.A. Cane, 2000: Suppression of El Nino during the mid-Holocene by changes in the Earth's orbit. *Paleoceanography,* 15(6), 731-737.
Clement, A.C., R. Seager, M.A. Cane, and S.E. Zebiak, 1996: An ocean dynamical thermostat. *Journal of Climate,* 9(9), 2190-2196.
Cobb, K.M., C.D. Charles, H. Cheng, and R.L. Edwards, 2003: El Nino/Southern Oscillation and tropical Pacific climate during the last millennium. *Nature,* 424(6946), 271-276.
Coe, M. T. and S. P. Harrison (2002). "The water balance of northern Africa during the mid-Holocene: an evaluation of the 6 ka BPPMIP simulations." Climate Dynamics 19(2): 155-166.
Cole, J., 2003: Global change - Dishing the dirt on coral reefs. *Nature,* 421(6924), 705-706.
Cole, J.E., and E.R. Cook, 1998: The changing relationship between ENSO variability and moisture balance in the continental United States. *Geophysical Research Letters,* 25(24), 4529-4532.
Cole, J.E., R.B. Dunbar, T.R. McClanahan, and N.A. Muthiga, 2000: Tropical Pacific forcing of decadal SST variability in the western Indian Ocean over the past two centuries. *Science,* 287(5453), 617-619.
Cook, E.R., B.M. Buckley, R.D. D'Arrigo, and M.J. Peterson, 2000: Warm-season temperatures since 1600 BC reconstructed from Tasmanian tree rings and their relationship to large-scale sea surface temperature anomalies. *Climate Dynamics,* 16(2-3), 79-91.
Cook, E.R., C.A. Woodhouse, C.M. Eakin, D.M. Meko, and D.W. Stahle, 2004b: Long-term aridity changes in the western United States. *Science,* 306(5698), 1015-1018.
Cook, E.R., J. Esper, and R.D. D'Arrigo, 2004a: Extra-tropical Northern Hemisphere land temperature variability over the past 1000 years. *Quaternary Science Reviews,* 23(20-22), 2063-2074.

Cook, E.R., J.G. Palmer, and R.D. D'Arrigo, 2002b: Evidence for a 'Medieval Warm Period' in a 1,100 year tree-ring reconstruction of past austral summer temperatures in New Zealand. *Geophysical Research Letters,* 29(14), art-1667.
Cook, E.R., R.D. D'Arrigo, and M.E. Mann, 2002a: A well-verified, multiproxy reconstruction of the winter North Atlantic Oscillation index since AD 1400. *Journal of Climate,* 15(13), 1754-1764.
Cortijo, E., L.D. Labeyrie, L. Vidal, M. Vautravers, M. Chapman, J.C. Duplessy, M. Elliot, M. Arnold, and G. Auffret, 1997: Changes in the sea surface hydrology associated with Heinrich event 4 in the North Atlantic Ocean (40-60°N). *Earth Planet. Sci. Lettt.,* 146, 29-45.
Cortijo, E., S. Lehman, L. Keigwin, M. Chapman, D. Paillard, and L. Labeyrie, 1999: Changes in meridional temperature and salinity gradients in the North Atlantic Ocean (30 degrees-72 degrees N) during the last interglacial period. *Paleoceanography,* 14(1), 23-33.
Cronin, T.M., 1999: *Priciples of Paleoclimatology.* Perspectives in Paleobiology and Earth History. Columbia University Press, New York, 560 pp.
Cronin, T.M., H.J. Dowsett, G.S. Dwyer, P.A. Baker, and M.A. Chandler, 2005: Mid-pliocene deep-sea bottom-water temperatures based on ostracode Mg/Ca ratios. *Marine Micropaleontology,* 54(3-4), 249-261.
Crouch, E.M., G.R. Dickens, H. Brinkhuis, M.P. Aubry, C.J. Hollis, K.M. Rogers, and H. Visscher, 2003: The Apectodinium acme and terrestrial discharge during the Paleocene-Eocene thermal maximum: new palynological, geochemical and calcareous nannoplankton observations at Tawanui, New Zealand. *Palaeogeography Palaeoclimatology Palaeoecology,* 194(4), 387-403.
Crowley, T.J., 1995: Ice-Age Terrestrial Carbon Changes Revisited. *Global Biogeochemical Cycles,* 9(3), 377-389.
Crowley, T.J., 1998: Significance of tectonic boundary conditions for paleoclimate simulations. In: *Tectonic Boundary Conditions for Climate Reconstructions* [T.J. Crowley, and K.C. Burke (eds.)]. Oxford Universtiy Press, New York, pp. 3-17.
Crowley, T.J., 2000: Causes of climate change over the past 1000 years. *Science,* 289(5477), 270-277.
Crowley, T.J., and T.S. Lowery, 2000: How warm was the medieval warm period? *Ambio,* 29(1), 51-54.
Crowley, T.J., S.K. Baum, K.Y. Kim, G.C. Hegerl, and W.T. Hyde, 2003: Modeling ocean heat content changes during the last millennium. *Geophysical Research Letters,* 30(18), art. no.-1932.
Crucifix, M., and C.D. Hewitt, 2005: Impact of vegetation changes on the dynamics of the atmosphere at the Last Glacial Maximum. *Climate Dynamics*, 25 (5): 447-459.
Crucifix, M., and M.F. Loutre, 2002: Transient simulations over the last interglacial period (126-115 kyr BP). *Climate Dynamics,* 19, 417-433.
Cuffey, K.M., and S.J. Marshall, 2000: Substantial contribution fo sea-level rise during the last interglacial from the Greenland ice sheet. *Nature,* 404, 591-594.
Cullen, H.M., A. Kaplan, P.A. Arkin, and P.B. Demenocal, 2002: Impact of the North Atlantic Oscillation on Middle Eastern climate and streamflow. *Climatic Change,* 55(3), 315-338.
Cumming, B.F., K.R. Laird, J.R. Bennett, J.P. Smol, and A.K. Salomon, 2002: Persistent millennial-scale shifts in moisture regimes in western Canada during the past six millennia. *Proceedings of the National Academy of Sciences of the United States of America,* 99(25), 16117-16121.
Dahl, K., A. Broccoli, and R. Stouffer, 2005: Assessing the role of North Atlantic freshwater forcing in millennial scale climate variability: a tropical Atlantic perspective. *Climate Dynamics,* 24(4), 325-346.
Dahl, S.O. and Nesje, A. , 1996: A new approach to calculating Holocene winter precipitation by combining glacier equilibrium-line altitudes and pine-tree limits: A case study from Hardangerjokulen, central southern Norway. *Holocene,* 6(4), 381-398.
Dahl-Jensen, D., K. Mosegaard, N. Gundestrup, G.D. Clow, S. Johnsen, A.W. Hansen, and N. Balling, 1998: Past temperature directly from the Greenland Ice Sheet. *Science,* 282, 268-271.
D'Arrigo, R., E.R. Cook, R.J. Wilson, R. Allan, and M.E. Mann, 2005: On the variability of ENSO over the past six centuries. *Geophysical Research Letters,* 32(3), art. no.-L03711.
D'Arrigo, R., R. Wilson, and G. Jacoby, 2006: On the long-term context for late twentieth century warming. *Journal of Geophysical Research-Atmospheres,* 111(D3) Doi: 10.1029/2005JD006352.
Davis, B.A.S., S. Brewer, A.C. Stevenson, J. Guiot, and D. contributors, 2003: The temperature of Europe during the Holocene reconstructed from pollen data. *Quaternary Science Reviews,* 22, 1701-1716.
de Menocal, P., J. Ortiz, T. Guilderson, and M. Sarnthein, 2000: Coherent high- and low-latitude climate variability during the holocene warm period. *Science,* 288(5474), 2198-2202.

de Noblet-Ducoudre, N., R. Claussen, et al. (2000). "Mid-Holocene greening of the Sahara: first results of the GAIM 6000 year BP Experiment with two asynchronously coupled atmosphere/biome models." Climate Dynamics 16(9): 643-659.
DeConto, R.M., and D. Pollard, 2003: Rapid Cenozoic glaciation of Antarctica induced by declining atmospheric CO2. *Nature,* 421(6920), 245-249.
Delworth, T.L., and M.E. Mann, 2000: Observed and simulated multidecadal variability in the Northern Hemisphere. *Climate Dynamics,* 16(9), 661-676.
deVernal, A., A. Rosell-Mele, M. Kucera, C. Hillaire-Marcel, F. Eynaud, M. Weinelt, T. Dokken, and M. Kageyama, in press: Multiproxy reconstruction of LGM sea-surface conditions in the northern North Atlantic. Quaternary Science Reviews. In press.
Dickens, G.R., and R.M. Owen, 1996: Sediment geochemical evidence for an early-middle Gilbert (early Pliocene) productivity peak in the North Pacific Red Clay Province. *Marine Micropaleontology,* 27(1-4), 107-120.
Dickens, G.R., M.M. Castillo, and J.C.G. Walker, 1997: A blast of gas in the latest Paleocene: Simulating first-order effects of massive dissociation of oceanic methane hydrate. *Geology,* 25(3), 259-262.
Ding, Z.L., E. Derbyshire, S.L. Yang, Z.W. Yu, S.F. Xiong, and T.S. Liu, 2002: Stacked 2.6-Ma grain size record from the Chinese loess based on five sections and correlation with the deep-sea delta O-18 record. *Paleoceanography,* 17(3).
Dlugokencky, E.J., L.P. Steele, P.M. Lang, and K.A. Masarie, 1994: The growth rate and distribution of atmospheric methane. *J. Geophys. Res.,* 99, 17021-17043.
Dokken, T.M., and E. Jansen, 1999: Rapid changes in the mechanism of ocean convection during the last glacial period. *Nature,* 401, 458-461.
Domack, E., D. Duran, A. Leventer, S. Ishman, S. Doane, S. McCallum, D. Amblas, J. Ring, R. Gilbert, and M. Prentice, 2005: Stability of the Larsen B ice shelf on the Antarctic Peninsula during the Holocene epoch. *Nature,* 436, 681-685.
Dowsett, H., J. Barron, and R. Poore, 1996: Middle Pliocene sea surface temperatures: A global reconstruction. *Marine Micropaleontology,* 27(1-4), 13-25.
Dowsett, H.J., and T.M. Cronin, 1990: High eustatic sea level during the middle Pliocene: evidence from southeastern U. S. Atlantic coastal plain. *Geology,* 18, 435-438.
Dowsett, H.J., M.A. Chandler, T.M. Cronin, and G.S. Dwyer, 2005: Middle Pliocene sea surface temperature variability. *Paleoceanography,* 20(2), 10.1029/2005PA001133.
Duplessy, J.C., E. Ivanova, I. Murdmaa, M. Paterne, and L. Labeyrie, 2001: Holocene paleoceanography of the northern Barents Sea and variations of the northward heat transport by the Atlantic ocean. *Boreas,* 30, 2-16.
Duplessy, J.C., L. Labeyrie, and C. Waelbroeck, 2002: Constraints on the ocean oxygen isotopic enrichment between the Last Glacial Maximum and the Holocene: Paleoceanographic implications. *Quaternary Science Reviews,* 21, 315-330.
Ehrmann, W.U., and A. Mackensen, 1992: Sedimentological Evidence for the Formation of an East Antarctic Ice-Sheet in Eocene Oligocene Time. *Palaeogeography Palaeoclimatology Palaeoecology,* 93(1-2), 85-112.
Elliot, M., L. Labeyrie, G. Bond, E. Cortijo, J.L. Turon, N. Tisnerat, and J.C. Duplessy, 1998: Millenial scale iceberg discharges in the Irminger Basin during the last glacial period: relationship with the Heinrich events and environmental settings. *Paleoceanography,* 13, 433-446.
Ellis, J.M. and Calkin, P.E., 1984: Chronology of Holocene glaciation, central Brooks Range, Alaska. *Geological Society of America Bulletin,* 95, 897-912.
Enting, I.G., 1987: On the use of smoothing splines to filter CO_2 data. *J. Geophys. Res.,* 92, 10977-10984.
EPICA community members, 2004: Eight glacial cycles from an Antarctic ice core. *Nature,* 429(6992), 623-628.
Esper, J., D.C. Frank, R.J.S. Wilson, and K.R. Briffa, 2005: Effect of scaling and regression on reconstructed temperature amplitude for the past millennium. *Geophysical Research Letters,* 32(7), doi:10.1029/2004GL021236.
Esper, J., E.R. Cook, and F.H. Schweingruber, 2002: Low-frequency signals in long tree-ring chronologies for reconstructing past temperature variability. *Science,* 295(5563), 2250-2253.
Etheridge, D.M., L.P. Steele, R.L. Langenfelds, R.J. Francey, J.M. Barnola, and V.I. Morgan, 1996: Natural and anthropogenic changes in atmospheric CO2 over the last 1000 years from air in Antarctic ice and firn. *Journal of Geophysical Research-Atmospheres,* 101(D2), 4115-4128.

Evans, M.N., A. Kaplan, and M.A. Cane, 2002: Pacific sea surface temperature field reconstruction from coral delta O-18 data using reduced space objective analysis. *Paleoceanography,* 17(1), art. no.-1007.
Eyer, M., Ph.D. thesis, Unversity of Bern, 2004, 2004: *Highly resolved d13C measurements on CO2 in air from Antarctic ice cores*, University of Bern, 113 pp.
Fairbanks, R.G., 1989: A 17,000 year glacio-eustatic sea level record: Influence of glacial melting rates on the Younger Dryas event and deep-ocean circulation. *Paleoceanography,* 342, 637-642.
Farrera, I., S.P. Harrison, I.C. Prentice, G. Ramstein, J. Guiot, P.J. Bartlein, and e. al., 1999: Tropical climates at the Last Glacial Maximum: a new synthesis of terrestrial palaeoclimate data. I. Vegetation, lake-levels and geochemistry. *Climate Dynamics,* 15, 823-856.
Ferretti, D.F., J.B. Miller, J.W.C. White, D.M. Etheridge, K.R. Lassey, D.C. Lowe, C.M. MacFarling Meure, M.F. Dreier, C.M. Trudinger, T.D. van Ommen, and R.L. Langenfelds, 2005: Unexpected changes to the global methane budget over the past 2000 years. *Science,* 309, 1714-1717.
Fischer, G., and G. Wefer, 1999: *Use of Proxies in Paleoceanography: Examples from the South Atlantic*. Springer, Berlin, 735 pp.
Fischer, H., D. Wagenbach, and S. Kipfstuhl, 1998: Sulfate and nitrate firn concentrations on the Greenland Ice Sheet 2. Temporal and anthropogenic deposition changes. *Journal of Geophysical Research,* 103(D17), 21935-21942.
Fleitmann, D., S.J. Burns, M. Mudelsee, U. Neff, J. Kramers, A. Mangini, and A. Matter, 2003: Holocene forcing of the Indian monsoon recorded in a stalagmite from southern Oman. *Science,* 300, 1737-1740.
Fligge, M., and S.K. Solanki, 2000: The solar spectral irradiance since 1700. *Geophysical Research Letters,* 27, 2157-2160.
Flückiger, J., A. Dällenbach, T. Blunier, B. Stauffer, T.F. Stocker, D. Raynaud, and J.M. Barnola, 1999: Variations in atmospheric N_2O concentration during abrupt climatic changes. *Science,* 285(5425), 227-230.
Flückiger, J., E. Monnin, B. Stauffer, J. Schwander, T.F. Stocker, J. Chappellaz, D. Raynaud, and J.-M. Barnola, 2002: High resolution Holocene N2O ice core record and its relationship with CH4 and CO2. *Glob. Biogeochem. Cycles,* 16, doi: 10.1029/2001GB001417.
Flückiger, J., T. Blunier, B. Stauffer, J. Chappellaz, R. Spahni, K. Kawamura, J. Schwander, T.F. Stocker, and D. Dahl-Jensen, 2004: N2O and CH4 variations during the last glacial epoch: Insight into global processes. *Global Biogeochemical Cycles,* 18, doi: 10.1029/2003GB002122.
Folland, C.K., T.R. Karl, J.R. Christy, R.A. Clarke, G.V. Gruza, J. Jouzel, M.E. Mann, J. Oerlemans, M.J. Salinger, and S.W. Wang, 2001: Observed climate variability and change. In: *Climate Change 2001: The scientific basis* [J.T. Houghton, and e. al. (eds.)]. Cambridge University Press, New York, pp. 99-181.
Forman, S.L., R. Oglesby, and R.S. Webb, 2001: Temporal and spatial patterns of Holocene dune activity on the Great Plains of North America: megadroughts and climate links. *Global and Planetary Change,* 29(1-2), 1-29.
Foster, S., 2004: *Reconstruction of Solar Irradiance Variations for use in Studies of Global Climate Change: Application of Recent SOHO Observations with Historic Data from the Greenwich Observatory*, Ph.D. Thesis, University of Southhampton, Southhampton.
Foukal, P., G. North, and T. Wigley, 2004: A stellar view on solar variations and climate. *Science,* 306(5693), 68-69.
Francois, L., P. Godderis, P. Warnant, G. Ramstein, N.I. de Noblet, and S.J. Lorenz, 1999: Carbon stocks and isotopic budgets of the terrestrial biospehere at mid-Holocene and last glacial maximum times. *Chemical Geology,* 159, 163-189.
Francois, L.M., C. Delire, P. Warnant, and G. Munhoven, 1998: Modelling the glacial-interglacial changes in the continental biosphere. *Global and Planetary Change,* 17, 37-52.
Freeman, K.H., and J.M. Hayes, 1992: Fractionation of carbon isotopes by phytophlankton and estimates of ancient CO2 levels. *Global Biogeochem. Cycles,* 6, 185-198.
Friedlingstein, P., P. Cox , R. Betts, L. Bopp, W. von Bloh, V. Brovkin, S. Doney, M. Eby, I. Fung, B. Govindasamy, J. John, C. Jones, F. Joos, T. Kato, M. Kawamiya, W. Knorr, K. Lindsay, H.D. Matthews, T. Raddatz, R. Rayner, C. Reick, E. Roeckner, K.-G. Schnitzler, R. Schnur, K. Strassmann, S. Thompson, A.J. Weaver, C. Yoshikawa, and N. N. Zeng, in press: Climate-carbon cycle feedback analysis, results from the C4MIP model intercomparison. *Journal of Climate*. In press.

Fröhlich, C., and J. Lean, 2004: Solar radiative output and its variability: evidence and mechanisms. *Astronomy and Astrophysics Review,* 12, 273-320.
Gaffen, D.J., B.D. Santer, J.S. Boyle, J.R. Christy, N.E. Graham, and R.J. Ross, 2000: Multidecadal changes in the vertical temperature structure of the tropical troposphere. *Science,* 287(5456), 1242-1245.
Gagan, M.K., L.K. Ayliffe, D. Hopley, J.A. Cali, G.E. Mortimer, J. Chappell, M.T. McCulloch, and M.J. Head, 1998: Temperature and surface-ocean water balance of the mid-Holocene tropical western Pacific. *Science,* 279, 1014-1018.
Ganopolski, A., and S. Rahmstorf, 2001: Rapid changes of glacial climate simulated in a coupled climate model. *Nature,* 409, 153-158.
Ganopolski, A., S. Rahmstorf, V. Petoukhov and M. Claussen, 1998: Simulation of modern and glacial climates with a coupled global model of intermediate complexity. Nature, 391, 351-356.
Gellatly, A.F., T.J. Chinn, and F. Rötlishberger, 1988: Holocene glacier variations in New-Zealand : a review. *Quaternary Science Reviews,* 7, 227-242.
Gerber, S., F. Joos, P. Brugger, T.F. Stocker, M.E. Mann, S. Sitch, and M. Scholze, 2003: Constraining temperature variations over the last millennium by comparing simulated and observed atmospheric CO2. *Climate Dynamics,* 20(2-3), 281-299.
Gersonde, R., X. Crosta, A. Abelmann, and L. Armand, 2005: Sea-surface temperature and sea ice distribution of the Southern Ocean at the EPILOG Last Glacial Maximum - a circum-Antarctic view based on siliceous microfossil records. *Quaternary Science Reviews*, 24 (7-9): 869-896
Gherardi, J.-M., L. Labeyrie, J.F. McManus, R. Francois, L.C. Skinner, and E. Cortijo, 2005: Evidence from the North Eastern Atlantic Basin for Variability of the Meridional Overturning Circulation through the last Deglaciation. *EPSL,* 240, 710-723.
Gladstone, R.M., I. Ross, P.J. Valdes, A. Abe-Ouchi, P. Braconnot, S. Brewer, M. Kageyama, A. Kitoh, A. Legrande, O. Marti, R. Ohgaito, B. Otto-Bliesner, and G. Vettoretti,,2005: Mid-Holocene NAO : a PMIP2 model intercomparison. *Geophysical Research Letters*, 32, L16707, doi:10.1029/2005GL023596.
Goldstein, B., F. Joos, and T.F. Stocker, 2003: A modeling study of oceanic nitrous oxide during the Younger Dryas cold period. *Geophysical Research Letters,* 30, doi: 10.1029/2002GL016418.
Goni, M.F.S., F. Eynaud, J.L. Turon, and N.J. Shackleton, 1999: High resolution palynological record off the Iberian margin: direct land-sea correlation for the Last Interglacial complex. *Earth and Planetary Science Letters,* 171(1), 123-137.
Gonzalez-Rouco, F., H. von Storch, and E. Zorita, 2003: Deep soil temperature as proxy for surface air-temperature in a coupled model simulation of the last thousand years. *Geophysical Research Letters,* 30(21), art. no.-2116.
Gonzalez-Rouco, J.F., H. Beltrami, E. Zorita, and H. von Storch, 2006: Simulation and inversion of borehole temperature profiles in surrogate climates: Spatial distribution and surface coupling. *Geophysical Research Letters,* 33(1) L01703, doi:10.1029/2005GL024693.
Goosse, H., H. Renssen, A. Timmermann, and R.S. Bradley, 2005a: Internal and forced climate variability during the last millennium: a model-data comparison using ensemble simulations. *Quaternary Science Reviews,* 24, 1345-1360.
Goosse, H., T.J. Crowley, E. Zorita, C.M. Ammann, H. Renssen, and E. Driesschaert, 2005b: Modelling the climate of the last millennium: what causes the differences between simulations? *Geophysical Research Letters,* 32, L06710.
Gosnold, W.D., P.E. Todhunter, and W. Schmidt, 1997: The borehole temperature record of climate warming in the mid- continent of North America. *Global and Planetary Change,* 15(1-2), 33-45.
Gradstein, F.M., J.G. Ogg, and A.G. Smith, 2004: *A Geologic Time Scale*. Cambridge University Press, Cambridge, 589 pp.
Greenblatt, J.B., and J.L. Sarmiento, 2004: Variabilty and climate feedback mechanisms in ocean uptake of CO2, The Global Carbon Cycle (eds., Field and Raupach). Island Press, Washington, D.C., 257-275.
Grove, J.M., 2004: *Little ice ages: ancient and modern*. Routeledge studies in physical geography and environment; 5,Routledge, New York. 718 pages.
Guilderson, T.P., R.G. Fairbanks, and J.L. Rubenstone, 1994: Tropical temperature variations since 20,000 years ago: modulating interhemispheric climate change. *Science,* 263, 663-665.
Guiot, J., A. Nicault, C. Rathgeber, J.L. Edouard, E. Guibal, G. Pichard, and C. Till, 2005: Last-millennium summer-temperature variations in western Europe based on proxy data. *Holocene,* 15(4), 489-500.
Guo, Z.T., N. Petit-Maire, and S. Kropelin, 2000: Holocene non-orbital climatic events in present-day arid areas of northern Africa and China. *Global and Planetary Change,* 26(1-3), 97-103.

Guo, Z.T., S.Z. Peng, Q.Z. Hao, P.E. Biscaye, Z.S. An, and T.S. Liu, 2004: Late Miocene-Pliocene development of Asian aridification as recorded in the Red-Earth Formation in northern China. *Global and Planetary Change,* 41(3-4), 135-145.
Gupta, A.K., D.M. Anderson, and J.T. Overpeck, 2003: Abrupt changes in the Asian southwest monsoon during the Holocene and their links to the North Atlantic ocean. *Nature,* 421, 354-357.
Hall, J.C., and G.M. Lockwood, 2004: The chromospheric activity and variability of cycling and flat activity solar-analog stars. *Astrophysical Journal,* 614, 942-946.
Hambrey, M.J., W.U. Ehrmann, and B. Larsen, 1991: *Cenozoic glacial record of the Prydz Bay continental shelf, East Antarctica.* Ocean Drilling Program, Texas, 77-131 pp.
Hanebuth, T., K. Stattegger, and P.M. Grootes, 2000: Rapid flooding of the Sunda Shelf: A late-glacial sea-level record. *Science,* 288(5468), 1033-1035.
Harrington, G.J., S.J. Kemp, and P.L. Koch, 2004: Palaeocene-Eocene paratropical floral change in North America: responses to climate change and plant immigration. *Journal of the Geological Society,* 161, 173-184.
Harris, R.N., and D.S. Chapman, 2001: Mid-Latitude (30 degrees-60 degrees N) climatic warming inferred by combining borehole temperatures with surface air temperatures. *Geophysical Research Letters,* 28(5), 747-750.
Harrison, S.P., 2005: Snowlines at the last glacial maximum and tropical cooling. *Quaternary International,* 138-139, 5-7.
Harrison, S. P., J. E. Kutzbach, et al. (2003). "Mid-Holocene climates of the Americas: a dynamical response to changed seasonality." Climate Dynamics 20(7-8): 663-688.
Harrison, S.P., and I.C. Prentice, 2003: Climate and CO2 controls on global vegetation distribution at the last glacial maximum: analysis based on palaeovegetation data, biome modelling and palaeoclimate simulations. *Global Change Biology,* 9, 983-1004.
Haug, G.H., K.A. Hughen, D.M. Sigman, L.C. Peterson, and U. Röhl, 2001: Southward Migration of the Intertropical Convergence Zone Through the Holocene. *Science,* 17(293), 1304-1308.
Hays, J.D., J. Imbrie, N.J. Shackleton, et al.. (1976) Variations in the Earth's orbit: pacemaker of the ice ages.*Science,* 194, 1121-1132.
Haywood, A.M., P. Dekens, A. C. Ravelo, and M. Williams, 2005: Warmer tropics during the mid-Pliocene? Evidence from alkenone paleothermometry and a fully coupled ocean-atmosphere GCM. *Geochem. Geophys. Geosyst,* 6, (Q03010, doi:10.1029/2004GC000799.).
Haywood, A.M., P.J. Valdes, and B.W. Sellwood, 2000: Global scale paleoclimate reconstruction of the middle Pliocene climate using the UKMO GCM: initial results. *Global Planet. Change,* 25, 239-256.
He, Y., W.H. Theakstone, Z.L. Zhang, T.D. Yao, T. Chen, Y.P. Shen, and H.X. Pang, 2004: Asynchronous Holocene climatic change across China. *Quaternary Research,* 61, 52-63.
Hegerl, G.C., T.J. Crowley, W.T. Hyde, and D.J. Frame, in press: Constrains on climate sensitivity from temperature reconstructions of the last seven centuries. *Nature*. In press.
Hemming, S.R., 2004: Heinrich events: Massive late pleistocene detritus layers of the North Atlantic and their global climate imprint. *Reviews of Geophysics,* 42(1), RG1005, doi:10.1029/2003RG000128.
Higgins, P.A.T., 2004: Biogeochemical and biophysical responses of the land surface to a sustained thermohaline circulation weakening. *Journal of Climate,* 17, 4135-4142.
Hodell, D.A., M. Brenner, and J.H. Curtis, 2005: Terminal Classic drought in the northern Maya lowlands inferred from multiple sediment cores in Lake Chichancanab (Mexico). *Quaternary Science Reviews,* 24(12-13), 1413-1427.
Hoerling, M., and A. Kumar, 2003: The perfect ocean for drought. *Science,* 299(5607), 691-694.
Hoffmann, G., E. Ramirez, J.D. Taupin, B. Francou, P. Ribstein, R. Delmas, H. Durr, R. Gallaire, J. Simoes, U. Schotterer, M. Stievenard, and M. Werner, 2003: Coherent isotope history of Andean ice cores over the last century. *Geophysical Research Letters,* 30(4), Doi: 10.1029/2002GL014870.
Holmgren, K., J.A. Lee-Thorp, G.R.J. Cooper, K. Lundblad, T.C. Partridge, L. Scott, R. Sithaldeen, A.S. Talma, and P.D. Tyson, 2003: Persistent millenial-scale climate variability over the past 25,000 years in Southern Africa. *Quaternary Science Reviews,* 2003, 2311-2326.
Holzhauser, H., M.J. Magny, and H.J. Zumbuhl, 2005: Glacier and lake-level variations in west-central Europe over the last 3500 years. *The Holocene,* 15(6), 789-801.
Hoyt, D.V., and K.H. Schatten, 1993: A discussion of plausible solar irradiance variations. *Journal of Geophysical Research,* 98, 18895-18906.

Huang, S.P., and H.N. Pollack, 1998: *Global borehole temperature database for climate reconstruction.* NOAA/NGDC Paleoclimatol. Program, Boulder, Colo., IGBP PAGES/World Data Center-A for Paleoclimatology Data Contribution Series #1998-044.
Huang, S.P., H.N. Pollack, and P.Y. Shen, 2000: Temperature trends ever the past five centuries reconstructed from borehole temperatures. *Nature,* 403(6771), 756-758.
Huber, C., M. Leuenberger, R. Spahni, J. Flückiger, J. Schwander, T.F. Stocker, S.J. Johnsen, A. Landais, and J. Jouzel, 2006: Isotope calibrated Greenland temperature record over Marine Isotope Stage 3 and its relation to CH4. *Earth and Planetary Science Letters,* in press.
Hughen, K.A., J.T. Overpeck, L.C. Peterson, and S. Trumbore, 1996: Rapid climate changes in the tropical Atlantic region during the last deglaciation. *Nature,* 380(6569), 51-54.
Hughen, K.A., T.I. Eglinton, L. Xu, and M. Makou, 2004: Abrupt tropical vegetation response to rapid climate changes. *Science,* 304(5679), 1955-1959.
Hughes, M.K., and H.F. Diaz, 1994: Was There a Medieval Warm Period, and If So, Where and When. *Climatic Change,* 26(2-3), 109-142.
Humlum, O., B. Elberling, A. Hormes, K. Fjordheim, O.H. Hansen, and J. Heinemeier, 2005: Late-Holocene glacier growth in Svalbard, documented by subglacial relict vegetation and living soil microbes. *Holocene,* 15(3), 396-407.
Hurrell, J.W., 1995: Decadal Trends in the North-Atlantic Oscillation - Regional Temperatures and Precipitation. *Science,* 269(5224), 676-679.
Huybers, P., 2005: Comment on "Hockey sticks, principal components, and spurious significance" by S. McIntyre and R. McKitrick. *Geophysical Research Letters,* 32(20), Doi:10.1029/2005GL023395.
Indermühle, A., E. Monnin, B. Stauffer, T.F. Stocker, and M. Wahlen, 2000: Atmospheric CO_2 concentration from 60 to 20 kyr BP from the Taylor Dome ice core, Antarctica. *Geophysical Research Letters,* 27(5), 735-738.
IPCC, 2001: *Climate Change 2001*. Cambridge University Press, Cambridge.
Jackson, S.C., and A.J. Broccoli, 2003: Orbital forcing of Arctic climate: mechanisms of climate response and implications for continental glaciation. *Climate Dynamics,* 21, 539-557.
Jansen, E., T. Fronval, F. Rack, and J.E.T. Channell, 2000: Pliocene-Pleistocene ice rafting history and cyclicity in the Nordic Seas during the last 3.5 Myr. *Paleoceanography,* 15(6), 709-721.
Jennings, A.E., K.L. Knudsen, M. Hald, C.V. Hansen, and J.T. Andrews, 2001: A mid-Holocene shift in Arctic sea-ice variability on the East Greenland Shelf. *The Holocene,* 12, 49-58.
Joerin, U.E., T.F. Stocker, and C. Schlüchter, accepted 2005: Multi-century glacier fluctuations in the Swiss Alps during the Holocene. *The Holocene*. Accepted.
Johnsen, S., D. Dahl-Jensen, N. Gundestrup, J.P. Steffenssen, H.B. Clausen, H. Miller, V. Masson-Delmotte, A.E. Sveinbjörnsdottir, and W. J., 2001: Oxygen isotope and palaeotemperature records from six Greenland ice-core stations: Camp Century, Dye-3, GRIP, GISP2, Renland and NorthGRIP. *Journal of Quaternary Science,* 16, 299-307.
Johnsen, S.J., D. DahlJensen, N. Gundestrup, J.P. Steffensen, H.B. Clausen, H. Miller, V. Masson-Delmotte, A.E. Sveinbjornsdottir, and J. White, 2001: Oxygen isotope and palaeotemperature records from six Greenland ice-core stations: Camp Century, Dye-3, GRIP, GISP2, Renland and NorthGRIP. *Journal of Quaternary Science,* 16(4), 299-307.
Jolly, D., S.P. Harrison, B. Damnati and R. Bonnefille, 1998: Simulated climate and biomes of Africa during the Late Quaternary: comparison with pollen and lake status data. Quat. Sci. Rev., **17**, 629-657.
Jones, P.D., and M.E. Mann, 2004: Climate over past millennia. *Reviews of Geophysics,* 42(2), art. no.-RG2002.
Jones, P. D. and A. Moberg (2003). "Hemispheric and large-scale surface air temperature variations: An extensive revision and an update to 2001." Journal of Climate 16(2): 206-223.
Jones, P.D., K.R. Briffa, and T.J. Osborn, 2003: Changes in the Northern Hemisphere annual cycle: Implications for paleoclimatology? *Journal of Geophysical Research-Atmospheres,* 108(D18), art. no.-4588.
Jones, P.D., K.R. Briffa, T.P. Barnett, and S.F.B. Tett, 1998: High-resolution palaeoclimatic records for the last millennium: interpretation, integration and comparison with General Circulation Model control-run temperatures. *Holocene,* 8(4), 455-471.
Jones, P.D., T.J. Osborn, and K.R. Briffa, 1997: Estimating sampling errors in large-scale temperature averages. *Journal of Climate,* 10(10), 2548-2568.
Jones, P.D., T.J. Osborn, and K.R. Briffa, 2001: The evolution of climate over the last millennium. *Science,* 292(5517), 662-667.

Joos, F., and I.C. Prentice, 2004: A paleo-perspective on changes in atmospheric CO_2 and climate. In: *The Global Carbon Cycle: Integrating Humans, Climate and the Natural World* [C.B. Field, and M.R. Raupach (eds.)]. Vol. SCOPE series 62. Island Press, Washington DC, USA, pp. 165-186.
Joos, F., G.K. Plattner, T.F. Stocker, O. Marchal, and A. Schmittner, 1999: Global warming and marine carbon cycle feedbacks on future atmospheric CO2. *Science,* 284, 464-467.
Joos, F., I.C. Prentice, S. Sitch, R. Meyer, G. Hooss, G.K. Plattner, S. Gerber, and K. Hasselmann, 2001: Global warming feedbacks on terrestrial carbon uptake under the Intergovernmental Panel on Climate Change (IPCC) emission scenarios. *Global Biogeochemical Cycles,* 15(4), 891-907.
Joos, F., S. Gerber, I.C. Prentice, B.L. Otto-Bliesner, and P.J. Valdes., 2004: Transient simulations of Holocene atmospheric carbon dioxide and terrestrial carbon since the Last Glacial Maximum. *Global Biogeochem. Cycles,* 18, doi:10.1029/2003GB002156.
Joussaume, S., K. E. Taylor, et al. (1999). "Monsoon changes for 6000 years ago: Results of 18 simulations from the Paleoclimate Modeling Intercomparison Project (PMIP)." Geophysical Research Letters 26(7): 859--862.
Kadomura, H., 1992: *Climatic change in the west African Sahel-Sudan zone since the Little Ice Age.* In Symposium on the Little Ice Age T. Mikami (ed.), Tokyo Metropolitan University, Tokyo, pp. 40-45.
Kageyama, M., A. Laine, A. Abe-Ouchi, P. Braconnot, E. Cortijo, M. Crucifix, A. de Vernal, J. Guiot, C.D. Hewitt, A. Kitoh, M. Kucera, O. Marti, R. Ohgaito, B.L. Otto-Bliesner, W.R. Peltier, A. Rosell-Mele, G. Vettoretti, N. Weber, and M.P. Members, In press: Last Glacial Maximum temperatures over the North Atlantic, Europe, and western Siberia: a comparison between PMIP models, MARGO sea-surface temperatures and pollen-base reconstructions. In press.
Kageyama, M., S. Charbit, C. Ritz, M. Khodri, and G. Ramstein, 2004: Quantifying ice-sheet feedbacks during the last glacial inception. *Geophysical Research Letters,* 31, doi:10.1029/2004GL021339.
Kaplan, J., N. Bigelow, I. Prentice, S. Harrison, P. Bartlein, T. Christensen, W. Cramer, N. Matveyeva, A. McGuire, D. Murray, V. Razzhivin, B. Smith, D. Walker, P. Anderson, A. Andreev, L. Brubaker, M. Edwards, and A. Lozhkin, 2003: Climate change and Arctic ecosystems: 2. Modeling, paleodata-model comparisons, and future projections. *J. Geophys. Res.,* 108**,** Doi:10.1029/2002JD002559.
Kaplan, J.O., I.C. Prentice, W. Knorr, and P.J. Valdes, 2002: Modeling the dynamics of terrestrial carbon storage since the Last Glacial Maximum. *Geophysical Research Letters,* 29, doi:10.1029/2002GL015230.
Karlen, W., J.L. Fastook, K. Holmgren, M. Malmstroem, J.A. Matthews, E. Odada, J. Risberg, G. Rosquist, P. Sandgren, A. Shemesh, and W. L.-O., 1999: Glacier fluctuations on Mount Kenya since ca 6000 cal.years BP: implications for Holocene climatic change in Africa. *Ambio,* 28(5), 409-418.
Karlen, W. and Kuylenstierna, J., 1996: On solar forcing of Holocene climate: evidence from Scandinavia. *Holocene,* 6, 359-365.
Kaspar, F. and U. Cubash. Simulations of the Eemian interglacial and the subsequent glacial inception with a coupled ocean-atmosphere general circulation model. The climate of past interglacials. [F. Sirocko, T. Litt, M. Claussen, M.F. Sánchez-Goñi (eds.)], Elsevier. Accepted.
Kaspar, F., N. Kuhl, U. Cubasch, and T. Litt, 2005: A model-data comparison of European temperatures in the Eemian interglacial.,Geophysical Research Letters, 32, L11703, doi:10.1029/2005GL022456.
Kaufman, D.S., T.A. Ager, N.J. Anderson, P.M. Anderson, J.T. Andrews, P.J. Bartlein, L.B. Brubaker, L.L. Coats, L.C. Cwynar, M.L. Duvall, A.S. Dyke, M.E. Edwards, W.R. Eisner, K. Gajewski, A. Geirsdottier, F.S. Hu, A.E. Jennings, M.R. Kaplan, M.W. Kerwin, A.V. Lorhkin, G.M. MacDonald, G.H. Miller, C.J. Mock, W.W. Oswald, B.L. Otto-Bliesner, D.F. Porinchu, K. Rühland, J.P. Smol, E.J. Steig, and B.B. Wolfe, 2004: Holocene thermal maximum in the western Arctic (0-180°W). *Quaternary Science Reviews,* 23, 529-560.
Keeling, C.D., and T.P. Whorf, 2005: *Atmospheric CO2 records from sites in the SIO air sampling network.* In In Trends: A Compendium of Data on Global Change. Carbon Dioxide Information Analysis Center, Oak Ridge National Laboratory, U.S. Department of Energy, Oak Ridge, Tenn., U.S.A.
Kennett, J.P., and L.D. Stott, 1991: Abrupt deep-sea warming, palaeoceanographic changes and benthic extinctions at the end of the Palaeocene. *Nature,* 353, 225-229.
Khodri, M., G. Ramstein, N. De Noblet, and M. Kageyama, 2003: Sensitivity of the northern extratropics hydrological cycle to the changing insolation forcing at 126 and 115 ky BP. *Climate Dynamics,* 21, 273-287.

Khodri, M., M.A. Cane, G.J. Kukla, J. Gavin, and P. Braconnot, 2005: The impact of precession changes on the Arctic climate during the last interglacial glacial transition. *Earth and Planetary Science Letters,* 236, 285-304.
Khodri, M., Y. Leclainche, et al. (2001). "Simulating the amplification of orbital forcing by ocean feedbacks in the last glaciation." Nature 410: 570-574.
Kim, J.H., N. Rimbu, S.J. Lorenz, G. Lohmann, S.I. Nam, S. Schouten, C. Ruhlemann, and R.R. Schneider, 2004: North Pacific and North Atlantic sea-surface temperature variability during the Holocene. *Quarternary Science Reviews,* 23, 2141-2154.
Kitoh, A., and S. Murakami, 2002: Tropical Pacific climate at the mid-Holocene and the Last Glacial Maximum simulated by a coupled ocean-atmosphere general circulation model. *Paleoceanography,* 17, Art. No. 1047.
Klitgaard-Kristensen, D., H.P. Sejrup, H. Haflidason, S. Johnsen, and M. Spurk, 1998: The short cold period 8,200 years ago documented in oxygen isotope records of precipitation in Europe and Greenland. *Journal of Quaternary Sciences,* 13(2), 165-169.
Knies, J., J. Matthiessen, C. Vogt, and R. Stein, 2002: Evidence of 'Mid-Pliocene (similar to 3 Ma) global warmth' in the eastern Arctic Ocean and implications for the Svalbard/Barents Sea ice sheet during the late Pliocene and early Pleistocene (similar to 3-1.7 Ma). *Boreas,* 31(1), 82-93.
Knox, J.C., 2000: Sensitivity of modern and Holocene floods to climate change. *Quaternary Science Reviews,* 19(1-5), 439-457.
Knutti, R., J. Flückiger, T.F. Stocker, and A. Timmermann, 2004: Strong hemispheric coupling of glacial climate through freshwater discharge and ocean circulation. *Nature,* 430(7002), 851-856.
Koç, N., and Jansen, E., 1994: Response of the high-latitude Northern Hemisphere to orbital climate forcing. *Geology,* 22, 523-526.
Koch, J., B. Menounos, J. Clague, and G.D. Osborn, 2004: Environmental Change in Garibaldi Provincial Park, Southern Coast Mountains, British Columbia. *Geoscience Canada,* 31(3), 127-135.
Koch, P.L., J.C. Zachos, and P.D. Gingerich, 1992: Correlation between Isotope Records in Marine and Continental Carbon Reservoirs near the Paleocene Eocene Boundary. *Nature,* 358(6384), 319-322.
Koerner, R.M., 1989: Ice Core Evidence for Extensive Melting of the Greenland Ice-Sheet in the Last Interglacial. *Science,* 244(4907), 964-968.
Kohfeld, K., and S.P. Harrison, 2001: DIRTMAP: the geological record of dust. *Earth-Science Reviews,* 54, 81-114.
Kohfeld, K.E., C. LeQuéré, S.P. Harrison, and R.F. Anderson, 2005: Role of marine biology in glacial-interglacial CO2 cycles. *Science,* 308, 74-78.
Köhler, P., F. Joos, S. Gerber, and R. Knutti, 2005: Simulating changes in vegetation distribution, land carbon storage, and atmospheric CO2 in response to a collapse of the North Atlantic thermohaline circulation. *Climate Dynamics,* 25 (7-8): 689-708.
Kreveld, S.v., M. Sarnthein, H. Erlenkeuser, P. Grootes, S. Jung, M.J. Nadeau, U. Pflaumann, and A. Voelker, 2000: Potential links between surging ice sheets, circulation changes, and the Dansgaard-Oeschger cycles in the Irminger Sea, 60-18 kyr. *Paleoceanography,* 15, 425-442.
Kucera, M., A. Rosell-Mele, R.R. Schneider, C. Waelbroeck, and M. Weinelt, 2005: Multiproxy approach for the reconstruction of the glacial ocean surface (MARGO). *Quaternary Science Reviews*, 24, 813-819.
Kuhnert, H., J. Patzold, B. Hatcher, K.H. Wyrwoll, A. Eisenhauer, L.B. Collins, Z.R. Zhu, and G. Wefer, 1999: A 200-year coral stable oxygen isotope record from a high- latitude reef off western Australia. *Coral Reefs,* 18(1), 1-12.
Kukla, G.J., and e. al., 2002: Last interglacial climates. *Quaternary Research,* 58, 2-13.
Kurtz, A.C., L.R. Kump, M.A. Arthur, J.C. Zachos, and A. Paytan, 2003: Early Cenozoic decoupling of the global carbon and sulfur cycles. . *Paleoceanography,,* 18(4), Doi: 10.1029/2003PA000908.
Laird, K.R., B.F. Cumming, S. Wunsam, J.A. Rusak, R.J. Oglesby, S.C. Fritz, and P.R. Leavitt, 2003: Lake sediments record large-scale shifts in moisture regimes across the northern prairies of North America during the past two millennia. *Proceedings of the National Academy of Sciences of the United States of America,* 100(5), 2483-2488.
Lamb, H.H., 1965. The early medieval warm epoch and its sequel. *Palaeogeography Palaeoclimatology Palaeoecology,* 1(13), 13-37.
Lamb, H.H., 1977: *Climates of the past, present and future* Vol. volumes I and II. Metheun, London.
Lamb, H.H., 1982: *Climate history and the modern world*. Routledge, London and New York, 433 pp.

Lambeck, K., 2002: Sea-level change from mid-Holocene to recent time: An Australian exemple with global implications. In: *Ice Sheets, Sea Level and the Dynamic Earth* [J.X. Mitrovica, and L.A. Vermeersen (eds.)]. Vol. 29, pp. 33-50.
Lambeck, K., and J. Chappell, 2001: Sea level change through the last glacial cycle. *Science,* 292(5517), 679-686.
Landais, A., V. Masson-Delmotte, J. Jouzel, D. Raynaud, S. Johnsen, C. Huber, M. Leuenberger, J. Schwander, and B. Minster, 2006: The glacial inception as recorded in the NorthGRIP Greenland ice core: timing, structure and associated abrupt temperature changes. *Climate Dynamics,* 26(2-3), 273-284.
Lauritzen, S.E., 2003: Reconstruction Holocene Climate records from Speleothems. In: *Global Change in the Holocene* [A. Mackay, Battarbee,R., Birks, J. & Oldfield, F. (eds) (ed.). Arnold, London, pp. p. 242-263.
Lea, D.W., D.K. Pak, L.C. Peterson, and K.A. Hughen, 2003: Synchroneity of tropical and high-latitude Atlantic temperatures over the last glacial termination. *Science,* 301(5638), 1361-1364.
Lean, J., 2000: Evolution of the sun's spectral irradiance since the Maunder Minimum. *Geophysical Research Letters,* 27(16), 2425-2428.
Lean, J.L., J.T. Mariska, K.T. Strong, H.S. Hudson, L.W. Acton, G.J. Rottman, T.N. Woods, and R.C. Willson, 1995: Correlated Brightness Variations in Solar Radiative Output from the Photosphere to the Corona. *Geophysical Research Letters,* 22(5), 655-658.
Lean, J.L., Y.M. Wang, and N.R. Sheeley, 2002: The effect of increasing solar activity on the Sun's total and open magnetic flux during multiple cycles: Implications for solar forcing of climate. *Geophysical Research Letters,* 29(24), art. no.-2224.
Lear, C.H., Y. Rosenthal, H.K. Coxall, and P.A. Wilson, 2004: Late Eocene to early Miocene ice sheet dynamics and the global carbon cycle. *Paleoceanography,* 19(4), Art. No., PA4015, doi:10.1029/2004PA001039.
LeGrande, A.N., G.A. Schmidt, D.T. Shindell, C.V. Field, R.L. Miller, D.M. Koch, G. Faluvegi, and G. Hoffmann, 2006: Consistent simulations of multiple proxy responses to an abrupt climate change event. *Proceedings of the National Academy of Sciences of the United States of America,* 103(4), 837-842.
Lemasurier, W.E., and S. Rocchi, 2005: Terrestrial record of post-Eocene climate history in Marie Byrd Land, West Antarctica. *Geografiska Annaler Series a-Physical Geography,* 87A(1), 51-66.
Levis, S., G. B. Bonan, et al. (2004). "Soil feedback drives the mid-Holocene North African monsoon northward in fully coupled CCSM2 simulations with a dynamic vegetation model." Climate Dynamics 23: 791-802.
Lhomme, N., G.K.C. Clarke, and C. Ritz, 2005a: Global budget of water isotopes inferred from polar ice sheets. *Geophysical Research Letters,* 32(20) Doi: 10.1029/2005GL023774.
Lhomme, N., G.K.C. Clarke, and S.J. Marshall, 2005b: Tracer transport in the Greenland Ice Sheet: constraints on ice cores and glacial history. *Quaternary Science Reviews,* 24, 173-194.
Lie, O., Dahl, S. O., Nesje, A., Matthews, J. A., Sandvold, S., 2004: Holocene fluctuations of a polythermal glacier in high-alpine eastern Jotunheimen, central-southern Norway. *Quaternary Science Reviews,* 23(18-19), 1925-1945.
Linsley, B.K., G.M. Wellington, D.P. Schrag, L. Ren, M.J. Salinger, and A.W. Tudhope, 2004: Geochemical evidence from corals for changes in the amplitude and spatial pattern of South Pacific interdecadal climate variability over the last 300 years. *Climate Dynamics,* 22(1), 1-11.
Lisiecki, L.E., and M.E. Raymo, 2005: A Pliocene-Pleistocene stack of 57 globally distributed benthic ∂18O records. *Paleoceanography,* 20, PA1003,doi:10.1029/2004PA001071.
Liu, K.B., 2004: Paleotempestology: Principles, methods, and examples from Gulf coast lake-sediments. In: Hurricanes and Typhoons: Past, Present and Future [R. Murnane, and K. Liu (eds.)]. Columbia University Press, New York, pp. 13-57.
Liu, Z., Harrison, SP, Kutzback, JE & Otto-Bleisner, B. , 2004: Global monsoons in the mid-Holocene and oceanic feedback. *Climate Dynamics,* 22, 157-182.
Liu, Z., J.E. Kutzbach, and L. Wu, 2000: Modeling climate shift of El Niño variability in the Holocene. *Geophysical Research Letters,* 27, 2265-2268.
Liu, Z., S. Shin, B.L. Otto-Bliesner, J.E. Kutzbach, E.C. Brady, and D. Lee, 2002: Tropical cooling at the last glacial maximum and extratropical ocean ventilation. *Geophysical Research Letters,* 29, Art. No. 1409.

Lockwood, M., and R. Stamper, 1999: Long-term drift of the coronal source magnetic flux and the total solar irradiance. *Geophysical Research Letters,* 26, 2461-2464.
Lorentz, S.J., J.-H. Kim, N. Rimbu, R.R. Schneider, and G. Lohmann, 2006: Orbitally driven insolation forcing on Holocene climate trends: evidence from alkenone data and climate modeling. *Paleoceanography,* 21, doi:10.1029/2005PA001152.
Loutre, M.F., 2003: Clues from MIS 11 to predict the future climate - a modelling point of view. *Earth and Planetary Science Letters,* 212, 213-224.
Loutre, M.F., and A.L. Berger, 2000: Future climatic changes: Are we entering an exceptionally long interglacial? *Climatic Change,* 46, 61-90.
Loutre, M.F., D. Paillard, F. Vimeux, and E. Cortijo, 2004: Does mean annual insolation have the potential to change the climate? *Earth and Planetary Science Letters,* 221(1-4), 1-14.
Lozhkin, A.V., and P.M. Anderson, 1995: The last interglaciation in northeast Siberia. *Quaternary Research,* 43, 147-158.
Lubinski, D.J., S.L. Forman, and G.H. Miller, 1999: Holocene glacier and climate fluctuations on Franz Josef Land, Arctic Russia, 80 degrees N. *Quaternary Science Reviews,* 18(1), 85-108.
Luckman, B.H., and M.S. Kearney, 1986: Reconstruction of Holocene Changes in Alpine Vegetation and Climate in the Maligne Range, Jasper National-Park, Alberta. *Quaternary Research,* 26(2), 244-261.
Luckman, B.H., and R.J.S. Wilson, 2005: Summer temperatures in the Canadian Rockies during the last millennium: a revised record. *Climate Dynamics,* 24(2-3), 131-144.
Luterbacher, J., D. Dietrich, E. Xoplaki, M. Grosjean, and H. Wanner, 2004: European seasonal and annual temperature variability, trends, and extremes since 1500. *Science,* 303(5663), 1499-1503.
Luterbacher, J., E. Xoplaki, D. Dietrich, R. Rickli, J. Jacobeit, C. Beck, D. Gyalistras, C. Schmutz, and H. Wanner, 2002: Reconstruction of sea level pressure fields over the Eastern North Atlantic and Europe back to 1500. *Climate Dynamics,* 18(7), 545-561.
Macayeal, D.R., 1993: Binge/Purge Oscillations of the Laurentide Ice-Sheet as a Cause of the North-Atlantics Heinrich Events. *Paleoceanography,* 8(6), 775-784.
MacDonald, G.M., and R.A. Case, 2005: Variations in the Pacific Decadal Oscillation over the past millennium. *Geophysical Research Letters,* 32(8), Doi: 10.1029/2005GL022478.
MacDonald, G.M., Velichko, A.A., Kremenetski, C.V., Borisova, O.K., Goleva, A.A., Andreev, A.A., Cwynar, L.C., Riding, R.T., Forman, S.L., Edwards, T.W.D., Aravena, R., Hammarlund, D., Szeicz, J.M., Gattaulin, V.N. , 2000: Holocene treeline history and climate change across northern Eurasia. *Quaternary Research,* 53, 302-311.
MacFarling Meure, C.M., 2004: *The variation of atmospheric carbon dioxide, methane and nitrous oxide during the Holocene from ice core analysis*, Ph.D. Thesis, Melbourne University, 178 pp.
Machida, T., T. Nakazawa, Y. Fujii, S. Aoki, and O. Watanabe, 1995: Increase in the atmospheric nitrous oxide concentration during the last 250 years. *Geophysical Research Letters,* 22, 2921-2924.
Mackay, A., R. Battarbee, J. Birks, and F.e. Oldfield, 2003: *Global Change in the Holocene*. Hodder Arnold, 480 pp.
Mahowald, N., K. Kohfeld, M. Hannson, Y. Balkanski, S.P. Harrison, I.C. Prentice, M. Schulz, and H. Rohde, 1999: Dust sources and deposition during the Last Glacial Maximum and current climate: A comparison of model results with paleodata from ice cores and marine sediments. *Journal of Geophysical Research,* 104, 15859-15916.
Mangerud, J., V. Astakhov, and J.-I. Svendsen, 2002: The extent of the Barents-Kara Ice Sheet during the Last Glacial Maximum. *Quaternary Science Reviews,* 21, 111-119.
Mann, M.E., and G.A. Schmidt, 2003: Ground vs. surface air temperature trends: Implications for borehole surface temperature reconstructions. *Geophysical Research Letters,* 30(12), art. no.-1607.
Mann, M.E., and P.D. Jones, 2003: Global surface temperatures over the past two millennia. *Geophysical Research Letters,* 30(15), art. no.-1820.
Mann, M. E., S. Rutherford, et al. (2003). "Optimal surface temperature reconstructions using terrestrial borehole data." Journal of Geophysical Research-Atmospheres 108(D7), 10.1029/2002JD002532.
Mann, M.E., M.A. Cane, S.E. Zebiak, and A. Clement, 2005b: Volcanic and solar forcing of the tropical Pacific over the past 1000 years. *Journal of Climate,* 18(3), 447-456.
Mann, M.E., R. Bradley, and M.K. Hughes, 2000: Long-Term Variability in the El Nino/Southern Oscillation and Associated Teleconnections. In: *El Nino and the Southern Oscillation: Multiscale Variability and Global and Regional Impacts* [H.F. Diaz, and V. Markgraf (eds.)]. University Press, Cambridge, pp. 357-412.

Mann, M.E., R.S. Bradley, and M.K. Hughes, 1998: Global-scale temperature patterns and climate forcing over the past six centuries. *Nature,* 392(6678), 779-787.
Mann, M.E., R.S. Bradley, and M.K. Hughes, 1999: Northern hemisphere temperatures during the past millennium: Inferences, uncertainties, and limitations. *Geophysical Research Letters,* 26(6), 759-762.
Mann, M.E., S. Rutherford, E. Wahl, and C.M. Ammann, 2005a: Testing the fidelity of methods used in 'proxy-based' reconstructions of past climate. *Journal of Climate*, 18 (20), 4097-4107.
Marchal, O., I. Cacho, T.F. Stocker, J.O. Grimalt, E. Calvo, B. Martrat, N. Shackleton, M. Vautravers, E. Cortijo, S.v. Kreveld, C. Andersson, N. Koc, M. Chapman, L. Sbaffi, J.-C. Duplessy, M. Sarnthein, J.-L. Turon, J. Duprat, and E. Jansen, 2002: Apparent long-term cooling of the sea surface in the northeast Atlantic and Mediterranean during the Holocene. *Quaternary Science Reviews*, 21 (4-6), 455-483.
Marchal, O., R. Francois, T.F. Stocker, and F. Joos, 2000: Ocean thermohaline circulation and sedimentary 231Pa/230Th ratio. *Paleoceanography,* 6, 625-641.
Marchal, O., T.F. Stocker, F. Joos, A. Indermühle, T. Blunier, and J. Tschumi, 1999: Modelling the concentration of atmospheric CO2 during the Younger Dryas climate event. *Climate Dynamics,* 15, 341-354.
Marchant, R., and H. Hooghiemstra, 2004: Rapid environmental change in African and South American tropics around 4000 years before present : a review. *Earth Science Reviews,* 66, 217-260.
Marchitto, T.N.J., D.W. Oppo, and W.B. Curry, 2002: Paired benthic foraminiferal Cd/Ca and Zn/Ca evidence for a greatly increased presence of Southern Ocean Water in the glacial North Atlantic. *Paleoceanography,* 17, 1038,10.1029/2000PA000598.
Marra, M.J., 2003: Last interglacial beetle fauna from New Zealand. *Quarternary Research,* 59, 122-131.
Masson, V., F. Vimeux, J. Jouzel, V. Morgan, M. Delmotte, P. Ciais, C. Hammer, S. Johnsen, V.Y. Lipenkov, E. Mosley-Thompson, J.-R. Petit, E. Steig, M. Stievenard, and R. Vaikmae, 2000: Holocene climate variability in Antarctica based on 11 ice cores isotopic records. *Quaternary Research,* 54, 348-358.
Masson-Delmotte, V., A. Landais, N. Combourieu-Nebout, U. von Grafenstein, J. Jouzel, N. Caillon, J. Chappellaz, D. Dahl-Jensen, S.J. Johnsen, and B. Stenni, 2005b: Rapid climate variability during warm and cold periods in polar regions and Europe. *Comptes Rendus Geoscience,* 337(10-11), 935-946.
Masson-Delmotte, V., J. Jouzel, A. Landais, M. Stievenard, S.J. Johnsen, J.W.C. White, M. Werner, A. Sveinbjornsdottir, and K. Fuhrer, 2005a: GRIP deuterium excess reveals rapid and orbital-scale changes in Greenland moisture origin. *Science,* 309(5731), 118-121.
Masson-Delmotte, V., M. Kageyama, P. Braconnot, S. Charbit, G. Krinner, C. Ritz, E. Guilyardi, J. Jouzel, A. Abe-Ouchi, M. Crucifix, R.M. Gladstone, C.D. Hewitt, A. Kitoh, A. Legrande, O. Marti, U. Merkel, T. Motoi, R. Ohgaito, B.L. Otto-Bliesner, W.R. Peltier, I. Ross, P.J. Valdes, G. Vettoretti, N. Weber, and F. Wolk, 2006: Past and future polar amplification of climate change: climate model intercomparisons and ice-core constraints. *Climate Dynamics,* 26 (5), 513-529.
Matthews, J.A., M.S. Berrisford, P.Q. Dresser, A. Nesje, S.O. Dahl, A.E. Bjune, J. Bakke, H. John, B. Birks, O. Lie, L. Dumayne-Peaty, and C. Barnett, 2005: Holocene glacier history of Bjornbreen and climatic reconstruction in central Jotunheimen, Norway, based on proximal glaciofluvial stream-bank mires. *Quaternary Science Reviews,* 24(1-2), 67-90.
Matthews, J.A., S.O. Dahl, A. Nesje, M.S. Berrisford, and C. Andersson, 2000: Holocene glacier variations in central Jotunheimen, southern Norway based on distal glaciolacustrine sediment cores. *Quaternary Science Reviews* , 19, 1625-1647.
Mayewski, P.A., E.E. Rohling, J.C. Stager, W. Karlen, K.A. Maasch, L.D. Meeker, E.A. Meyerson, F. Gasse, S.v. Kreveld, K. Holmgren, J. Lee-Thorp, G. Rosvist, F. Rack, M. Staubwasser, R.R. Schneider, and E.J. Steig, 2004: Holocene climate variability. *Quaternary Reseach,* 62 (3), 243-255.
McDermott, F., D.P. Mattey, and C. Hawkesworth, 2001: Centennial-scale holocene climate variability revealed by a high-resolution speleothem delta O-18 record from SW Ireland. *Science,* 294(5545), 1328-1331.
McElwain, J.C., and W.G. Chaloner, 1995: Stomatol density and index of fossil plants track atmospheric carbon dioxide in the Palaeozoic. *Annals of Botany,* 76, 389-395.
McGregor, H.V., and M.K. Gagan, 2004: Western Pacific coral delta O-18 records of anomalous Holocene variability in the El Nino-Southern Oscillation. *Geophysical Research Letters,* 31(11), Doi:10.1029/2004GL019972.

McIntyre, S., and R. McKitrick, 2003: Corrections to the Mann et al. (1998) proxy database and northern hemispheric average temperature series. *Energy and Environment,* 14, 751-771.

McIntyre, S., and R. McKitrick, 2005: Hockey sticks, principal components, and spurious significance. *Geophysical Research Letters,* 32(3), art. no.-L03710.

McManus, J.F., D.W. Oppo, L. Keigwin, J. Cullen, and G. Bond, 2002: Thermohaline circulation and prolonged interglacial warmth in the North Atlantic. *Quaternary Research,* 58, 17-21.

McManus, J.F., R. Francois, J.-M. Gherardi, L. Keigwin, and S. Brown-Leger, 2004: Collapse and rapid resumption of Atlantic meridional circulation linked to deglacial climate changes. *Nature,* 428, 834-837.

Meissner, K.J., A.J. Weaver, H.D. Matthews, and P.M. Cox, 2003: The role of land surface dynamics in glacial inception: a study with the UVic Earth System Model. *Climate Dynamics,* 21, 7-8.

Meland, M.Y., E. Jansen, and H. Elderfield, 2005: Constraints on SST estimates for the northern North Atlantic/Nordic Seas during the LGM. *Quaternary Science Reviews,* 24 (7-9), 835-852.

Menounos, B., J.S. Koch, G. Osborn, J. Clague, and D. Mazzucchi, 2004: Early Holocene glacier advance, southern Coast Mountains, British Columbia, Canada. *Quaternary Science Reviews,* 23(14-15), 1543-1550.

Mickley, L.J., D.J. Jacob, and D. Rind, 2001: Uncertainty in preindustrial abundance of tropospheric ozone: Implications for radiative forcing calculations. *Journal of Geophysical Research-Atmospheres,* 106(D4), 3389-3399.

Mieding, B., 2005: *Rekonstruktion tausendjähriger aerosolchemischer Eiskernzeitreihen aus Nordostgrönland: Quantifizierung zeitlicher Veränderungen in Atmosphärenzirkulation, Emission und Deposition.* Alfred-Wegener-Inst. für Polar- und Meeresforschung, Bremerhaven. 119 pp.

Mix, A.C., A.E. Morey, N.G. Pisias, and S.W. Hostetler, 1999: Foraminiferal faunal estimates of paleotemperature: Circumventing the no-analog problem yields cool ice age tropics. *Paleoceanography,* 14, 350-359.

Moberg, A., D.M. Sonechkin, K. Holmgren, N.M. Datsenko, and W. Karlen, 2005: Highly variable Northern Hemisphere temperatures reconstructed from low- and high-resolution proxy data. *Nature,* 433(7026), 613-617.

Monnin, E., A. Indermühle, A. Dällenbach, J. Flückiger, B. Stauffer, T.F. Stocker, D. Raynaud, and J.M. Barnola, 2001: Atmospheric CO_2 concentrations over the last glacial termination. *Science,* 291(5501), 112-114.

Monnin, E., E.J. Steig, U. Siegenthaler, K. Kawamura, J. Schwander, B. Stauffer, T.F. Stocker, D.L. Morse, J.M. Barnola, B. Bellier, D. Raynaud, and H. Fischer, 2004: Evidence for substantial accumulation rate variability in Antarctica during the Holocene, through synchronization of CO2 in the Taylor Dome, Dome C and DML ice cores. *Earth and Planetary Science Letters,* 224(1-2), 45-54.

Monnin, E.A., A. Indermühle, A. Dallenbach, J. Fluckiger, B. Stauffer, T.F. Stocker, R. D., and J.M. Barnola, 2001: Atmospheric CO2 concentrations over the last glacial termination. *Science,* 291, 112-114.

Montoya, M., A. Griesel, A. Levermann, J. Mignot, M. Hofmann, A. Ganopolski, and S. Rahmstorf, 2005: The Earth System Model of Intermediate Complexity CLIMBER-3α Part I: description and performance for present day conditions. *Climate Dynamics,* 25, 237-263.

Montoya, M., H. von Storch, and T.J. Crowley, 2000: Climate simulation for 125 kyr BP with a coupled ocean-atmosphere general circulation model. *Journal of Climate,* 13, 1057-1072.

Moros, M., J.T. Andrews, D.E. Eberl, and E. Jansen, in press: The Holocene history of drift ice in the northern North Atlantic: Evidence for different spatial and temporal modes. *Paleoceangraphy*. In press.

Morrill, C., J. Overpeck, J.E. Cole, K.-B. Liu, C. Shen, and L. Tang, 2006: Holocene variations in the Asian monsoon inferred from the geochemistry of lake sediments in central Tibet. *Quaternary Research,* 65(2), 232-243.

Morrill, C., J.T. Overpeck, and J.E. Cole, 2003: A synthesis of abrupt changes in the Asian summer monsoon since the last deglaciation. *The Holocene,* 13, 465-476.

Moy, C.M., G.O. Seltzer, D.T. Rodbell, and D.M. Anderson, 2002: Variability of El Nino/Southern Oscillation activity at millennial timescales during the Holocene epoch. *Nature,* 420, 162-165.

Mudelsee, M., 2001: The phase relations among atmospheric CO_2 content, temperature and global ice volume over the past 420 ka. *Quaternary Science Reviews,* 20, 583-589.

Muhs, D.R., K.R. Simmons, and B. Steinke, 2002: Timing and warmth of the last interglacial period: New U-series evidence from Hawaii and Bermuda and a new fossil compilation for North America. *Quaternary Science Reviews,* 21, 1355-1383.
Muhs, D.R., T.A. Ager, and J.E. Beget, 2001: Vegetation and paleoclimate of the last interglacial period, central Alaska. *Quaternary Science Reviews,* 20, 41-61.
Muscheler, R., F. Joos, J. Beer, S.A. Müller, M. Vonmoos, and I. Snowball, accepted: Changes in solar activity during the last 1000 years inferred from radionuclide records. *Quaternary Science Reviews.* Accepted.
Muscheler, R., F. Joos, S.A. Müller, and I. Snowball, 2005: Climate - How unusual is today's solar activity? *Nature,* 436(7050), E3-E4.
Myhre, G., E.J. Highwood, K.P. Shine, and F. Stordal, 1998: New estimates of radiative forcing due to well mixed greenhouse gases. *Geophysical Research Letters,* 25, 2715-1718.
Nesje, A., and S.O. Dahl, 2003: The 'Little Ice Age' - only temperature? *Holocene,* 13(1), 139-145.
Nesje, A., Jansen, E., Birks, J.B., Bjune, A.E., Bakke, J., Andersson, C., Dahl, S.O., Kristensen, K., Lauritzen, S.E., Lie, O, Risebrobakken, B., Svendsen, J.-I., 2005: Holocene Climate Variability in the Northern North Atlantic Rewgion: A Review of Terrestrial and Marine Evidence. In: *The Nordic Seas: An Integrated Perspective. Geophysical Monograph Series 158* [AGU (ed.), pp. 289-322.
Nesje, A., Olaf Dahl, S, et al., 2000: The lacustrine sedimentary sequence in Sygneskardvatnet, western Norway: a continuous, high-resolution record of the Jostedalsbreen ice cap during the Holocene. *Quaternary Science Reviews,* 19, 1047-1065.
Nesje, A., S.O. Dahl, and J. Bakke, 2004: Were abrupt lateglacial and early-Holocene climatic changes in northwest Europe linked to freshwater outbursts to the North Atlantic and Arctic oceans? *The Holocene,* 14, 299-310.
Nguetsop, V.F., S. Servant-Vildary, and M. Servant, 2004: Late Holocene climatic changes in west Africa, a high resolution diatom record from equatorial Cameroon. *Quaternary Science Reviews,* 23(5-6), 591-609.
North Greenland Ice Core Project, 2004: High-resolution record of Northern Hemisphere climate extending into the last interglacial period. *Nature,* 431, 147-151.
Oerlemans, J., 2005: Extracting a climate signal from 169 glacier records. *Science,* 308(5722), 675-677.
Oppenheimer, M., and R.B. Alley, 2005: Ice sheets, global warming, and Article 2 of the UNFCCC. *Climatic Change,* 68(3), 257-267.
Oppo, D.W., J.F. McManus, and J.L. Cullen, 2003: Deepwater variability in the Holocene epoch. *Nature,* 422, 277-278.
Osborn, G., and B.H. Luckman, 1988: Holocene Glacier Fluctuations in the Canadian Cordillera (Alberta and British-Columbia). *Quaternary Science Reviews,* 7(2), 115-128.
Osborn, T., and K.R. Briffa, 2006: The spatial extent of 20th-century warmth in the context of the past 1200 years. *Science,* 311(5762), 841-844.
Osborn, T.J., and K.R. Briffa, 2004: The real color of climate change? *Science,* 306(5296), 621-622.
Osborn, T.J., Raper, S.C.B., Briffa, K.R.: (in press): Simulated climate change during the last 1,000 years: comparing the ECHO-G general circulation model with the MAGICC simple climate model. Climate Dynamics. DOI 10.1007/s00382-006-0129-5. In press.
Otterå, O.H., H. Drange, M. Bentsen, N.G. Kvamsto, and D.B. Jiang, 2004: Transient response of the Atlantic meridional overturning circulation to enhanced freshwater input to the Nordic Seas-Arctic Ocean in the Bergen climate model. *Tellus Series a-Dynamic Meteorology and Oceanography,* 56(4), 342-361.
Otto-Bliesner, B.L., 1999: El Nino La Nina and Sahel precipitation during the middle Holocene. *Geophysical Research Letters,* 26, 87-90.
Otto-Bliesner, B.L., E.C. Brady, G. Clauzet, R. Tomas, S. Levis, and Z. Kothavala, in press-b: Last Glacial Maximum and Holocene Climate in CCSM3. *Journal of Climate*. In press.
Otto-Bliesner, B.L., E.C. Brady, S.I. Shin, Z.Y. Liu, and C. Shields, 2003: Modeling El Nino and its tropical teleconnections during the last glacial-interglacial cycle. *Geophysical Research Letters,* 30(23) doi:10.1029/2003GL018553.
Otto-Bliesner, B.L., S.J. Marshall, J.T. Overpeck, and G. Miller, in press-a: Simulating polar amplification of orbital forcing for the Last Interglacial. *Science*. In press.
Overpeck, J., and K.E. Trenberth, 2004: *CLIVAR/PAGES/IPCC Workshop: A multi-millennia perspective on drought and implications for the future.*, UCAR, Boulder CO.

Overpeck, J.T., B.L. Otto-Bliesner, G.H. Miller, D. Muhs, R. Alley, and J.T. Kiehl, in press: Paleoclimatic Evidence for Future Ice Sheet Instability and Rapid Sea Level Rise. *Science*. In press.

Pagani, M., J.C. Zachos, K.H. Freeman, B. Tipple, and S. Bohaty, 2005: Marked decline in atmospheric carbon dioxide concentrations during the Paleogene. *Science,* 309(5734), 600-603.

Paillard, D., 1998: The timing of Pleistocene glaciations from a simple multiple-state climate model. *Nature,* 391, 378-381.

Pearson, P.N., P.W. Ditchfield, J. Singano, K.G. Harcourt-Brown, C.J. Nicholas, R.K. Olsson, N.J. Shackleton, and M.A. Hall, 2001: Warm tropical sea surface temperatures in the Late Cretaceous and Eocene epochs. *Nature,* 413, 481-487.

Peltier, W.R., 1996: Mantle viscosity and ice age ice sheet topography. *Science,* 273, 1359-1364.

Peltier, W.R., 1998: Postglacial variations in the level of the sea: Implications for climate dynamics and solid-earth geophysics. *Reviews of Geophysics,* 36(4), 603-689.

Peltier, W.R., 2002: On eustatic sea level history: Last Glacial Maximum to Holocene. *Quaternary Science Reviews,* 21(1-3), 377-396.

Peltier, W.R., 2004: Global glacial isostasy and the surface of the ice-age Earth: The ICE-5G (VM2) model and GRACE. *Annual Reviews of Earth and Planetary Sciences,* 32, 111-149.

Peltier, W.R., and L.P. Solheim, 2002: Dynamics of the ice age earth: solid mechanics and fluid mechanics. *J. Phys. IV France,* 12, 85-104.

Peltier, W.R., and R.G. Fairbanks, accepted: Global glacial ice volume and last glacial maximum duration from an extended Barbados sea level record. *Quarternary Science Reviews*. Accepted.

Peltier, W.R., I. Shennan, R. Drummond, and B. Horton, 2002: On the postglacial isostatic adjustment of the British Isles and the shallow viscoelastic structure of the Earth. *Geophysical Journal International,* 148(3), 443-475.

Pépin, L., D. Raynaud, J.-M. Barnola, and M.F. Loutre, 2001: Hemispheric roles of climate forcings during glacial-interglacial transitions, as deduced from the Vostok record and LLN-2D model experiments. *Journal of Geophysical Research,* 106(D23), 31,885-31,892.

Peteet, D., 1995: Global Younger Dryas. *Quaternary International,* 28, 93-104.

Peterson, L.C., G.H. Haug, K.A. Hughen, and U. Röhl, 2000: Rapid changes in the hydrologic cycle of the tropical Atlantic during the last glacial. *Science,* 290, 1947-1951.

Petit, J.R., J. Jouzel, D. Raynaud, N.I. Barkov, J.-M. Barnola, I. Basile, M. Bender, J. Chappellaz, M. Davis, G. Delaygue, M. Delmotte, V.M. Kotlyakov, M. Legrand, V.Y. Lipenkov, C. Lorius, L. Pépin, C. Ritz, E. Saltzman, and M. Stievenard, 1999: Climate and atmospheric history of the past 420,000 years from the Vostok ice core, Antarctica. *Nature,* 399, 429-436.

Petoukhov, V., A. Ganopolski, V. Brovkin, M. Claussen, A. Eliseev, C. Kubatzki, and S. Rahmstorf, 2000: CLIMBER-2: a climate system model of intermediate complexity. Part I: model description and performance for present climate. *Climate Dynamics,* 16(1), 1-17.

Pettersson, O., 1914: Climate variations in historic and prehistoric time. *Svenska Hydrogr. - Biol.Komm. Skriften 5, pp. 1-26.*

Peyron, O., C. Begeot, S. Brewer, O. Heiri, and M. Magny, 2005: Lateglacial climate in the Jura Mountains (France) based on different quantitative reconstruction approaches from pollen, lake-levels, and chironomids. *Quaternary Research,* 62 (2), pp. 197-211.

Plattner, G.K., F. Joos, T.F. Stocker, and O. Marchal, 2001: Feedback mechanisms and sensitivities of ocean carbon uptake under global warming. *Tellus Series B-Chemical and Physical Meteorology,* 53(5), 564-592.

Pollack, H.N., and J.E. Smerdon, 2004: Borehole climate reconstructions: Spatial structure and hemispheric averages. *Journal of Geophysical Research-Atmospheres,* 109(D11), art. no.-D11106.

Pollack, H.N., and S.P. Huang, 2000: Climate reconstruction from subsurface temperatures. *Annual Review of Earth and Planetary Sciences,* 28, 339-365.

Pollard, D., and S.L. Thompson, 1997: Climate and ice-sheet mass balance at the last Glacial maximum from the GENESIS Version-2 global climate model. *Quaternary Science Reviews,* 16, 841-863.

Porter, S.C., 2001: Snowline depression in the tropics during the Last Glaciation. *Quaternary Science Reviews,* 20, 1067-1091.

Prentice, I.C., D. Jolly and BIOME 6000 participants, 2000: Mid-Holocene and glacial-maximum vegetation geography of the northern continents and Africa. *Journal of Biogeography,* 27, 507-519.

Prentice, I.C., and T. Webb, 1998: BIOME 6000: reconstructing global mid-Holocene vegetation patterns from palaeoecological records. *Journal of Biogeography*, 25 (6), 997-1005.

Rahmstorf, S., 2001: Abrupt Climate Change. In: *Encyclopedia of Ocean Sciences* [J. Steele, S. Thorpe, and K. Turekian (eds.)]. Vol. 1. Academic Press, London, pp. 1-6.
Rahmstorf, S., 2002: Ocean circulation and climate during the past 120,000 years. *Nature,* 419, 207-214.
Rahmstorf, S., and H.J. Schellnhuber, 2006: *Der klimawandel*. Beck Verlag, Munich, 144 pp.
Rahmstorf, S., M. Crucifix, A. Ganopolski, H. Goosse, I. Kamenkovich, R. Knutti, G. Lohmann, R. Marsh, L.A. Mysak, Z.M. Wang, and A.J. Weaver, 2005: Thermohaline circulation hysteresis: A model intercomparison. *Geophysical Research Letters,* 32(23), doi:10.1029/2005GL023655.
Ramankutty, N., and J.A. Foley, 1999: Estimating historical changes in global land cover: Croplands from 1700 to 1992. *Global Biogeochemical Cycles,* 13(4), 997-1027.
Ravelo, A.C. et al., 1997: Pliocene carbonate accumulation along the California margin. *Paleoceangraphy,* 12, 729-741.
Raymo, M.E., and G.H. Rau, 1992: Plio-Pleistocene atmospheric CO2 levels inferred from POM d13C at DSDP Site 607. *Eos,* 73, 95.
Raymo, M.E., B. Grant, M. Horowitz, and G.H. Rau, 1996: Mid-Pliocene warmth: Stronger greenhouse and stronger conveyor. *Marine Micropaleontology,* 27(1-4), 313-326.
Raymo, M.E., W. F. Ruddiman, J. Backman, B. M. Clement, and D.G. Martinson, 1989: Late Pliocene variation in northern hemisphere ice sheets and North Atlantic deep water circulation. *Paleoceanography,* 4, 413-446.
Raynaud, D., J.-M. Barnola, R. Souchez, R. Lorrain, J.-R. Petit, P. Duval, and V.Y. Lipenkov, 2005: The record for marine isotopic stage 11. *Nature, 436 (7047), 39-40.*
Renssen, H., and Vandenberghe, 2003: Investigation of the relationship between permafrost distribution in NW Europe and extensive winter sea-ice cover in the North Atlantic Ocean during the cold phases of the Last Glaciation. *Quaternary Science Reviews,* 22, 209-223.
Renssen, H., H. Goosse, and T. Fichefet, 2002: Modeling the effect of freshwater pulses on the early Holocene climate : the influence of high frequency climate variability. *Paleoceanography,* 17, Art. No. 1020.
Renssen, H., H. Goosse, T. Fichefet, and J.M. Campin, 2001: The 8.2 kyr BP event simulated by a global atmosphere-sea-ice-ocean model. *Geophysical Research Letters,* 28(8), 1567-1570.
Renssen, H., V. Brovkin, T. Fichefet, and H. Goosse, 2003: Holocene climate instability during the termination of the African humid period. *Geophysical Research Letters,* 30, Art. No. 1184.
Ridgwell, A.J., A.J. Watson, M.A. Maslin, and J.O. Kaplan, 2003: Implications of coral reef buildup for the controls on atmospheric CO2 since the Last Glacial Maximum *Paleoceanography,* 18(4), Doi: 10.1029/2003PA000893.
Rimbu, N., G. Lohmann, S.J. Lorenz, J.H. Kim, and R.R. Scheider, 2004: Holocene climate variability as derived from alkenone sea surface temperature and coupled ocean-atmosphere model experiments. *Climate Dynamics,* 23, 215-227.
Rind, D., and M.A. Chandler, 1991: Increased ocean heat transports and warmer climate. *J. Geophys. Res.,* 96, 7437-7461.
Rind, D., J. Perlwitz, and P. Lonergan, 2005: AO/NAO response to climate change: 1. Respective influences of stratospheric and tropospheric climate changes. *Journal of Geophysical Research-Atmospheres,* 110(D12), Doi: 10.1029/2004JD005103.
Risebrobakken, B., E. Jansen, C. Andersson, E. Mjelde, and K. Hevroy, 2003: A high resolution study of Holocene paleoclimatic and paleoceanographic changes in the Nordic Seas. *Paleoceanography,* 18, 1-14.
Risebrobakken, B., T.M. Dokken, and E. Jansen, 2005: Extent and variability of the meridional atlantic circulation in the eastern nordic seas during marine isotope stage 5 and its influence on the inception of the last glacial. In: *The Nordic Seas: An Integrated Perspective* [H. Drange, T. Dokken, T. Furevik, R. Gerdes, and A. Berger (eds.)]. Vol. 158. AGU, Washington D.C., pp. 323-340.
Robertson, A., J. Overpeck, D. Rind, E. Mosley-Thompson, G. Zielinski, J. Lean, D. Koch, J. Penner, I. Tegen, and R. Healy, 2001: Hypothesized climate forcing time series for the last 500 years. *Journal of Geophysical Research-Atmospheres,* 106(D14), 14783-14803.
Robock, A., and M.P. Free, 1995: Ice Cores as an Index of Global Volcanism from 1850 to the Present. *Journal of Geophysical Research-Atmospheres,* 100(D6), 11549-11567.
Roche, D., D. Paillard, and E. Cortijo, 2004: Constraints on the duration and freshwater release of Heinrich event 4 through isotope modelling. *Nature,* 432, 379-382.
Rodbell, D.T., G.O. Seltzer, D.M. Anderson, M.B. Abbott, D.B. Enfield, and J.H. Newman, 1999: An ~15,000-year record of El Niño-driven alluviation in southwestern Ecuador. *Science,* 283, 516-520.

Roethlisberger, F., and M.A. Geyh, 1985: Glacier variations in Himalayas and Karakorum. *Zeitschrift fuer Gletscherkunde und Glaizialgeolgy,* 21, 237-249.
Rosell-Mele, A., E. Bard, K.-C. Emeis, B. Grieger, C.D. Hewitt, P. Muller, J., and R.R. Schneider, 2004: Sea surface temperature anomalies in the oceans at the LGM estimated from the alkenone-$U^{K'}_{37}$ index: comparison with GCMs. *Geophysical Research Letters,* 31, L03208.
Rosenthal, Y., and A.J. Broccoli, 2004: In search of Paleo-ENSO. *Science,* 304, 219-221.
Rostami, K., W.R. Peltier, and A. Mangini, 2000: Quaternary marine terraces, sea-level changes and uplift history of Patagonia, Argentina. Comparisons with predictions of ICE-4G (VM2) model of the global process of glacial isostatic adjustment. *Quat.Sci.Rev,* 19, 1495-1525.
Röthlisberger, R., M. Bigler, E.W. Wolff, F. Joos, E. Monnin, and M.A. Hutterli, 2004: Ice core evidence for the extent of past atmospheric CO_2 change due to iron fertilisation. *Geophysical Research Letters,* 31(16), *Art. No. L16207*.
Royer, D., 2003: Estimating latest Cretaceous and Tertiary atmospheric CO2 from stomatal indices. In: *Causes and Consequences of Globally Warm Climates in the Early Paleogene* [S.L. Wing, P.D. Gingerich, B. Schmitz, and E. Thomas (eds.)]. Vol. 369. Geological Society of America Special Paper, pp. 79-93.
Royer, D.L., in press: CO2-forced climate thresholds during the Phanerozoic. *Geochimica Et Cosmochimica Acta*. In press.
Royer, D. L., R. A. Berner, et al. (2004). "CO2 as a primary driver of Phanerozoic climate." GSA Today 14(3): 4-10.
Royer, D.L., S.L. Wing, D.J. Beerling, D.W. Jolley, P.L. Koch, L.J. Hickey, and R.A. Berner, 2001: Paleobotanical evidence for near present-day levels of atmospheric CO2 during part of the tertiary. *Science,* 292(5525), 2310-2313.
Ruddiman, W.F., 1997: *Tectonic Uplift and Climate Change.* [W.F. Ruddiman (ed). Plenum Press, 535 pp.
Ruddiman, W.F., 2003: Orbital insolation, ice volume and greenhouse gases. *Quaternary Science Reviews,* 15-17, 1597-1629.
Ruddiman, W.F., 2005: Cold climate during the closest Stage 11 analog to recent Millennia. *Quaternary Science Reviews,* 24, 1111-1121.
Ruddiman, W.F., and J.S. Thomson, 2001: The case for human causes of increased atmospheric CH4. *Quaternary Science Reviews,* 20(18), 1769-1777.
Ruddiman, W.F., S.J. Vavrus, and J.E. Kutzbach, 2005: A test of the overdue-glaciation hypothesis. *Quaternary Science Reviews,* 24, 1-10.
Ruddiman, W. F., 2000: Title: Earth's Climate: Past and Future. Freeman. 465 pp.
Russell, J.M., T.C. Johnson, and M.R. Talbot, 2003: A 725 yr cycle in the climate of central Africa during the late Holocene. *Geology,* 31(8), 677-680.
Rutberg, R.L., S.R. Hemming, and S.L. Goldstein, 2000: Reduced North Atlantic deep water flux to the glacial Southern Ocean inferred from neodymium isotope ratios. *Nature,* 405, 935-938.
Rutherford, S., and M.E. Mann, 2004: Correction to "Optimal surface temperature reconstructions using terrestrial borehole data" by Mann et al. *Journal of Geophysical Research-Atmospheres,* 109(D11107), *doi*: 10.1029/2003JD004163.
Rutherford, S., M.E. Mann, T.J. Osborn, R.S. Bradley, K.R. Briffa, M.K. Hughes, and P.D. Jones, 2005: Proxy-based Northern Hemisphere surface temperature reconstructions: Sensitivity to method, predictor network, target season, and target domain. *Journal of Climate,* 18(13), 2308-2329.
Rutherford, S., M.E. Mann, T.L. Delworth, and R.J. Stouffer, 2003: Climate field reconstruction under stationary and nonstationary forcing. *Journal of Climate,* 16(3), 462-479.
Sànchez Goñi, M.F., I. ICacho, J.-L. Turon, J. Guiot, F.J. Sierro, J.-P. Peypouquet, J. Grimalt, and N.J. Shackleton, 2002: Sinchroneity between marine and terrestrial responses to millennial scale climatic varriability during the last glacial period in the Mediterranean region. *Climate Dynamics,* 19, 95-105.
Sarnthein, M., R. Gersonde, S. Niebler, U. Pflaumann, R. Spielhagen, J. Thiede, G. Wefer, and M. Weinelt, 2003b: Overview of the Glacial Atlantic Ocean Mapping (GLAMAP 2000). *Paleoceanography,* 18, 1030, doi:10.1029/2002PA000769.
Sarnthein, M., U. Pflaumann, and M. Weinelt, 2003a: Past extent of sea ice in the northern North Atlantic inferred from foraminiferal paleotemperature estimates. *Paleoceanography,* 18, doi:10.1029/2002PA000771.
Scherer, R.P., A. Aldahan, S. Tulaczyk, G. Possnert, H. Engelhardt, and B. Kamb, 1998: Pleistocene collapse of the West Antarctic ice sheet. *Science,* 281(5373), 82-85.

Scholze, M., W. Knorr, and M. Heimann, 2003: Modelling terrestrial vegetation dynamics and carbon cycling for an abrupt climate change event. *The Holocene,* 13, 327-333.
Schubert, S.D., M.J. Suarez, P.J. Pegion, R.D. Koster, and J.T. Bacmeister, 2004: Causes of long-term drought in the US Great Plains. *Journal of Climate,* 17(3), 485-503.
Schulz, M., A. Paul, and A. Timmermann, 2004: Glacial-interglacial contrast in climate variability at centennial-to-millenial timescales: observations and conceptual model. *Quaternary Science Reviews,* 23, 2219-2230.
Schwander, J., J.M. Barnola, C. Andrie, M. Leuenberger, A. Ludin, D. Raynaud, and B. Stauffer, 1993: The Age of the Air in the Firn and the Ice at Summit, Greenland. *Journal of Geophysical Research-Atmospheres,* 98(D2), 2831-2838.
Seager, R., Y. Kushnir, C. Herweijer, N. Naik, and J. Velez, 2005: Modeling of tropical forcing of persistent droughts and pluvials over western North America: 1856-2000. *Journal of Climate,* 18(19), 4065-4088.
Seppa, H., and H.J.B. Birks, 2001: July mean temperature and annual precipitation trends during the Holocene in the Fennoscandian tree-line area: pollen-based climate reconstructions. *Holocene,* 11, 527-539.
Severinghaus, J.P., and E.J. Brook, 1999: Abrupt climate change at the end of the last glacial period inferred from trapped air in polar ice. *Science,* 286(5441), 930-934.
Shackleton, N., J.C. Hall, and D. Pate, 1995: Pliocene stable isotope stratigraphy of ODP Site 846. Proceedings of the Ocean Drilling Program, Scientific Results, (138), 337-356 pp.
Shackleton, N.J., 1977: Carbon-13 in Uvigerina: Tropical rainforest history and the equatorial Pacific carbonate dissolution cycles. In: *The fate of fossil fuel CO2 in the ocean* [Andersen ,N and A. Malahoff (ed.). Plenum, New York, pp. 401-428.
Shackleton, N.J., 2000: The 100,000-year ice-age cycle identified and found to lag temperature, carbon dioxide, and orbital eccentricity. *Science,* 289, 1897-1902.
Shackleton, N.J., M.A. Hall, and A. Boersma, 1984: Oxygen and Carbon Isotope Data from Leg-74 Foraminifers. *Initial Reports of the Deep Sea Drilling Project,* 74(MAR), 599-612.
Shin, S.I., P.D. Sardeshmukh, R.S. Webb, R.J. Oglesby, and J.J. Barsugli, in press : Understanding the mid-Holocene climate. *Journal of Climate*. In press.
Shin, S.I., Z. Liu, B.L. Otto-Bliesner, E.C. Brady, J.E. Kutzbach, and S.P. Harrison, 2003: A simulation of the Last Glacial Maximum Climate using the NCAR CSM. *Climate Dynamics,* 20, 127-151.
Shindell, D.T., G.A. Schmidt, M.E. Mann, and G. Faluvegi, 2004: Dynamic winter climate response to large tropical volcanic eruptions since 1600. *Journal of Geophysical Research-Atmospheres,* 109(D5), art. no.-D05104.
Shindell, D.T., G.A. Schmidt, M.E. Mann, D. Rind, and A. Waple, 2001: Solar forcing of regional climate change during the maunder minimum. *Science,* 294(5549), 2149-2152.
Shindell, D.T., G.A. Schmidt, R.L. Miller, and M.E. Mann, 2003: Volcanic and solar forcing of climate change during the preindustrial era. *Journal of Climate,* 16(24), 4094-4107.
Shulmeister, J., and B.G. Lees, 1995: Pollen evidence from tropical Australia for the onset of an ENSO-dominated climate at c. 4000 BP. *The Holocene,* 5, 10-18.
Shuman, B., W. Thompson, P. Bartlein, and J.W. Williams, 2002: The anatomy of a climatic oscillation: vegetation change in eastern North America during the Younger Dryas chronozone. *Quaternary Science Reviews,* 21(16-17), 1777-1791.
Siegenthaler, U., E. Monnin, K. Kawamura, R. Spahni, J. Schwander, B. Stauffer, T.F. Stocker, J.M. Barnola, and H. Fischer, 2005a: Supporting evidence from the EPICA Dronning Maud Land ice core for atmospheric CO_2 changes during the past millennium. *Tellus Series B-Chemical and Physical Meteorology,* 57(1), 51-57.
Siegenthaler, U., T.F. Stocker, E. Monnin, D. Luthi, J. Schwander, B. Stauffer, D. Raynaud, J.M. Barnola, H. Fischer, V. Masson-Delmotte, and J. Jouzel, 2005b: Stable carbon cycle-climate relationship during the late Pleistocene. *Science,* 310(5752), 1313-1317.
Sigman, D.M., and E.A. Boyle, 2000: Glacial/interglacial variations in atmospheric carbon dioxide. *Nature,* 407, 859-869.
Six, D., Reynaud, L., Letréguilly, A., 2001: Bilans de masse des glaciers alpins et scandinaves, leurs relations avec l oscillation du climat de l Atlantique nord. *C. R. Acad. Sci. Paris, Sciences de la Terre et des planètes / Earth and Planetary Sciences* 333, 693–698.
Sloan, L.C., T.J. Crowley, and D. Pollard, 1996: Modeling of middle Pliocene climate with the NCAR GENESIS general circulation model. *Mar. Micropaleontol.,* 27, 51-61.

Smerdon, J.E., H.N. Pollack, V. Cermak, J.W. Enz, M. Kresl, J. Safanda, and J.F. Wehmiller, 2004: Air-ground temperature coupling and subsurface propagation of annual temperature signals. *Journal of Geophysical Research-Atmospheres,* 109(D21), art. no.-D21107.
Smerdon, J.E., H.N. Pollack, V. Cermak, J.W. Enz, M. Kresl, J. Safanda, and J.F. Wehmiller, in press: Daily, seasonal and annual relationships between air and subsurface temperatures. *Journal of Geophysical Research-Atmospheres*. In press.
Smith, J.A., G.O. Seltzer, D.L. Farber, D.T. Rodbell, and R.C. Finkel, 2005: Early local last glacial maximum in the tropical Andes. *Science,* 308, 678-681.
Sokratov, S.A., and R.G. Barry, 2002: Intraseasonal variation in the thermoinsulation effect of snow cover on soil temperatures and energy balance *Journal of Geophysical Research-Atmospheres,* 107(D19), art. no.-4374.
Solanki, S.K., and N.S. Krivova, 2003: Can solar variability explain global warming since 1970? *Journal of Geophysical Research - Space Physics,* 108, Art. No. 1200.
Solanki, S.K., I.G. Usoskin, B. Kromer, M. Schüssler, and J. Beer, 2004: Unusual activity of the Sun during recent decades compared to the previous 11,000 years. *Nature,* 431, 1084-1087.
Soon, W., and S. Baliunas, 2003: Proxy climatic and environmental changes of the past 1000 years. *Climate Research,* 23(2), 89-110.
Spahni, R., J. Chappellaz, T.F. Stocker, L. Loulergue, G. Hausammann, K. Kawamura, J. Flückiger, J. Schwander, D. Raynaud, V. Masson-Delmotte, and J. Jouzel, 2005: Atmospheric methane and nitrous oxide of the late Pleistocene from Antarctic ice cores. *Science,* 310(5752), 1317-1321.
Spahni, R., J. Schwander, J. Flückiger, B. Stauffer, J. Chappellaz, and D. Raynaud, 2003: The attenuation of fast atmospheric CH_4 variations recorded in polar ice cores. *Geophysical Research Letters,* 30(11), Doi: 10.1029/2003GL017093.
Stager, J.C., and P.A. Mayewski, 1997: Abrupt Early to Mid-Holocene Cliamtic transition registered at the Equator and the Poles. *Science,* 276, 1834 - 1836.
Stager, J.C., B.F. Cumming, and L.D. Meeker, 2003: A 10,000-year high-resolution diatom record from Pilkington Bay, Lake Victoria, East Africa. *Quaternary Research,* 59(2), 172-181.
Stager, J.C., D. Ryves, B.F. Cumming, L.D. Meeker, and J. Beer, 2005: Solar variability and the levels of Lake Victoria, East Africa, during the last millenium. *Journal of Paleolimnology,* 33(2), 243-251.
Stahle, D.W., and M.K. Cleaveland, 1992: Reconstruction and analysis of spring rainfall over southeastern U.S. for the past 1000 years. *Bulletin of the American Meteorological Society,* 73, 1947-1961.
Stahle, D.W., R.D. D'Arrigo, P.J. Krusic, M.K. Cleaveland, E.R. Cook, R.J. Allan, J.E. Cole, R.B. Dunbar, M.D. Therrell, D.A. Gay, M.D. Moore, M.A. Stokes, B.T. Burns, J. Villanueva-Diaz, and L.G. Thompson, 1998: Experimental dendroclimatic reconstruction of the Southern Oscillation. *Bulletin of the American Meteorological Society,* 79(10), 2137-2152.
Stauffer, B., G. Fischer, A. Neftel, and H. Oeschger, 1985: Increase of Atmospheric Methane Recorded in Antarctic Ice Core. *Science,* 229(4720), 1386-1388.
Steele, L.P., E.J. Dlugokencky, P.M. Lang, P.P. Tans, R.C. Martin, and K.A. Masarie, 1992: Slowing down of the accumulation of atmospheric methane uring the 1980s. *Nature,* 358, 313-16.
Stendel, M., I.A. Mogensen, and J.H. Christensen, 2006: Influence of various forcings on global climate in historical times using a coupled atmosphere-ocean general circulation model. *Climate Dynamics,* 26(1), 1-15.
Stenni, B., V. Masson-Delmotte, S. Johnsen, J. Jouzel, A. Longinelli, E. Monnin, R. Rothlisberger, and E. Selmo, 2001: An oceanic cold reversal during the last deglaciation. *Science,* 293, 2074-2077.
Stern, D.I., 2005: Global sulfur emissions from 1850 to 2000. *Chemosphere,* 58, 163-175.
Stieglitz, M., S.J. Dery, V.E. Romanovsky, and T.E. Osterkamp, 2003: The role of snow cover in the warming of arctic permafrost. *Geophysical Research Letters,* 30(13), art. no.-1721.
Stocker, T.F., 1998: Climate change - The seesaw effect. *Science,* 282(5386), 61-62.
Stocker, T.F., and E. Monnin, 2003: Past rates of carbon dioxide changes and their relevance for future climate. *Pages News,* 11(1), 6-8.
Stocker, T.F., and S.J. Johnsen, 2003: A minimum thermodynamic model for the bipolar seesaw. *Paleoceanography,* 18(4), Doi: 10.1029/2003PA000920.
Stott, L., K. Cannariato, R. Thunell, G.H. Haug, A. Koutavas, and S. Lund, 2004: Decline in surface temperature and salinity in the western tropical Pacific ocean in the Holocene epoch. *Nature,* 431, 56-59.
Stouffer, R.J., J. Yin, J.M. Gregory, K.W. Dixon, M.J. Spelman, W. Hurlin, A.J. Weaver, M. Eby, G.M. Flato, H. Hasumi, A. Hu, J. Jungclaus, V. Kamenkovich, A. Levermann, M. Montoya, S. Murakami,

S. Nawarth, A. Oka, W.R. Peltier, D.Y. Robitaille, A. Solokov, G. Vettoretti, and N. Weber, in press: Investigating the causes of the response of the thermohaline circulation to the past and future climate changes. *Journal of Climate*. In press.
Sutton, R.T., and D.L.R. Hodson, 2005: Atlantic Ocean forcing of North American and European summer climate. *Science,* 309(5731), 115-118.
Svendsen, J.I., and J. Mangerud, 1997: Holocene glacial and climatic viriations on Spitsbergen, Svalbard. *The Holocene,* 7, 45-57.
Svensen, H., and e. al., 2004: Release of methane from a volcanic basin as a mechanism for initial Eocene global warming. *Nature,* 429, 542-545.
Tarasov, L., and W.R. Peltier, 2003: Greenland glacial history, borehole constraints, and Eemian extent. *Journal of Geophysical Research,* 108, 2143,doi:10.1029/2001JB001731.
Tarasov, L., and W.R. Peltier, 2005: Arctic freshwater forcing of the Younger Dryas cold reversal. *Nature,* 435(7042), 662-665.
Taylor, K.E., C.D. Hewitt, P. Braconnot, A.J. Broccoli, C. Doutriaux, J.F.B. Mitchell, and P.P. Groups, 2000: Analysis of forcing, response, and feedbacks in a paleoclimate modeling experiment. In: *Paleoclimate Modelling Intercomparison Project (PMIP)* [P. Braconnot (ed.). Vol. WCRP-111, WMO/TD-No. 1007, pp. 43-49.
Tett, S.F.B., R. Betts, T.J. Crowley, J.M. Gregory, T.C. Johns, A. Jones, T.J. Osborn, E. Ostrom, D.L. Roberts, and M.J. Woodage, in press: The impact of natural and anthropogenic forcings on climate and hydrology since 1550. *Climate Dynamics*. In press.
Thomas, E., 2003: *Extinction and food at the seafloor: A high-resolution benthic foraminiferal record across the initial Eocene thermal maximum, Southern Ocean site 690.*, 319-332. pp.
Thompson, L.G., 2000: Ice core evidence for climate change in the Tropics: implications for our future. *Quaternary Science Reviews,* 19(1-5), 19-35.
Thompson, L.G., 2001: Stable isotopes and their relationship to temperature as recorded in low latitude ice cores. In: *Geological perspectives of global climate change* [L.C. Gerhard, W.E. Harrison, and B.M. Hanson (eds.)], American Ass. of Petroleum Geologists, pp. 99-119.
Thompson, L.G., T. Yao, E. Mosley-Thompson, M.E. Davis, K.A. Henderson, and P.N. Lin, 2000: A high-resolution millennial record of the South Asian Monsoon from Himalayan ice cores. *Science,* 289(5486), 1916-1919.
Thompson, R.S., 1991: Pliocene environments and climates in the Western United States. *Quat. Sci. Rev.,* 10, 115-132.
Thompson, R.S., and R.F. Fleming, 1996: Middle Pliocene vegetation: reconstructions, paleoclimate inferences, and boundary conditions for climate modeling. *Mar. Micropaleontol.,* 27, 27-49.
Tinner, W., and A.F. Lotter, 2001: Central European vegetation response to abrupt climate change at 8.2 ka. *Geology,* 29, 551-554.
Toracinta, E.R., R.J. Oglesby, and D.H. Bromwich, 2004: Atmospheric response to modified CLIMAP ocean boundary conditions during the Last Glacial Maximum. *Journal of Climate,* 17, 504-522.
Trenberth, K.E., and B.L. Otto-Bliesner, 2003: Toward integrated reconstruction of past climates. *Science,* 300(5619), 589-591.
Tripati, A.K., and H. Elderfield, 2004: Abrupt hydrographic changes in the equatorial Pacific and subtropical Atlantic from foraminiferal Mg/Ca indicate greenhouse origin for the thermal maximum at the Paleocene-Eocene Boundary. *Geochemistry Geophysics Geosystems,* 5, DOI 10.1029/2003GC000631.
Tudhope, A.W., C.P. Chilcott, M.T. McCulloch, E.R. Cook, J. Chappell, R.M. Ellam, D.W. Lea, J.M. Lough, and G.B. Shimmield, 2001: Variability in the El Niño-Southern Oscillation through a glacial-interglacial cycle. *Science,* 291, 1511-1517.
Tzedakis, P.C., 2005: Towards an understanding of the response of southern European vegetation to orbital and suborbital climate variability. *Quaternary Science Reviews,* 24, 1585-1599.
Urban, F.E., J.E. Cole, and J.T. Overpeck, 2000: Influence of mean climate change on climate variability from a 155-year tropical Pacific coral record. *Nature,* 407(6807), 989-993.
Usoskin, I. G., S. K. Solanki, et al. (2003). "Millennium-Scale Sunspot Number Reconstruction: Evidence for an Unusually Active Sun since the 1940s." Physical Review Letters 91(19 Nov), 211101.
Vellinga, M., and R.A. Wood, 2002: Global climatic impacts of a collapse of the Atlantic thermohaline circulation. *Climatic Change,* 54(3), 251-267.
Verschuren, D., 2001: Reconstructing fluctuations of a shallow East African lake during the past 1800 yrs from sediment stratigraphy in a submerged crater basin. *Journal of Paleolimnology,* 25(3), 297-311.

Veski, S., H. Seppa, and A.E.K. Ojala, 2004: Cold event at 8200 yr BP recorded in annually laminated lake sediments in eastern Europe. *Geology,* 32(8), 681-684.
Vidal, L., L. Labeyrie, and T.C.E. van Weering, 1998: Benthic delta O-18 records in the North Atlantic over the last glacial period (60-10 kyr): Evidence for brine formation. *Paleoceanography,* 13(3), 245-251.
Villalba, R., A. Lara, J.A. Boninsegna, M. Masiokas, S. Delgado, J.C. Aravena, F.A. Roig, A. Schmelter, A. Wolodarsky, and A. Ripalta, 2003: Large-scale temperature changes across the southern Andes: 20th-century variations in the context of the past 400 years. *Climatic Change,* 59(1-2), 177-232.
Vincent, C., P. Ribstein, V. Favier, P. Wagnon, B. Francou, E. Le Meur, and D. Six, 2005: Glacier fluctuations in the Alps and in the tropical Andes. *Comptes Rendus Geoscience,* 337(1-2), 97-106.
Voelker, A.H.L., 2002: Global distribution of centennial-scale records for Marine Isotope Stage (MIS) 3: a database. *Quaternary Science Reviews,* 21(10), 1185-1212.
von Grafenstein, U., E. Erlenkeuser, J. Müller, J. Jouzel, and S. Johnsen, 1998: The cold event 8,200 years ago documented in oxygen isotope records of precipitation in Europe and Greenland. *Climate Dynamics,* 14, 73-81.
von Storch, H., and E. Zorita, 2005: Comment on "Hockey sticks, principal components, and spurious significance" by S. McIntyre and R. McKitrick. *Geophysical Research Letters,* 32(20), Doi: 10.1029/2005GL022753.
Von Storch, H., E. Zorita, J.M. Jones, Y. Dimitriev, F. Gonzalez-Rouco, and S.F.B. Tett, 2004: Reconstructing past climate from noisy data. *Science,* 306(5296), 679-682.
Vuille, M., and M. Werner, 2005: Stable isotopes in precipitation recording South American summer monsoon and ENSO variability: observations and model results. *Climate Dynamics,* 25(4), 401-413.
Vuille, M., M. Werner, R.S. Bradley, and F. Keimig, 2005: Stable isotopes in precipitation in the Asian monsoon region. *Journal of Geophysical Research-Atmospheres,* 110(D23), Doi: 10.1029/2005JD006022.
Waelbroeck, C., L. Labeyrie, E. Michel, J.C. Duplessy, J.F. McManus, K. Lambeck, E. Balbon, and M. Labracherie, 2002: Sea-level and deep water temperature changes derived from benthic foraminifera isotopic records. *Quaternary Science Reviews,* 21(1-3), 295-305.
Waelbroeck, C., S. Mulitza, H. Spero, T. Dokken, T. Kiefer, and E. Cortijo, 2005: A global compilation of late Holocene planktonic foraminiferal d18O: relationship between surface water temperature and d18O. *Quarternary Science Reviews,* 24, 853-858.
Wahl, E.R., and C.M. Ammann, accepted: Robustness of the Mann, Bradley, Hughes reconstruction of Northern Hemisphere surface temperatures: Examination of criticisms based on the nature and processeing of proxy climate evidence. *Climatic Change*. Accepted.
Wahl, E.R., and D.M. Ritson, accepted: Reconstruction of century-scale temperature variations. *Science*. Accepted.
Wang, Y., H. Cheng, R.L. Edwards, Y. He, X. Kong, Z. An, J. Wu, M.J. Kelly, C.A. Dykoski, and X. Li, 2005b: The Holocene Asian Monsoon: Links to Solar Changes and North Atlantic Climate *Science,* 308, 854-857.
Wang, Y., L.A. Mysak, Z.M. Wang, and V. Brovkin, 2005a: The greening of the McGill paleoclimate model. Part II: Simulation of Holocene millennial-scale natural climate changes. *Climate Dynamics,* 24(5), 481-496.
Wang, Y.J., H. Cheng, R.L. Edwards, Z.S. An, J.Y. Wu, C.C. Shen, and J.A. Dorale, 2001: A high-resolution absolute-dated late Pleistocene monsoon record from Hulu Cave, China. *Science,* 294, 2345-2348.
Wang, Y.M., and N.R. Sheeley, 2003: Modeling the Sun's large-scale magnetic field during the Maunder minimum. *Astrophysical Journal,* 591(2), 1248-1256.
Wang, Y.M., J.L. Lean, and N.R. Sheeley, 2005: Modeling the sun's magnetic field and irradiance since 1713. *Astrophysical Journal,* 625, 522-538.
Wang, Z., and L.A. Mysak, 2002: Simulation of the last glacial inception and rapid ice sheet growth in the McGill Paleoclimate model. *Geophysical Research Letters,* 29, doi:10.1029/2002GL015120.
Webb, R.S., S.J. Lehman, D. Rind, R. Healy, and D. Sigman, 1997: Influence of ocean heat transport on the climate of the Last Glacial Maximum. *Nature,* 385, 695-699.
Williams, J.W., D.M. Post, L.C. Cwynar, A.F. Lotter, and A.J. Levesque, 2002: Rapid and widespread vegetation responses to past climate change in the North Atlantic region. *Geology,* 30(11), 971-974.
Williams, J.W., T.I. Webb, P.H. Richard, and P. Newby, 2000: Late Quaternary biomes of Canada and the eastern United States. *Journal of Biogeography,* 27, 585-607.

Williams, P.W., D.N.T. King, J.-X. Zhao, and K.D. Collerson, 2004: Speleothem master chronologies : combined Holocene 18O and 13C records from the north Island of New Zealand and their palaeoenvironmental interpretation. *The Holocene,* 14, 194-208.

Wing, S.L., G.J. Harrington, F.A. Smith, J.I. Bloch, D.M. Boyer, and K.H. Freeman, 2005: Transient floral change and rapid global warming at the Paleocene-Eocene boundary. *Science,* 310(5750), 993-996.

Wise, S.W.J., J.R. Breza, D.M. Harwood, and W. Wei, 1991: Paleogene glacial history of Antarctica. In: *Controversies in Modern Geology: Evolution of Geological Theories in Sedimentology, Earth History and Tectonics* [D.W. Müller, J.A. McKenzie, and H. Weissert (eds.)]. Cambridge University Press, Cambridge, pp. 133-171.

Wohlfahrt, J., S.P. Harrison, and P. Braconnot, 2004: Synergestic feedbacks between ocean and vegetation on mid- and high- latitude climates during the mid-Holocene. *Climate Dynamics,* 22, 223-238.

Woodhouse, C.A., and J.T. Overpeck, 1998: 2000 years of drought variability in the central United States. *Bulletin of the American Meteorological Society,* 79(12), 2693-2714.

Wyputta, U., and B.J. McAvaney, 2001: Influence of vegetation changes during the Last Glacial Maximum using the BMRC atmospheric general circulation model. *Climate Dynamics,* 17, 923-932.

Xia, Q.K., H.X. Zhao, and K.D. Collerson, 2001: Early-Mid Holocene climatic variations in Tasmania, Australia: multi-proxy records in a stalagmite from Lynds Cave. *Earth and Planetary Science Letters,* 194(1-2), 177-187.

Yapp, C.J., and H. Poths, 1992: Ancient atmospheric CO2 pressures inferred from natural goethites. *Nature,* 355, 342-344.

Yokoyama, Y., K. Lambeck, P. De Deckker, P. Johnston, and L.K. Fifield, 2000: Timing of the Last Glacial Maximum from observed sea-level minima. *Nature,* 406(6797), 713-716.

Yokoyama, Y., K. Lambeck, P. De Deckker, P. Johnston, and L.K. Fifield, 2001: correction: Timing of the Last Glacial Maximum from observed sea-level minima. *Nature,* 406, 99.

Zachos, J., M. Pagani, L. Sloan, E. Thomas, and K. Billups, 2001: Trends, rhythms, and aberrations in global climate 65 Ma to present. *Science,* 292(5517), 686-693.

Zachos, J.C., D. Kroon, P. Blum, and e. al., 2004: *Early cenozoic extreme climates: the Walvis ridge transcet, Sites 1262-1267.* Ocean Drilling Program, Texas.

Zachos, J.C., M.W. Wara, S. Bohaty, M.L. Delaney, M.R. Petrizzo, A. Brill, T.J. Bralower, and I. Premoli-Silva, 2003: A transient rise in tropical sea surface temperature during the Paleocene-Eocene Thermal Maximum. *Science,* 302((5650)), 1551-1554.

Zachos, J. C., D. Kroon, et al. (2004). Early Cenozoic Extreme Climates: The Walvis Ridge Transect. Proceedings of the Ocean Drilling Program, Initial Reports Leg 208. College Station, Texas.

Zachos, J.C., U. Rohl, S.A. Schellenberg, A. Sluijs, D.A. Hodell, D.C. Kelly, E. Thomas, M. Nicolo, I. Raffi, L.J. Lourens, H. McCarren, and D. Kroon, 2005: Rapid acidification of the ocean during the Paleocene-Eocene thermal maximum. *Science,* 308(5728), 1611-1615.

Zhang, D.e., 2005: Severe Drought Events as Revealed in the Climate Record of China and Their Temperature Situations over the Last 1000 Years. *National Climate Center*(4), 485-491.

Zhang, R., and T.L. Delworth, 2005: Simulated tropical response to a substantial weakening of the Atlantic thermohaline circulation. *Journal of Climate,* 18(12), 1853-1860.

Zhao, Y., P. Braconnot, O. Marti, S.P. Harrison, C. Hewitt, A. Kitoh, Z. Liu, U. Mikolajewicz, B. Otto-Bliesner, S.L. Weber, 2005: A multi-model analysis of the role of the ocean on the African and Indian monsoon during the mid-Holocene, *Climate Dynamics*, 25, (7-8), 777-800.

Zielinski, G.A., 2000: Use of paleo-records in determining variability within the volcanism–climate system. *Quaternary Science Reviews,* 19(1), 417-438.

Zorita, E., F. Gonzalez-Rouco, and S. Legutke, 2003: Testing the Mann et al. (1998) approach to paleoclimate reconstructions in the context of a 1000-yr control simulation with the ECHO-G coupled climate model. *Journal of Climate,* 16(9), 1378-1390.

Question 6.1: What Caused the Ice Ages and Other Important Climate Changes Before the Industrial Era?

Climate on Earth has changed on all time scales, long before human activity could have played a role. Great progress has been made in understanding the causes and mechanisms of these climate changes. There is not one major cause or "driver" of past climate changes, but several. For each case – be it the Ice Ages, the warmth at the time of the dinosaurs or the ups-and-downs of the past millennium – the specific causes must be established individually. In many cases this can now be done with good confidence, and many past climate changes can be reproduced with quantitative models.

Our global climate is determined by the radiation balance of the planet (see Chapter 1, Question 1.1). There are three fundamental ways to change the radiation balance and hence cause a climate change: (1) changing the incoming solar radiation (e.g., by changes in the Earth's orbit or in the sun itself), (2) changing the fraction of solar radiation that is reflected (this fraction is called the albedo – it can be changed e.g., by changes in cloud cover, aerosols or land cover), and (3) altering the long-wave back-radiation (e.g., by changes in the greenhouse gas concentration). In addition, local climate also depends on how heat is distributed by winds and ocean currents. All of these factors have played a role in past climate changes.

Starting with the Ice Ages that have come and gone in regular cycles for the past nearly 3 million years, it is now well established that these are caused by regular variations in the Earth's orbit around the sun, the so-called Milankovich cycles. These cycles change the amount of solar radiation received at each latitude in each season (but hardly the global, annual mean), and they can be calculated with astronomical precision. There is still some discussion how exactly this starts and ends ice ages, but the most likely scenario is that the amount of summer sunshine on northern continents is crucial: if it drops below a critical value, snow from the past winter does not melt away in summer and an ice sheet starts to grow as more and more snow accumulates. Climate model simulations confirm that an Ice Age can indeed be started in this way (e.g., Khodri et al., 2001, Loutre, 2003), while simple conceptual models have been used to successfully "hind-cast" the onset of past glaciations based on the orbital changes (Paillard, 1998). The next large minimum in northern summer insolation, similar to ones that started past Ice Ages, is due in ~50,000 years.

Although it is not their primary cause, atmospheric CO_2 also plays an important role in the Ice Ages. Antarctic ice core data show that CO_2 concentration is low in the cold glacial times (~190 ppm), and high in the warm interglacials (~280 ppm); atmospheric CO_2 follows the climate changes with a lag of some hundreds of years. Because the climate changes at the beginning and end of ice ages take several thousand years, most of these changes are affected by a positive CO_2 feedback; i.e., a small initial cooling due to the Milankovich cycles is subsequently amplified as the CO_2 concentration falls. Model simulations of Ice Age climate (see discussion in Section 6.4.2.1) yield realistic results only if the role of CO_2 is accounted for.

Within the Ice Ages, over 20 abrupt and dramatic climate shifts have occurred that are particularly prominent in records around the northern Atlantic (see Section 6.3). These differ from the glacial-interglacial cycles in that they probably do not involve large changes in global mean temperature: changes are not synchronous in Greenland and Antarctica, and they have the opposite sign in South and North Atlantic. This means we do not need to look for a major change in global radiation balance as their cause; a redistribution of heat within the climate system will suffice. There is indeed strong evidence that changes in ocean circulation and heat transport can explain many features of these abrupt events; sediment data and model simulations show that some of these changes could have been triggered by instabilities in the ice sheets surrounding the Atlantic at the time.

Much warmer times have also occurred in climate history – during most of the past 500 million years our planet was probably completely free of ice sheets (geologists can tell from the marks ice leaves on rock), unlike today, where Greenland and Antarctica are ice covered. Data on greenhouse gases going back beyond a million years, that is beyond the reach of Antarctic ice cores, are still rather uncertain, but analysis from sediment cores suggest that the warm ice-free periods coincide with high atmospheric CO_2 levels. On million-year time scales, CO_2 levels change due to tectonic activity, which affects the rates of CO_2-exchange of ocean and atmosphere with the solid Earth. See Box 6.1 for more about these ancient climates.

Another likely cause of past climatic changes has been variations in the energy output of the sun. We know from measurements over recent decades that the solar output varies slightly (by close to 0.1%) in an 11-year cycle, and that these variations are correlated with the number of sunspots, as well as with cosmic rays reaching the Earth's surface. Hence, sunspot observations (going back to the 17th Century), as well as cosmogenic isotope data provide evidence for longer-term changes in solar activity. Such data show that the coldest periods of the past millennium coincide with minima in solar activity – for example, the Maunder minimum around the year 1700 (see Section 6.5). Data correlation, as well as model simulations, indicate that solar variability and volcanic activity are likely to be leading reasons for climate variations of the past millennium, before the start of the industrial era.

These examples illustrate that different climate changes in the past had different causes. However, these natural causes very likely cannot explain the warming of the past few decades. Milankovich cycles or tectonic changes act too slowly; solar activity shows no clear trend since 1940 (although it has increased until then, changes in oceanic or atmospheric circulation could not explain a global warming trend, and neither can volcanic activity.

Question 6.2: Is the Current Climate Change Unusual Compared to Earlier Changes in Earth's History?

Climate has changed on all time scales throughout Earth's history. Some aspects of the current climate change are not unusual, but others are. CO_2 concentration in the atmosphere has reached a million-year record high at an exceptionally fast rate. Current global temperatures are as warm as they have ever been during the past eight centuries, probably even for millennia. And faster rates of global-mean warming than those of the past 30 years (about 0.19ºC per decade) are at least not documented in the records from the past. If warming continues unabated, the resulting climate change within this century would be extremely unusual even in geological terms.

When comparing the current climate change to earlier, natural ones, we need to make three distinctions. First, we need to be clear which variable we are comparing: is it greenhouse gas concentration or temperature (or some other climate parameter), and is it their absolute value or their rate of change? Second, we must not confuse local with global changes. Local climate changes are often much larger than global ones, since local factors (e.g., changes in oceanic or atmospheric circulation) can shift the delivery of heat or moisture from one place to another and local feedbacks operate (e.g., sea ice feedback). Large changes in global mean, in contrast, require some global forcing (such as a change in greenhouse gas concentration or solar activity). Third, we must distinguish between time scales. Climate changes over millions of years can be much larger and have different causes (e.g., continental drift) compared to climate changes on a century time-scale.

The main reason for the current concern about climate change is the rise in atmospheric CO_2 concentration, which is very unusual for the Quaternary (about the last 2 million years). CO_2 concentration is now known accurately almost half a million years back in time from Antarctic ice cores, and the new EPICA core will provide a record 700,000 years back in time, when analyses are finished. During this time, CO_2 concentration has varied between a low of 190 ppm during cold glacial times and a high of 290 ppm during warm interglacials. Over the past two centuries, it has increased to 380 ppm (see Chapter 2). For comparison, the ~80 ppm rise in CO_2 concentration at the end of the past Ice Ages generally took over 5,000 years. Higher values than at present have only occurred many millions of years ago (see Question 6.1).

Temperature is a more difficult variable to reconstruct than CO_2 (a globally well-mixed gas), as it does not have the same value all over the globe, so that a single record (e.g., an ice core) is only of limited value. Local temperature fluctuations, even those over just a few decades, can be several degrees, which is larger than the global warming signal of the past century of ~0.6ºC. Hence, in most places the global "signal" does not clearly exceed the "noise" of natural variability, and some regions of the Earth are cooling despite the global warming trend (see Chapter 3). Although they must not be over-interpreted, local records can still be interesting. For example, oxygen isotope data of the Dye 3 ice core from southern Greenland, which is the closest to the Medieval Viking settlement, shows that in the mid-20th Century the highest oxygen-18 values were reached, suggesting the warmest temperatures for several millennia in this region.

More meaningful for global changes is an analysis of large-scale (global or hemispheric) averages, where much of the local variations average out and variability is smaller. Sufficient coverage of instrumental records only goes back ~150 years. On this time scale, the current warming is clearly unusual – the globally warmest years on record are 1998, 2002, 2003, and 2001 (see Chapter 3). Further back in time we have compilations of proxy data from tree rings, ice cores etc., going back 1–2 millennia, with decreasing spatial coverage for earlier periods (see Section 6.5). While there are still differences between those reconstructions and significant uncertainties remain, all published reconstructions find that temperatures were warm during the Middle Ages, and then cooled to low values in the 17th, 18th, and 19th centuries, warming rapidly after that. The medieval level of warmth was reached again in the mid-20th Century, and has thus been exceeded since then. Independent support for this conclusion comes from models driven by reconstructed forcings, including solar variability. Since proxies indicate similar solar activity in the mid-20th Century as in medieval times, this conclusion is robust with respect to a scaling of the amplitude of solar variability, or any possible amplifying mechanisms.

Proxy data for the period before 2000 years ago have not been systematically compiled into large-scale averages, but they do not provide evidence for warmer-than-present global annual-mean temperatures going back through the Holocene (the last 11,600 years – see Section 6.4), or even at the peak of the previous interglacial period (~125,000 years ago – see Section 6.3). Models can reproduce past warm climates when orbital forcing (Milankovich cycles, see Question 6.1) is accounted for. There are strong indications that a still warmer climate, with much reduced global ice cover, prevailed until around 3 million years ago. Hence, current warmth appears unusual in the context of the past millennia, but not unusual on longer time scales for which changes in tectonic activity become relevant (see Box 6.1).

A different matter is the current rate of warming of 0.19ºC per decade. Are more rapid *global* climate changes recorded in proxy data? The largest temperature changes of the past million years are the glacial cycles, during which the global mean temperature changed by 4–7ºC between ice ages and warm interglacial periods (local changes were much larger, for example near the continental ice sheets). However, the data indicate that the global warming at the end of an ice age was a gradual process taking ~5,000 years, yielding a mean rate of around 0.01ºC per decade (see Section 6.3). The much-discussed abrupt climate shifts during glacial times (also see Section 6.3) are not counter-examples, since they were probably due to changes in ocean heat-transport which would hardly affect the global mean temperature.

Further back in time, beyond ice core data, the time resolution of sediment cores and other archives does not resolve changes as fast as the present warming. Hence, although large climate changes have occurred in the past, we have no evidence of these proceeding at a faster rate than present warming. Neither do we know of a mechanism other than a rapid greenhouse gas release that could lead to equally rapid global warming. If the more pessimistic projections of ~5ºC warming in this century are realised, then the Earth will have experienced the same amount of global-mean warming as it did at the end of the last Ice Age; however, this rate of future change would then very likely be much faster than any comparable global temperature increase of the last 50 million years.

Tables

Table 6.1. Records of Northern Hemisphere temperature shown in Figure 6.11.

Series	Period	Description		Reference
[I1]	1856–2004	HadCRUT2v land & marine temperatures for the full NH		Jones and Moberg, 2003
[I2]	1856–2004	Standard errors for [I1]		Jones et al., 1997
[I3]	1781–2004	CRUTEM2v land only temperatures for the NH		Jones and Moberg, 2003; extended using data from Jones et al., 2003
[I4]	1721–2003	Average of central England, de Bilt, Berlin & Uppsala		
Proxy-based reconstructions of temperature				
Series	**Period**	**Season**	**Region**	**Reference**
[R1]	1000–1991	Summer	Land, 20–90°N	Jones et al., 1998; calibrated by Jones et al., 2001
[R2]	1000–1980	Annual	Land+marine, 0–90°N	Mann et al., 1999
[R3]	1402–1960	Summer	Land, 20–90°N	Briffa et al., 2001
[R4]	831–1992	Annual	Land, 20–90°N	Esper et al., 2002; recalibrated by Cook et al., 2004a
[R5]	1–1993	Summer	Land, 20–90°N	Briffa, 2000; calibrated by Briffa et al., 2004
[R6]	200–1980	Annual	Land+marine, 0–90°N	Mann and Jones, 2003
[R7]	1400–1960	Annual	Land+marine, 0–90°N	Rutherford et al., 2005
[R8]	1–1979	Annual	Land+marine, 0–90°N	Moberg et al., 2005
[R9]	713–1995	Annual	Land, 20–90°N	D'Arrigo et al., 2006
[R10]	558–1960	Annual	Land, 20–90°N	Hegerl et al., in press
[R11]	1500–2000	Annual	Land, 0–90°N	Pollack and Smerdon, 2004; reference level adjusted following Moberg et al., 2005
[R12]	1600–1990	Summer	Global land	Oerlemans, 2005

Table 6.2. Climate model simulations shown in Figure 6.13a-d.

Series	**Label**	**Model**	**Model type**	**Forcings[a]**	**Reference**
[S1]	GSZ2003	ECHO-G	GCM	SV-G----	Gonzalez-Rouco et al., 2003; von Storch et al., 2004
[S2]	ORB2006	ECHO-G/MAGICC	GCM adjusted using EBM	SV-G-A-O	Osborn et al., in press
[S3]	TBC..2006	HadCM3	GCM	SVOG-ALO	Tett et al., in press
[S4]	AJS..2006	NCAR CSM	GCM	SV-G-A-O	Mann et al., 2005a
[S5]	BLC..2002	MoBiDiC	EMIC	SV-G-AL-	Bertrand et al., 2002b
[S6]	CBK..2003	-	EBM	SV-G-A--	Crowley et al., 2003
[S7]	GRT..2005	ECBilt-CLIO	EMIC	SV-G-A--	Goosse et al., 2005b
[S8]	GJB..2003	Bern CC	EBM	SV-G-A-O	Gerber et al., 2003
[S9]	B..03-14C	Climber2	EMIC (solar from ^{14}C)	SV----C-L-	Bauer et al., 2003
[S10]	B..03-10Be	Climber2	EMIC (solar from ^{10}Be)	SV----C-L-	Bauer et al., 2003
[S11]	GBZ..2006	ECHO-G	GCM	SV-G----	Gonzalez-Rouco et al., 2006
[S12]	SMC2006	ECHAM4/OPYC3	GCM	SV-G-A-O	Stendel et al., 2006

Notes:
(a) Forcings: S=solar, V=volcanic, O=orbital, G=well-mixed greenhouse gases, C=CO_2 but not other greenhouse gases, A=tropospheric sulphate aerosol, L=land-use change, O=tropospheric and/or stratospheric ozone changes and/or halocarbons

Table 6.3. Simulations with intermediate complexity climate models shown in Figure 6.13e.

Models:	
Bern2.5CC	Plattner et al., 2001
Climber2	Petoukhov et al., 2000
Climber3α	Montoya et al., 2005
Forcings:	
Volcanic	Forcing from Crowley, 2000, used in all runs
Solar	'Bard25' runs used strong solar irradiance changes, based on ^{10}Be record scaled to give a Maunder Minimum irradiance 0.25% lower than today, from Bard et al., 2000 'Bard08-WLS' runs used weak solar irradiance changes, using sunspot records and a model of the Sun's magnetic flux for the period since 1610, from Wang et al., 2005, and extended before this by the ^{10}Be record scaled to give a Maunder Minimum irradiance 0.08% lower than today
Anthropogenic	'All' runs included anthropogenic forcings after 1765, from Joos et al., 2001 'Nat' runs did not include any anthropogenic forcings

Appendix 6.A: Glossary

Alkalinity
A measure of the buffering capacity of water, or the capacity of bases to neutralize acids.

Alkenones
Complex organic molecules found in fossil shells of plant plankton and used to reconstruct past temperatures.

Allerød
An abrupt warming event around 13,000 years ago seen in Greenland and elsewhere. See also the Bølling event; the two are often referred to together as the Bølling-Allerød Period: 14,500–12,900 years ago, characterized by warmer conditions in many places and for much of the time.

Bølling
An abrupt warming event around 14,500 years ago. See also the Allerød event.

Calendar-based time
Age determination in actual years, distinguished from 14C based time,

Carbonate compensation depth
The level in the oceans at which the rate of supply of calcium carbonate (calcite and aragonite) equals the rate of dissolution, such that no calcium carbonate is preserved.

Chronology
Arrangement of events according to dates or times of occurrence.

Clathrate (methane)
A partly frozen slushy mix of methane gas and ice, usually found in sediments.

Cosmogenic isotopes
Rare isotopes which are created when a high-energy cosmic ray interacts with the nucleus of an in situ atom. Often used as indications of solar magnetic activity (which can shield cosmic rays) or as a tracer of atmospheric transport. Also called cosmogenic nuclides.

Dansgaard-Oeschger (DO) events
Abrupt warming events followed by gradual cooling. Seen in Greenland ice cores and other areas at intervals of 1500 to 7000 years during glacial intervals.

Diatom
Silt-sized algae that live in surface waters of lakes, rivers, and oceans and form shells of opal. Their distribution in ocean cores is often related to past sea surface temperatures.

Eccentricity
The extent to which the Earth's orbit around the Sun departs from a perfect circle.

Eocene
The Eocene epoch (55–34 million years ago) is a major division of the geologic timescale and the second epoch of the Palaeogene period in the Cenozoic era.

Foraminifera (planktonic)
Sand-sized organisms (protozoans) that live in ocean surface waters and form shells made out of $CaCO_3$. Their distribution in ocean cores is often used as an indication of sea surface temperatures in past climates.

Gravitational equilibrium
The state in which gravitational forces pulling inward on a particle are balanced by some outward pressure.

Ground surface temperatures (GST)
The temperature of the ground near the surface (often within the first 10 cm).

Heinrich event
An interval of rapid flow of icebergs from the margins of ice sheets into the North Atlantic Ocean, causing deposition of sediment eroded from the land. Indicative of cold events, followed by rapid warming. During the last glacial time period, six such events occurred in the last 75,000 years.

Holocene Climate Optimum
The Holocene Climate Optimum is vague term to denote a warm period during roughly the interval 9,000 to 5,000 years ago. This event has also been known by many other names, including: Hypisthermal, Altithermal, Climatic Optimum, Holocene Optimum, Holocene Thermal Maximum, and Holocene Megathermal. In reality the warming was primarily during Northern Hemisphere summer, and was not synchronous across the hemisphere.

Holocene Thermal Optimum (HTO)
See Holocene Climatic Optimum

Ice core
Cylinders of ice drilled out of glaciers and polar ice sheets

Insolation
The amount of solar radiation arriving at the top of Earth's atmosphere by latitude and by season.

Interglacial
The periods between ice age glaciations

Lake Agassiz
Once the largest proglacial lake in North America. Evidence of glacial Lake Agassiz occurs over an area of roughly 365,000 square miles, an area five times the size of the state of North Dakota, although at no single time did the lake ever cover this entire area. Ice margin positions and lowering of outlets by erosion combined to limit the size of the lake at any given time. Glacial Lake Agassiz was the latest in a series of proglacial lakes that must have formed in the Red River Valley many times during the Ice Age, each time north-draining rivers were impounded by ice sheets spreading south out of Canada and again as the glaciers receded.

Last Interglacial (LIG)
Time period previous to the present when the Earth did not have land ice sheets outside Greenland and Antarctica. Dated approximately from 129,000 to 115,000 years ago.

Laurentide ice sheet
The largest of the Northern Hemisphere ice sheets that grow and shrink at orbital cycles, covering east-central Canada and the northern United States east of the Rockies.

Little Ice Age
An interval between approximately 1400 and 1900 AD when temperatures in the Northern Hemisphere were generally colder than today's, especially in Europe.

Medieval Warm Period (MWP)
An interval between 1000 and 1300 AD in which some Northern Hemisphere regions were warmer than in the Little Ice Age that followed.

Megadrought
Long-drawn out and pervasive drought much longer than normal, usually lasting a decade or more.

Neoglaciation

Advances, often associated with mountain glaciers, of smaller extent than the major glaciations of the ice ages. Term also often applies to cooling associated with advancing glaciers.

Ocean plankton
Organisms that float in the upper layers of oceans.

O-isotopes [oxygen isotope ratio]
Ratio of oxygen-18 to oxygen-16 as determined from foraminifera tests of deep-ocean cores, as well as coral skeletons, ice layers of ice sheets, and other types of paleoclimatic sample.

Paleocene
The Paleocene epoch (65–55 million years ago) is the first geologic epoch of the Palaeogene period in the modern Cenozoic era.

Paleocene-Eocene Thermal Maximum (PETM)
Beginning at the end of the Paleocene the PETM (55.5 to 54.8 million years before present), was one of the most rapid and extreme global warming events recorded in geologic history.

Paleosols
A soil horizon that formed on the surface during the geologic past, that is, an ancient soil. Also know as a buried soil; fossil soil.

Permafrost
A permanently frozen mixture of rocks, soil and water occurring in very cold regions.

Pleistocene
The earlier of two Quaternary epochs, extending from the end of the Pliocene, about 1.8 million years ago, until the beginning of the Holocene about 10,000 years ago.

Pliocene
The Pliocene epoch is the period in the geologic timescale that extends from 5.3 million to 1.8 million years before present.

Pollen [analysis]
A technique of both relative dating and environmental reconstruction, consisting of the identification and counting of pollen types preserved in peats, lake sediments, and other deposits.

Preboreal Oscillation (PBO)
In northern and central Europe, early Preboreal warming was soon followed by a short climatic reversal. The cooling began some hundreds of years after the end of the Younger Dryas, with the event then occurring between about 11,300 and 11,150 years ago.

Quaternary
The period of geological time following the Tertiary Period. It is formed of two epochs, the Pleistocene and Holocene, and it extends form 1.8 million years ago until the present.

Radiometric dating
The process of determining the age of rocks from the decay of their radioactive elements.

Reconstructions
The use of climate indicators to help determine (generally past) climates.

See-saw
Oscillation envisioned as possible in the climate-system, perhaps between the two polar regions.

Sr/Ca ratios

The ratio between strontium and calcium in biologically-precipitated CaCO3 that has been successfully used as a temperature proxy (e.g., in corals and sclerosponges) to represent past ocean temperature variations.

Tree-rings
Concentric rings of secondary wood evident in a cross-section of the stem of a woody plant. The difference between the dense, small-celled late wood of one season and the wide-celled early wood of the next enables the age of a tree to be estimated, and the ring widths or density can be related to climate parameters such as temperature and precipitation.

Younger Dryas
Younger Dryas Period: 12,900–11,600 years ago, characterized by colder conditions in many locations, especially circum-North Atlantic.

13C
Stable isotope of carbon having molecular weight 13.

14C
Unstable isotope of carbon having molecular weight 14 and a half-life of about 5700 years, often used for dating purposes. Its variation in time is affected by the magnetic fields of the sun and earth.

231Pa/230Th
As part of the uranium radioactive decay, Protactinium-231 decays to Thorium-230 with a half-life of 32,000 yrs; used for longer-term dating.

8.2K-event
Following the post-glacial warming, a rapid climate oscillation with a cooling of about 400 years occurred at about 8,200 years ago.

Chapter 6: Paleoclimate

Coordinating Lead Authors:
Eystein Jansen, Jonathan Overpeck

Lead Authors:
Keith R. Briffa, Jean-Claude Duplessy, Fortunat Joos, Valérie Masson-Delmotte, Daniel O. Olago, Bette Otto-Bliesner, Wm. Richard Peltier, Stefan Rahmstorf, Rengaswamy Ramesh, Dominique Raynaud, David H. Rind, Olga Solomina, Ricardo Villalba, De'er Zhang.

Contributing Authors:
Jean-Marc Barnola, Eva Bauer, Mark Chandler, Julia Cole, Edward R. Cook, Elsa Cortijo, Trond Dokken, Dominik Fleitmann, Myriam Khodri, Laurent Labeyrie, Anders Levermann, Øyvind Lie, Marie-France Loutre, Erik Monnin, Daniel Muhs, Tim Osborn, Frederic Parrenin, Gian-Kasper Plattner, Henry N. Pollack, Øyvind Paasche, Lowell Stott, Ellen Mosley-Thompson, Renato Spahni, Guo-Zheng-Tang, Lonnie Thompson, Claire Waelbroeck, Jim Zachos.

Review Editors: Jean Jouzel, John Mitchell

Date of Draft: 7 March 2006

Notes: TSU compiled version

Figures

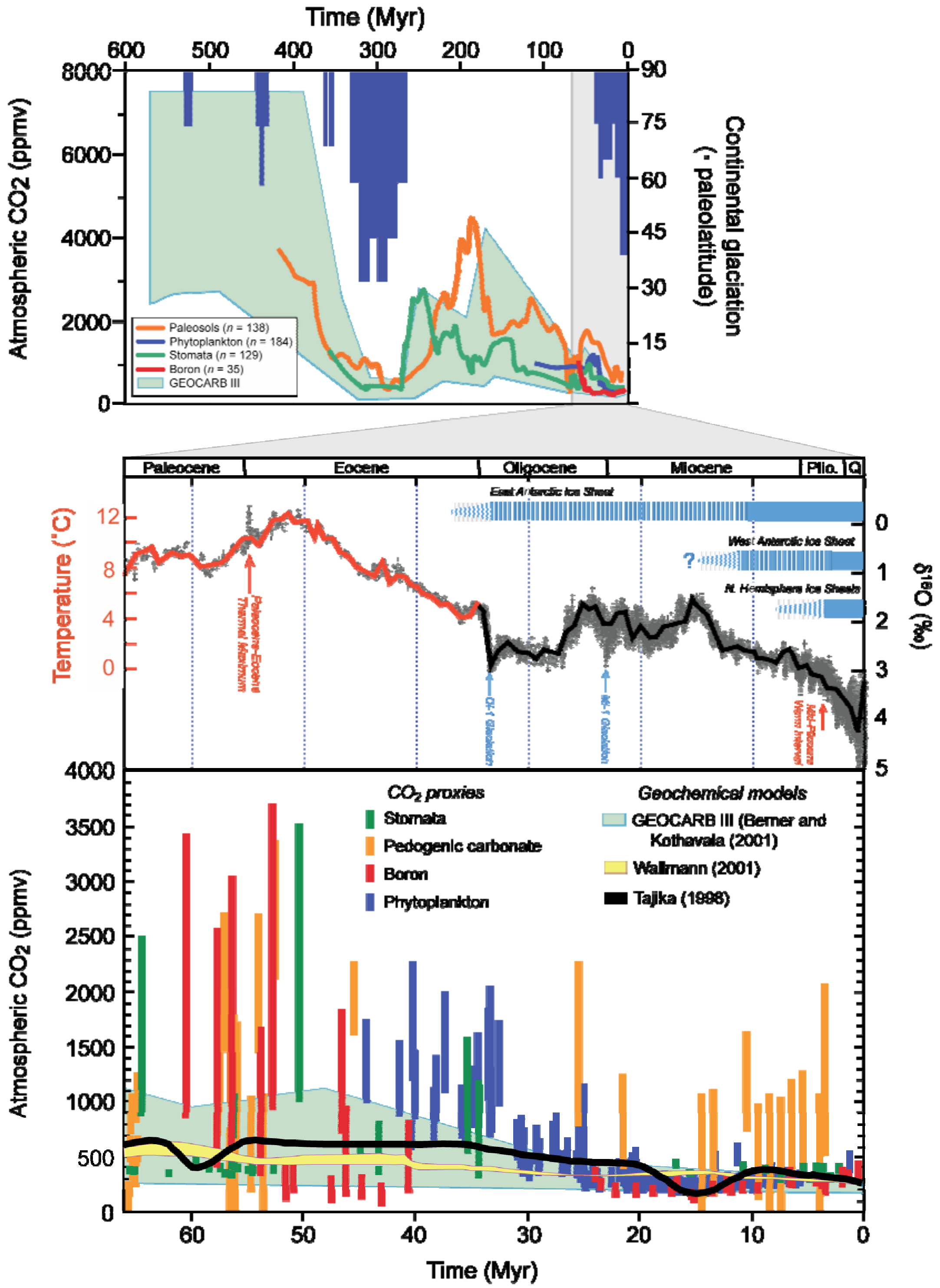

Figure 6.1. Top panel: Records of atmospheric CO_2 and continental glaciation for the Phanerozoic Eon (542 Myr ago to present). Vertical blue bars mark the timing and paleolatitudinal extent of continental glaciations (after Crowley, 1998). The plotted CO_2 records represent five-point running averages of CO_2 reconstructions from each of the four major proxies (see Royer, in press for details of compilation). Also plotted are the plausible ranges of CO_2 predictions from the geochemical carbon cycle model GEOCARB III (Berner and Kothavala, 2001). All data have been adjusted to the Gradstein et al. (2004) timescale.
Middle panel: The global compilation of deep sea benthic foraminifera oxygen isotope records from 40 DSDP and ODP sites (Zachos et al., 2001) updated with the addition of high-resolution records for the interval spanning the Eocene through Miocene (Billups et al., 2002; Bohaty and Zachos, 2003; Lear et al., 2004). Most data were derived from analyses of two common and long-lived benthic taxa, *Cibicidoides* and

Nuttallides. To correct for genus-specific isotope vital effects, the ^{18}O values were adjusted by +0.64 and +0.4 (Shackleton et al., 1984), respectively. The ages are relative to the GPTS of Berggren et al. (1995). The raw data were smoothed using a five-point running mean, and curve-fitted with a locally weighted mean. The ^{18}O temperature scale was computed assuming an ice-free ocean [~1.2 Standard Mean Ocean Water (SMOW)], and thus only applies to the time preceding the onset of large-scale glaciation on Antarctica (~35 Myr ago). From that time (early Oligocene) to the present, much of the variability (~70%) in the ^{18}O record reflects changes in Antarctica and Northern Hemisphere ice volume. The presumption of a negligible contribution from ice sheets prior to about 35 Myr ago, and large ice-sheets thereafter, is supported by several lines of evidence, including the distribution of glaciomarine sediment or ice-rafted debris near or on Antarctica, and by changes in the distribution and abundances of clay minerals associated with physical weathering in proximal margin and deep-sea sediments (e.g., Hambrey et al., 1991; Wise et al., 1991; Ehrmann and Mackensen, 1992). The horizontal bars (shown in light blue) provide a qualitative representation of ice volume in Northern Hemisphere and Antarctic ice sheets. The dashed bars represent periods of partial or ephemeral ice, while the solid bars represent ice sheets of modern or greater size. The evolution and stability of the West Antarctic ice sheet (e.g. Lemasurier and Rocchi, 2005) remains an important area of uncertainty that could impact estimates of future sea level rise.
Bottom panel: Detailed record of CO_2 for the last 65 Myr. Individual records of CO_2 and associated errors are color-coded by proxy method; when possible, records are based on replicate samples (see Royer, in press for details). Error terms for age are typically <±1 Myr. Also plotted are the plausible ranges of CO_2 predictions from three geochemical carbon cycle models.

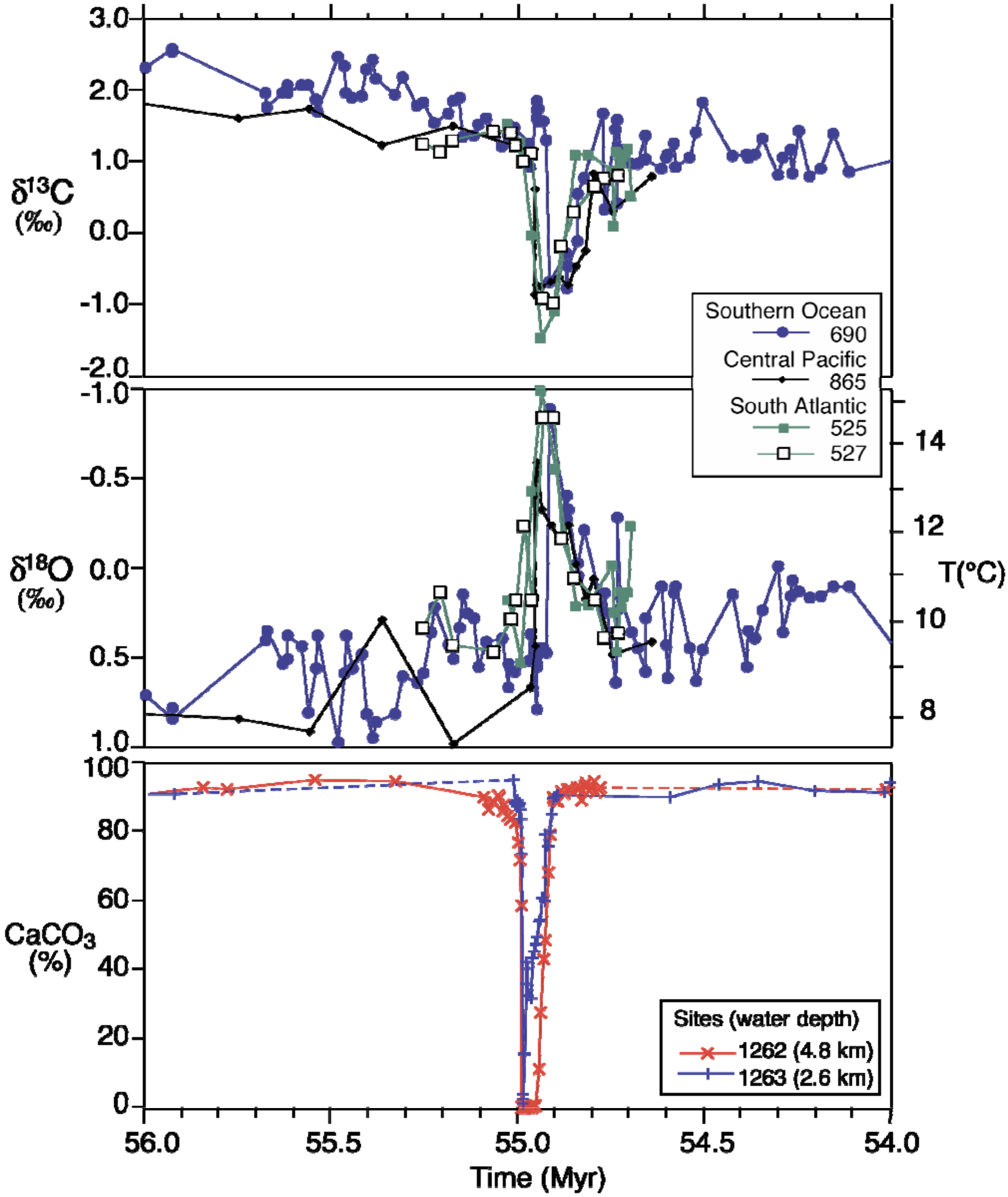

Figure 6.2. The Paleocene-Eocene Thermal Maximum (PETM) as recorded in benthic (bottom dwelling) foraminifer (*N. truempyi*) isotopic records from sites in the Antarctic, south Atlantic and Pacific (see Zachos et al., 2003 for details). The rapid decrease in carbon isotope ratios in the top panel is indicative of a large increase in atmospheric greenhouse CO_2 and CH_4, that was coincident with ~5°C global warming (center panel). Using the carbon isotope records, numerical models show that CH_4 released by the rapid decomposition of marine hydrates might have been a major component (~2000 GtC) of the carbon flux (Dickens and Owen, 1996). Testing of this and other models requires an independent constraint on the carbon fluxes. In theory, the much of the additional greenhouse carbon would have been absorbed by the

ocean, thereby lowering seawater pH and causing widespread dissolution of seafloor carbonates. Such a response is evident in the lower panel which shows a transient reduction in the carbonate content of sediments in two cores from the south Atlantic (Zachos et al., 2004; Zachos et al., 2005). The observed patterns indicate that the oceans carbonate saturation horizon rapidly shoaled over 2 km, and then gradually recovered as buffering processes slowly restored the chemical balance of the ocean. Initially, most of the carbonate dissolution is of sediment deposited prior to the event, a process that offsets the apparent timing of the dissolution horizon relative to the base of the benthic foraminifer carbon isotope excursion. Model simulations show that the recovery of the carbonate saturation horizon should precede the recovery in the carbon isotopes by as much as 100 kyr (Dickens and Owen, 1996), another feature that is evident in the sediment records.

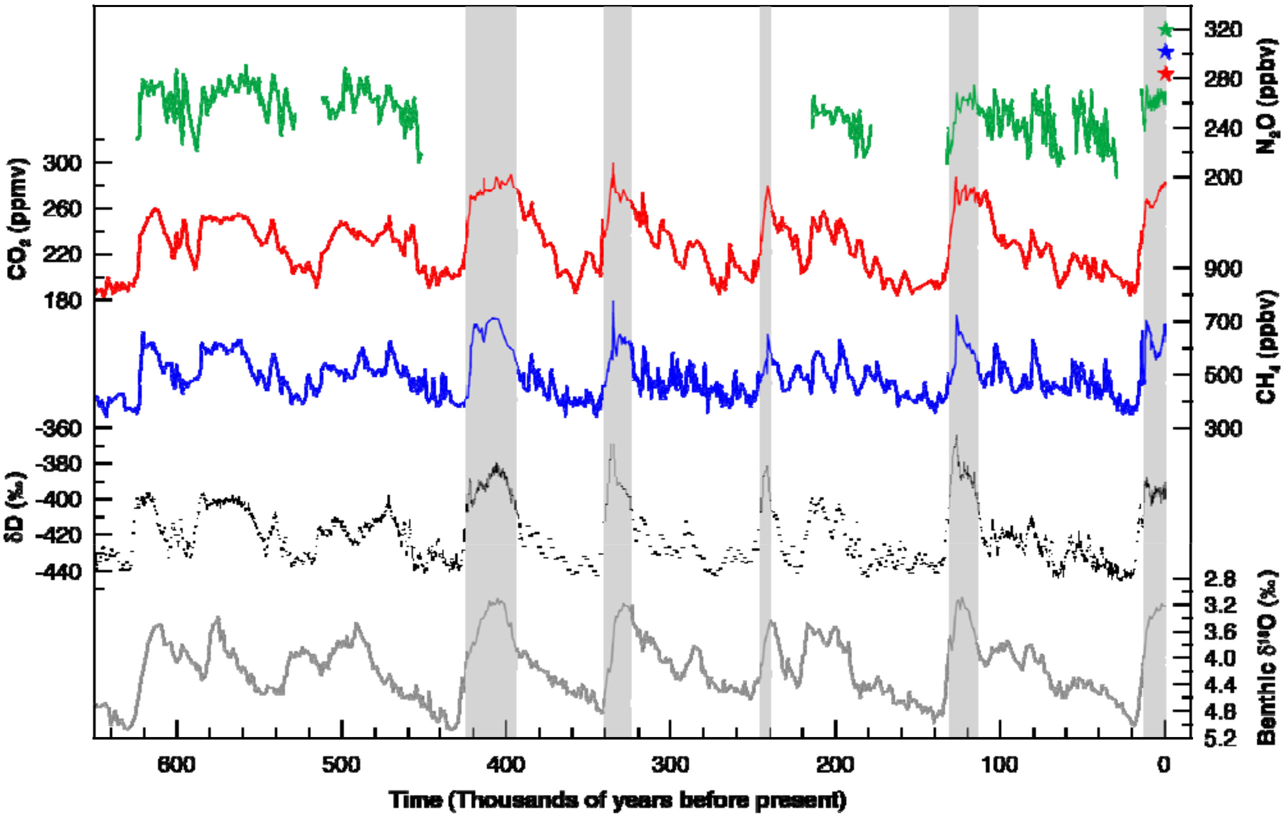

Figure 6.3. Variations of deuterium in Antarctic ice, a proxy for local temperature, and the atmospheric concentrations of the greenhouse gases carbon dioxide, methane, and nitrous oxide derived from air trapped within ice cores from Antarctica and from recent atmospheric measurements(Petit et al., 1999; Indermühle et al., 2000; EPICA community members, 2004; Spahni et al., 2005; Siegenthaler et al., 2005b). The shading indicates the last interglacial warm periods. There is clear evidence for interglacial periods prior to 450,000 years, but these were apparently colder than the typical interglacials of the latest Quaternary. The length of the current interglacial is not unusual in the context of the last 650,000 years. The stack of 57 globally distributed benthic δ^{18}O marine records, a proxy for global ice volume fluctuations (Lisiecki and Raymo, 2005), is displayed in the bottom part of the figure for comparison with the ice core data. Larger ice volume is expressed downwards. Note that the shaded vertical bars are based on the ice core age model (EPICA community members, 2004), and that the marine record is plotted on its original time scale based on tuning to the orbital parameters (Lisiecki and Raymo, 2005).

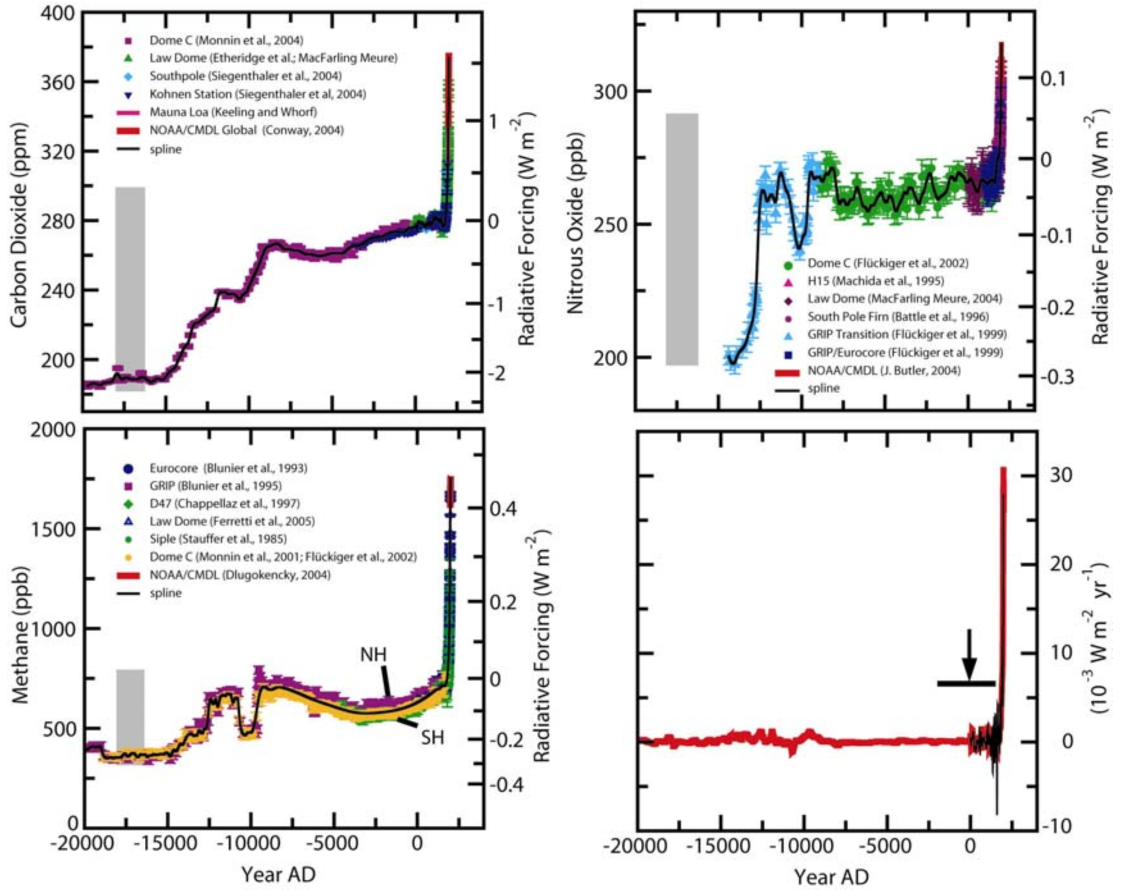

Figure 6.4. The concentrations and radiative forcing by (a) carbon dioxide (CO_2), (b) methane (CH_4), (c) nitrous oxide (N_2O), and (d) the rate of change in their combined radiative forcing over the last 20,000 years reconstructed from Antarctic and Greenland ice and firn data (symbols) and direct atmospheric measurements (red and magenta lines). The grey ranges show the reconstructed ranges of natural variability for the past 650,000 years (Siegenthaler et al., 2005b; Spahni et al., 2005). Radiative forcing has been computed with the simplified expressions of chapter 2 (Myhre et al., 1998). The rate of change in radiative forcing (red line) has been computed from spline fits (Enting, 1987) of the concentration data (thin black lines in panel a-c). The width of the age distribution of the bubbles in ice varies from ~20 years for sites with a high accumulation of snow such as Law Dome, Antarctica, to ~200 years for low accumulation sites such as Dome Concordia, Antarctica. The Law Dome ice and firn data, covering the past two millennia, have been splined with a cut-off period of 40 years and the resulting rate of change in radiative forcing is shown by the thin black line in d. The arrow indicates how the anthropogenic peak would have been recorded in ice during the last glacial transition. It shows the peak in the rate of change in radiative forcing after the anthropogenic signals of CO_2, CH_4, and N_2O have been smoothed with a model describing the enclosure process of air in ice (Spahni et al., 2003) applied for conditions at the low accumulation Dome Concordia site. The CO_2 data are from (Etheridge et al., 1996; Monnin et al., 2001; MacFarling Meure, 2004; Monnin et al., 2004; Siegenthaler et al., 2005a), the CH_4 data from (Stauffer et al., 1985; Steele et al., 1992; Blunier et al., 1993; Dlugokencky et al., 1994; Blunier et al., 1995; Chappellaz et al., 1997; Monnin et al., 2001; Flückiger et al., 2002; Ferretti et al., 2005), the N_2O data from (Machida et al., 1995; Battle et al., 1996; Flückiger et al., 1999; Flückiger et al., 2002; MacFarling Meure, 2004). Atmospheric data are from the NOAA global air sampling network, representing global average concentrations (Steele et al., 1992; Dlugokencky et al., 1994), and from Mauna Loa, Hawaii (Keeling and Whorf, 2005).

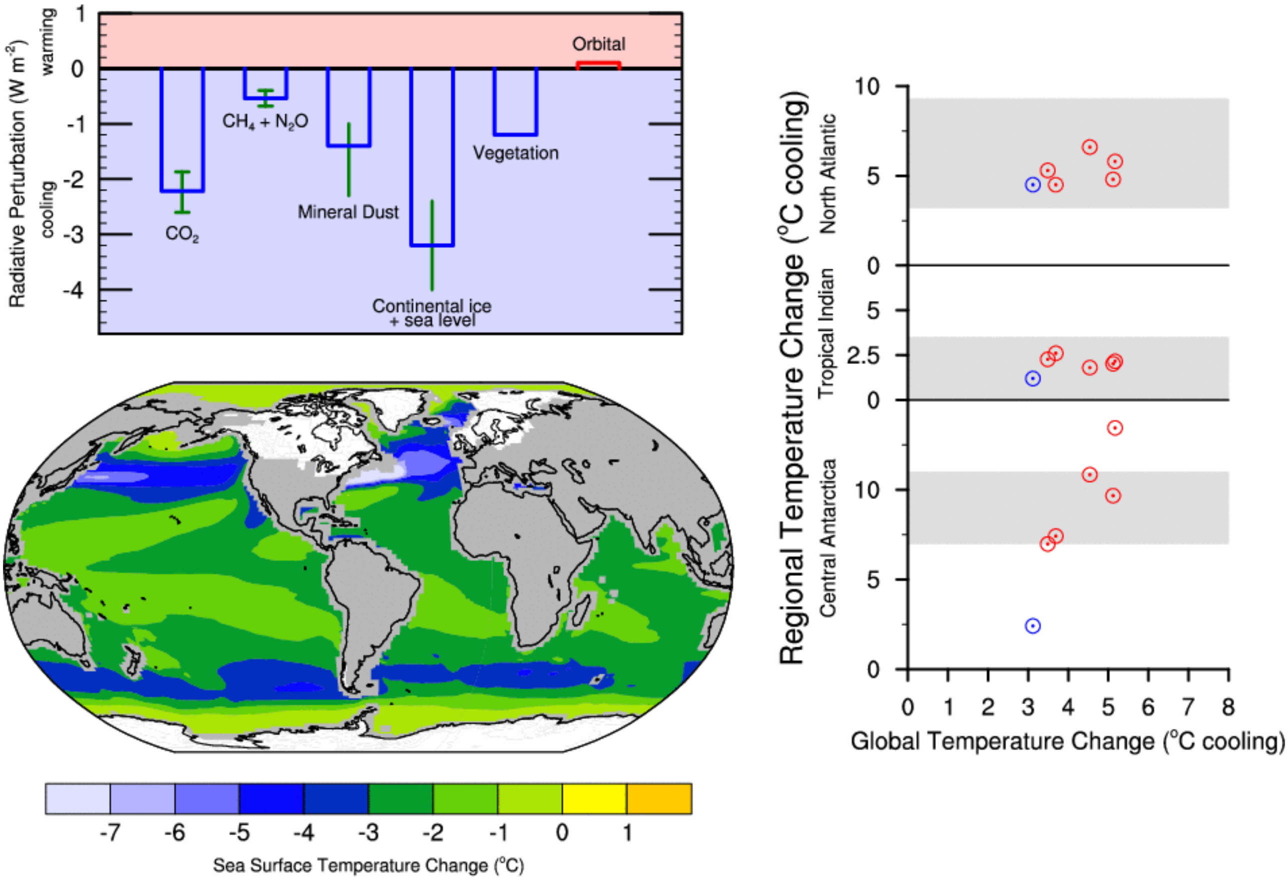

Figure 6.5. The Last Glacial Maximum (around 21kyrs ago) relative to pre-industrial (1750). See text for more details and references. Top left: Global annual mean radiative influences (W m^{-2}) of LGM climate change agents, generally feedbacks on glacial-interglacial cycles but specified in most AOGCM simulations for LGM. The heights of the rectangular bars denote best estimate values guided by published values of the forcing and physical understanding. Vertical lines about rectangular bars are ranges as follows: greenhouse gases include uncertainties in ice core measurements and errors in simplified expressions for converting concentrations to radiative perturbations (see Chapter 2); mineral dust aerosols include range of estimates from modeling studies of direct effects only; continental ice sheets/sea level is range of PMIP-2 AOGCMs, all using prescribed ICE-5G ice sheet and does not include uncertainties of LGM ice sheet extent or height. No range is available for LGM vegetation changes. Bottom left: Multi-model average SST change for LGM PMIP-2 simulations by five AOGCMs (CCSM, FGOALS, HadCM, IPSL, and MIROC). Ice extent over continents is shown in white. Right: LGM regional cooling as compared to LGM global cooling as simulated in PMIP-2, AOGCM results shown as red circles, EMIC (ECBilt-CLIO) result shown as blue circle. Regional averages are defined as Antarctica, annual for inland ice cores; tropical Indian Ocean, annual for 15°S–15°N, 50–100°E; North Atlantic Ocean, July-August-September for 42–57°N, 35°W–20°E. Grey shading indicates range of proxy estimates of regional cooling: Antarctica (Stenni et al., 2001), tropical Indian Ocean (Barrows and Juggins, 2005), North Atlantic Ocean (Rosell-Mele et al., 2004; deVernal et al., 2005; Kucero and al., 2005).

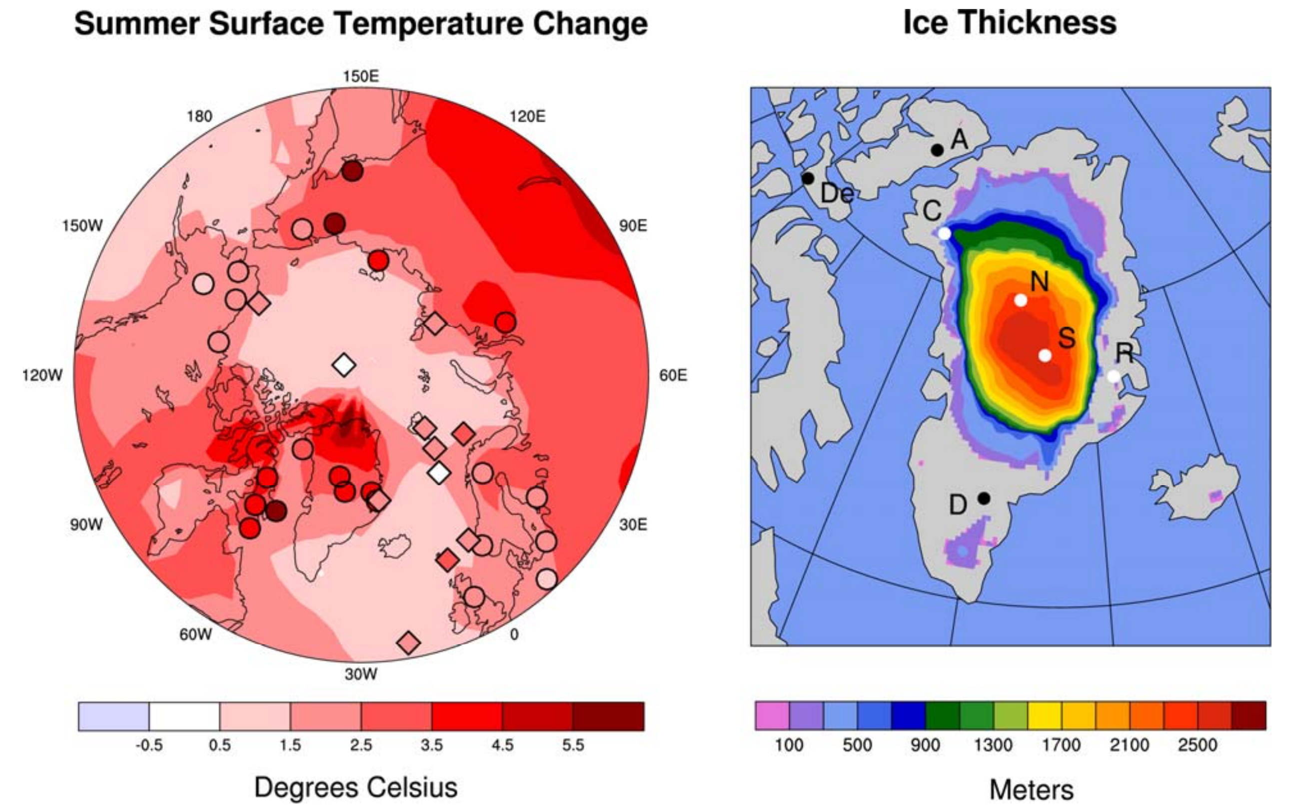

Figure 6.6. Summer surface air temperature change over the Arctic and annual ice thickness and extent for Greenland and western Arctic glaciers for the Last Interglacial at approximately 130–125 kyr ago~~)~~ from a multi-model and a multi-proxy synthesis. The summer warming simulated by the NCAR CCSM (Otto-Bliesner et al., 2006) and ECHO-G model (Kaspar et al., 2005) is contoured in the left panel and is overlain by proxy estimates of maximum summer warming from terrestrial (circles) and marine (diamonds) sites as compiled in the syntheses published by the CAPE Project Members (2006) and Kaspar et al. (2005). Extents and thicknesses of the Greenland ice sheet and western Canadian and Iceland glaciers are shown at their minimum extent for the Last Interglacial as a multi-model average from three ice models (Tarasov and Peltier, 2003; Lhomme et al., 2005b; Otto-Bliesner et al., 2006). Ice core observations (Koerner, 1989; North Greenland Ice Core Project, 2004) indicate Last Interglacial ice (white dots) at Renland (R), NGRIP (N), Summit (S, GRIP and GISP2), and possibly Camp Century (C), but no LIG ice (black dots) at Dye-3 (D), Devon (De), and Agassiz (A).

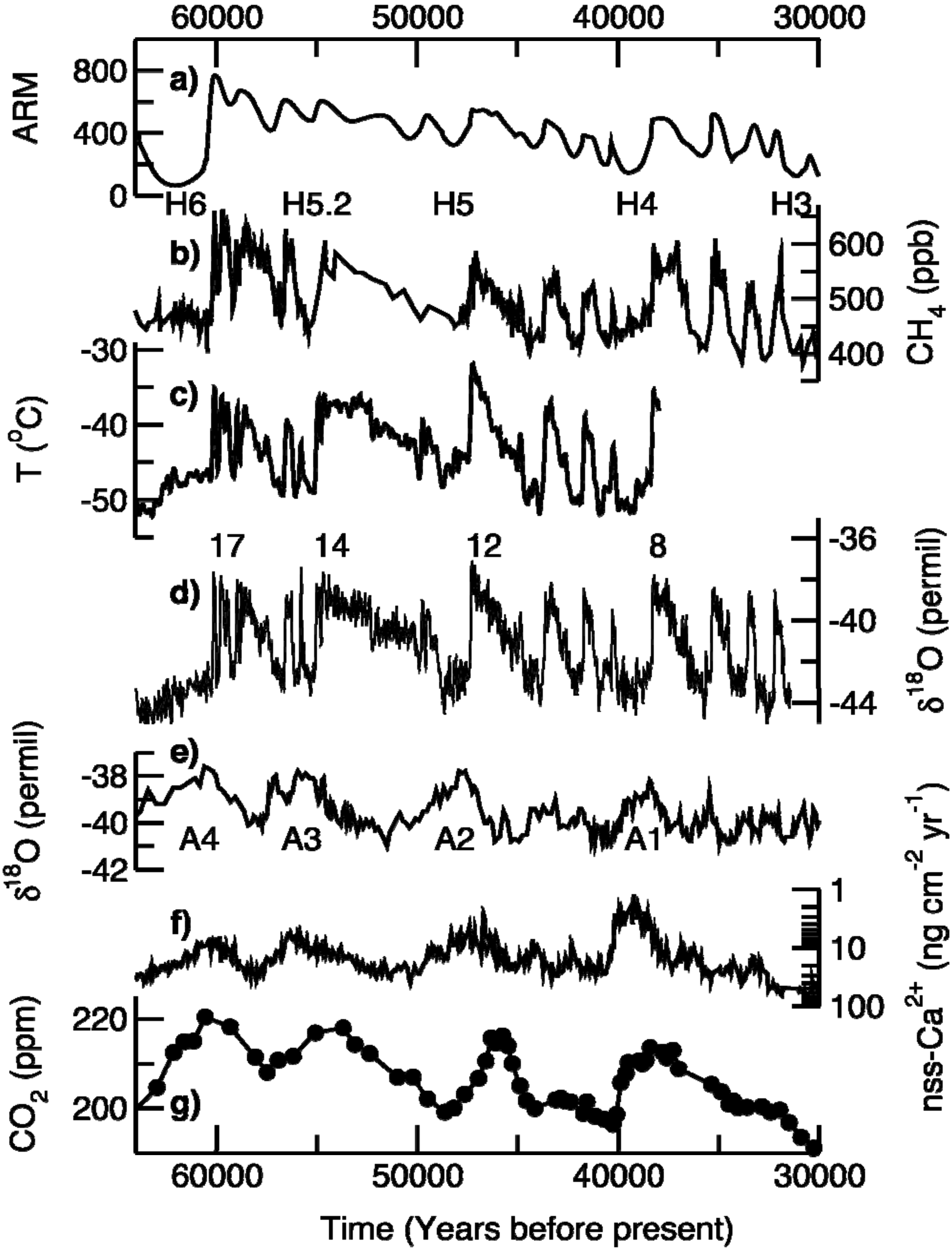

Figure 6.7. The evolution of climate indicators from the Northern Hemisphere (panels a to d) and from Antarctica (panels e to f) over the period 64,000 to 30,000 years before present. a) Anhysteretic remanent magnetisation (ARM), here a proxy of the northward extent of Atlantic Meridional Overturning circulation, from an ocean sediment core from the Nordic Seas (Dokken and Jansen, 1999); b) methane as recorded in

Greenland ice cores at the GRIP, GISP (data from 40 to 64 thousand years ago), and NorthGRIP sites (Blunier and Brook, 2001; Flückiger et al., 2004; Huber et al., 2006). CH_4 data for the period 40 to 30 thousand years ago were selected for the GRIP site and for 64 to 40 thousand years ago for the GISP site when sample resolution is highest in the cores; c) surface temperature estimated from nitrogen isotope ratios that are influenced by thermal diffusion (Huber et al., 2006); d) $\delta^{18}O$, a proxy for surface temperature, from NorthGRIP (North Greenland Ice Core Project, 2004); e) $\delta^{18}O$ from Byrd, Antarctica (Blunier and Brook, 2001); f) nss-Ca^{2-}, a proxy of dust and iron deposition, from Dome C, Antarctica (Röthlisberger et al., 2004); g) CO_2 as recorded in ice from Taylor Dome, Antarctica (Indermühle et al., 2000). The Dansgard/Oeschger Northern Hemisphere warm events 8, 12, 14, and 17, the Heinrich events, periods of massive ice rafted debris recorded in marine sediments, H3, H4, H5, H5.2, and H6, as well as the Antarctic warm events A1 to A4 are shown. All data are plotted on the Greenland SS09sea time scale. CO_2 and CH_4 are well mixed in the atmosphere. CH_4 variations are synchronous (within the resolution of ±50 years) with variations in Greenland temperature. CO_2 co-varied with the Antarctic temperature (The exact synchronisation between Taylor Dome and Byrd is not without uncertainties making the determination of lead or lags between temperature and CO_2 elusive). The evolution of Greenland and Antarctic temperature is consistent with a reorganisation of the heat fluxes and the Meriodional Overturning Circulation in the Atlantic (Knutti et al., 2004).

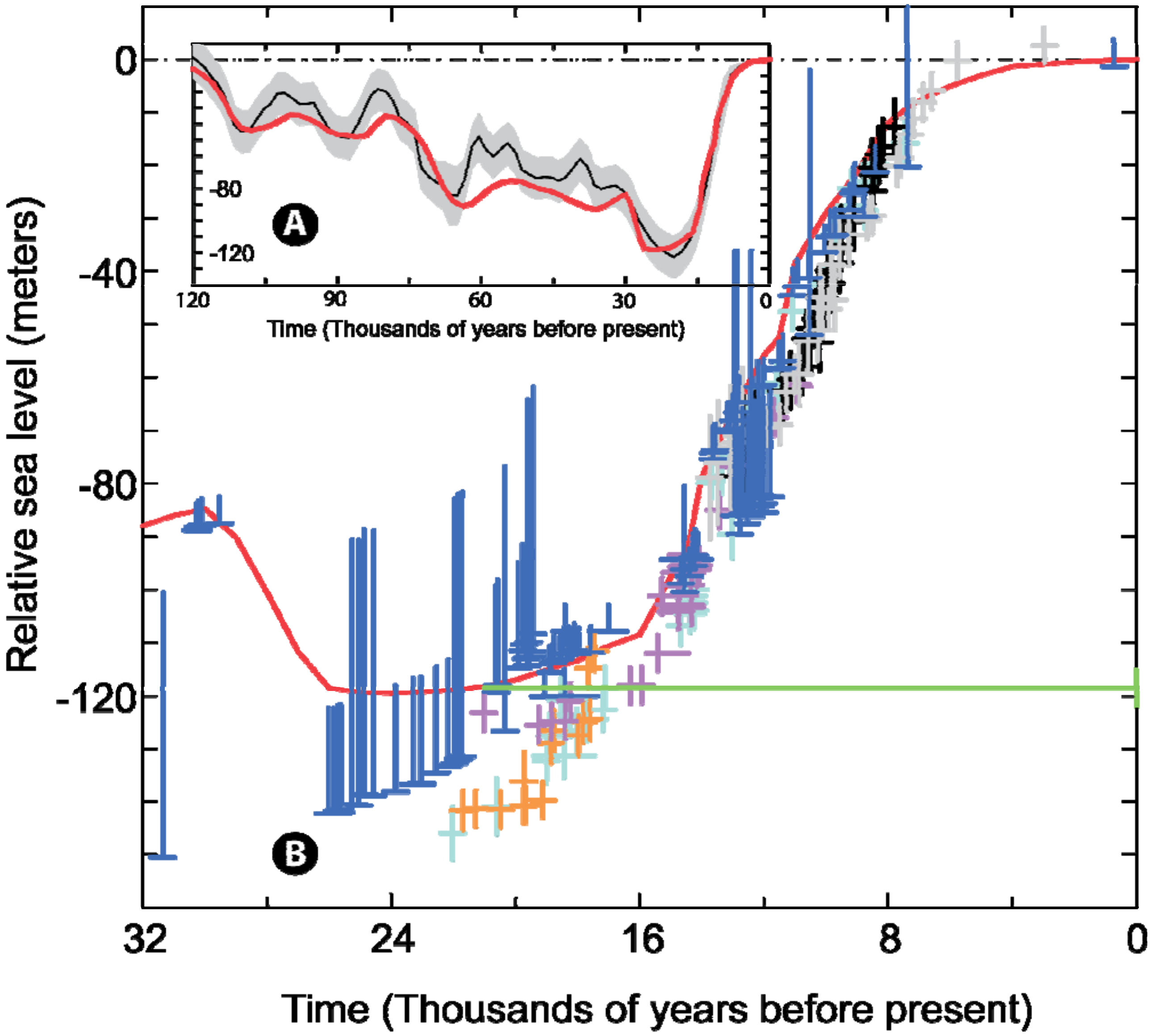

Figure 6.8. (a) The ice equivalent eustatic sea level history over the last glacial-interglacial cycle according to the reconstruction of Waelbroeck et al. (2002). The black line defines the mid-point of their estimates for each age and the surrounding hatched region an estimate of error. The red line is the prediction of the ICE-5G(VM2) model for the Barbados location for which the relative sea level observations themselves provide a close approximation to the ice equivalent eustatic sea level curve.
(b) The fit of the ICE-5G(VM2) model prediction (red line) to the coral based record of relative sea level history from the island of Barbados in the Caribbean Sea (Fairbanks, 1989; Peltier and Fairbanks, accepted) over the age range from the present day to 30,000 years before present. The individual coral based estimates of relative sea level (blue) have an attached error bar that depends upon the coral species. The estimates denoted by the short error bars are derived from the *Acropora Palmata* species which provide the tightest constraints upon relative sea level as this species is found to live within approximately 5m of sea level in the modern ecology. The estimates denoted by the longer error bars are derived either from the *Monastrea Annularis* species of coral (error bars of intermediate length) or from further species which are found over a wide range of depths with respect to sea level (longest error bars). These data are most useful in providing a lower bound for the sea level depression. The data denoted by the colored crosses are from the ice equivalent eustatic sea level reconstruction of Lambeck and Chappell (2001). The color code employed for these data is as follows: cyan (Barbados), grey (Tahiti), black (Huon), orange (Bonaparte Gulf), purple (Sunda Shelf). The green line denotes the conventionally inferred LGM sea level lowering of 120 m (eg. Shackleton, 2000)

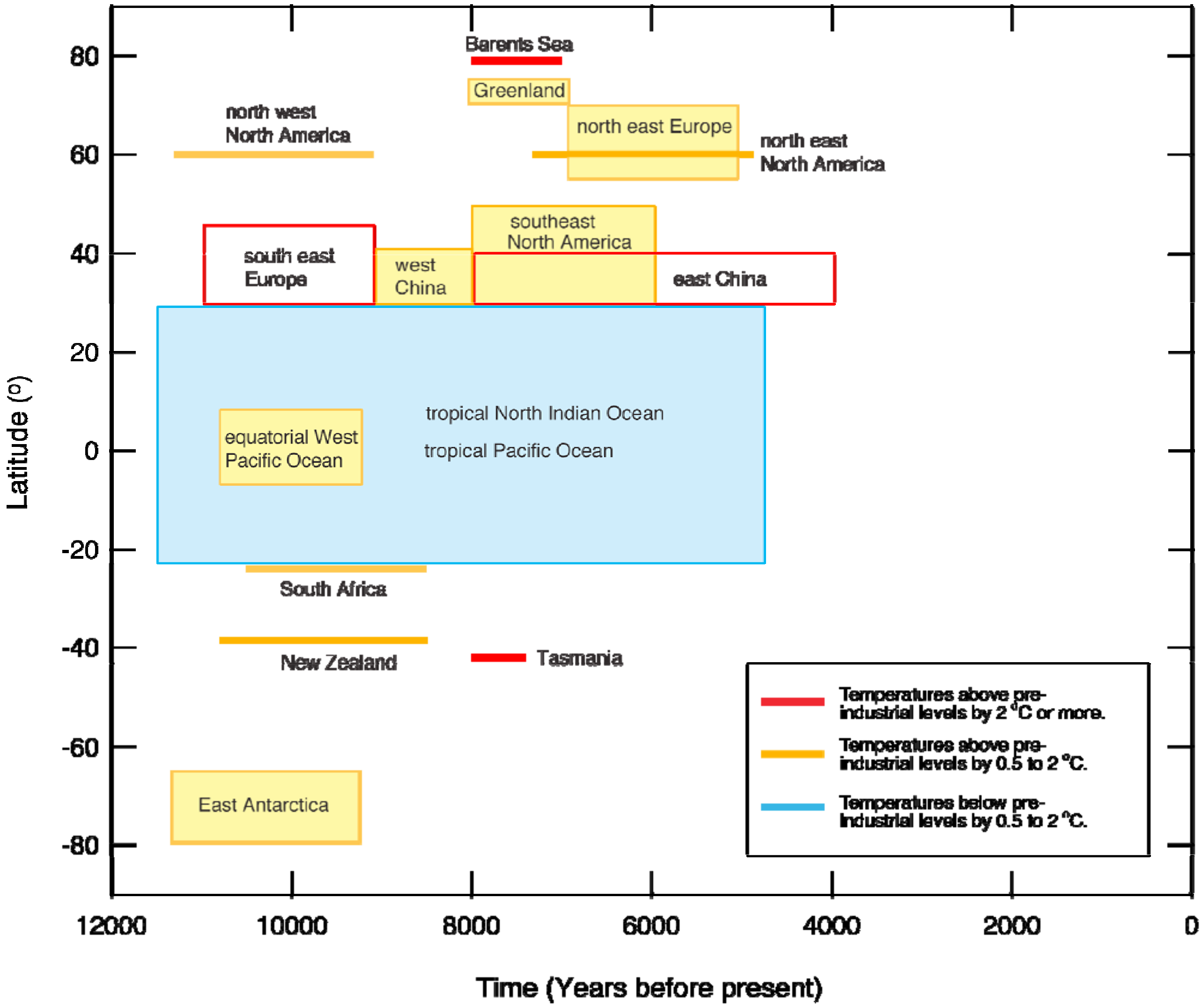

Figure 6.9. Timing and intensity of maximum temperature deviation from pre-industrial levels, as a function of latitude (vertical axis) and time (horizontal axis, in thousands of years before present, 1950 A.D.). Temperatures above pre-industrial levels by 0.5°C to 2°C appear in orange (above 2°C in red). Temperatures below pre-industrial levels by 0.5°C to 2°C appear in blue. References for datasets are : Barents Sea (Duplessy et al., 2001), Greenland (Johnsen et al., 2001), Europe (Davis et al., 2003), northwest and northeast America (Kaufman et al., 2004) (MacDonald et al., 2000), China (He et al., 2004), tropical oceans (Rimbu et al., 2004) (Stott et al., 2004) (Lorentz et al., 2006), north Atlantic (Marchal et al., 2002) (Kim et al., 2004), Tasmania (Xia et al., 2001), East Antarctica (Masson et al., 2000), south Africa (Holmgren et al., 2003), New Zealand (Williams et al., 2004).

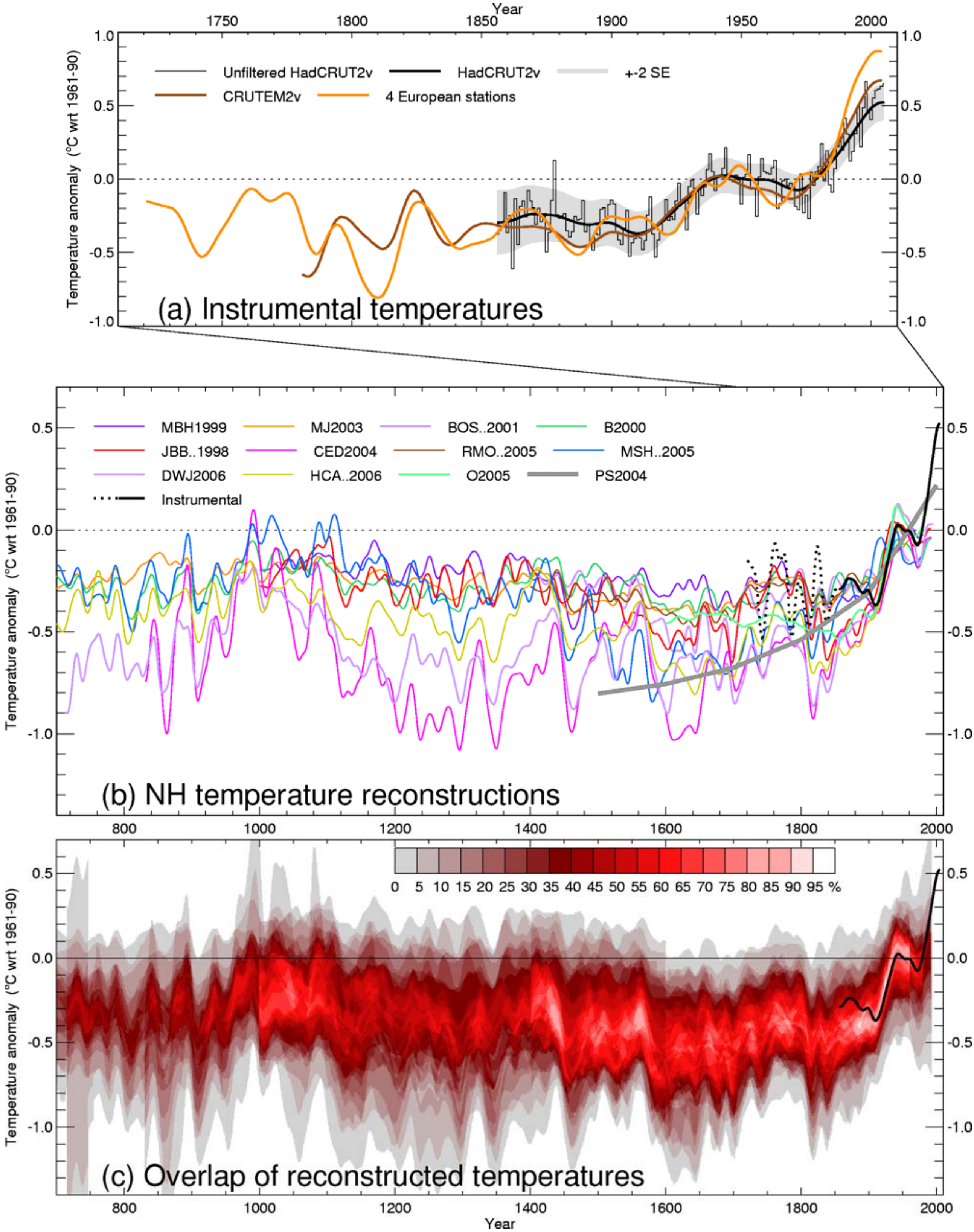

Figure 6.10. Records of Northern Hemisphere temperature variation during the last 1300 years. (a) Annual-mean instrumental temperature records: black = land and marine temperatures for the full NH (series [I1] in Table 6.1), with annual values (thin line) and ±2 standard errors ([I2], grey shading); brown = land only temperatures for the NH [I3]; orange = average of temperatures from 4 stations in Europe [I4]. (b) Reconstructions using multiple climate proxy records: red (JBB..1998) = [R1]; dark purple (MBH1999) = series [R2]; light blue (BOS..2001) = [R3]; pink (CED2004) = [R4]; green (B2000) = [R5]; orange

(MJ2003) = [R6]; brown (RMO..2005) = [R7]; dark blue (MSH..2005) = [R8]; light purple (DWJ2006) = [R9]; yellow (HCA..2006) = [R10]; thick grey (PS2004) = [*R11*]; black (Instrumental) = composite of [I4] and [I3] (dotted) and [I1] (solid).
(c) Composite of series [R1] to [R12] (excluding [R7] and [R11]) and their published uncertainty ranges indicating the number of overlapping reconstructions (regions within the ±1 standard error [SE] of a reconstruction score 10%, regions within ±2 SE score 5%; maximum 100% obtained for temperatures that fall within ±1 SE of all 10 reconstructions). Series [I1] is shown in black.

All series have been smoothed with a Gaussian-weighted filter to remove fluctuations on time scales less than 30 years; smoothed values are obtained up to both ends of each record by extending the records with the mean of the adjacent existing values. All temperatures represent anomalies (°C) from the 1961–1990 mean.

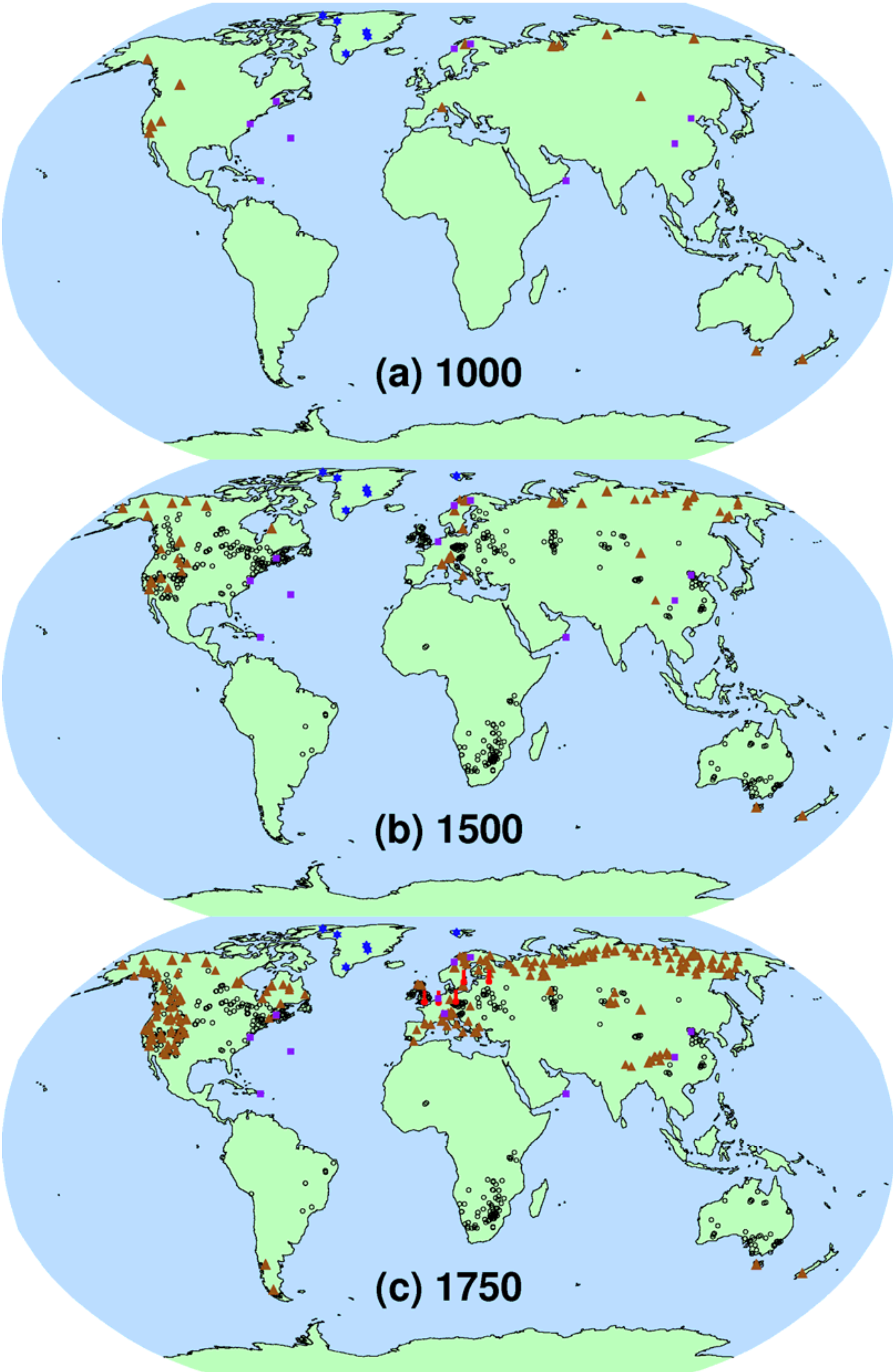

Figure 6.11. Locations of temperature-sensitive proxy records with data back to 1000, 1500 and 1750 (instrumental records: red thermometers; tree-ring: brown triangles; boreholes: black circles; ice-core/ice-boreholes: blue stars; other records including low-resolution records: purple squares). All proxies used in reconstructions [R1] to [R11] of Northern Hemisphere temperatures (see Table 6.1 and Figure 6.10) or used to indicate Southern Hemisphere regional temperatures (Figure 6.12) are included.

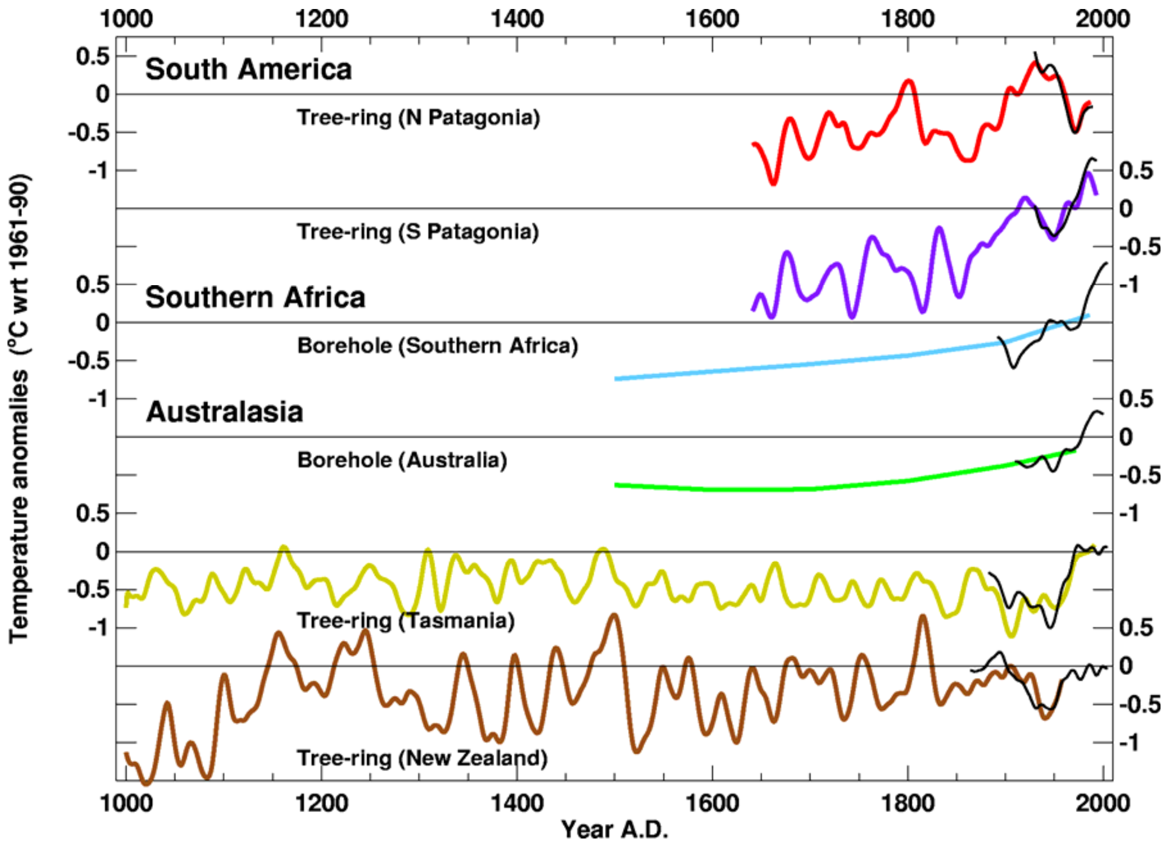

Figure 6.12. Temperature reconstructions for regions in the Southern Hemisphere: two annual temperature series from South American tree-ring data (Villalba et al., 2003); annual temperature estimates from borehole inversions for southern Africa and Australia (derived using the approach of Pollock and Smerdon (2004); summer temperature series from Tasmania and New Zealand tree-ring data (Cook et al., 2000; Cook et al., 2002a). The black curves show summer or annual instrumental temperatures for each region. All tree-ring and instrumental series have been smoothed with a 25-year filter and represent anomalies (°C) from the 1961–1990 mean (indicated by the horizontal lines).

1

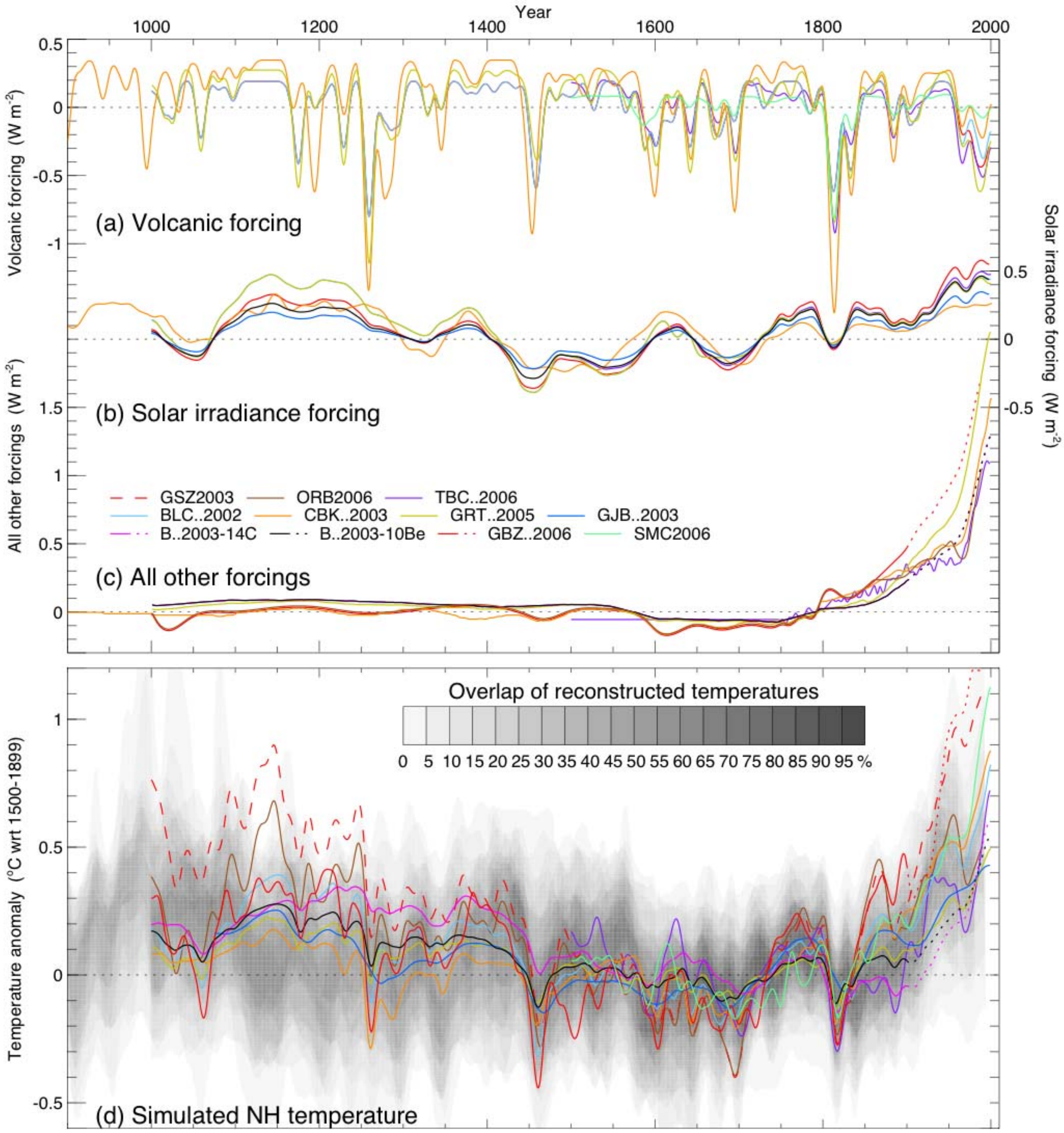

Year
1000
1200
1400
1600
1800
2000
Volcanic forcing (W m^{-2})
(a) Volcanic forcing
Solar irradiance forcing (W m^{-2})
(b) Solar irradiance forcing
All other forcings (W m^{-2})
GSZ2003
ORB2006
TBC..2006
BLC..2002
CBK..2003
GRT..2005
GJB..2003
B..2003-14C
B..2003-10Be
GBZ..2006
SMC2006
(c) All other forcings
Overlap of reconstructed temperatures
0 5 10 15 20 25 30 35 40 45 50 55 60 65 70 75 80 85 90 95 %
Temperature anomaly (°C wrt 1500-1899)
(d) Simulated NH temperature

2

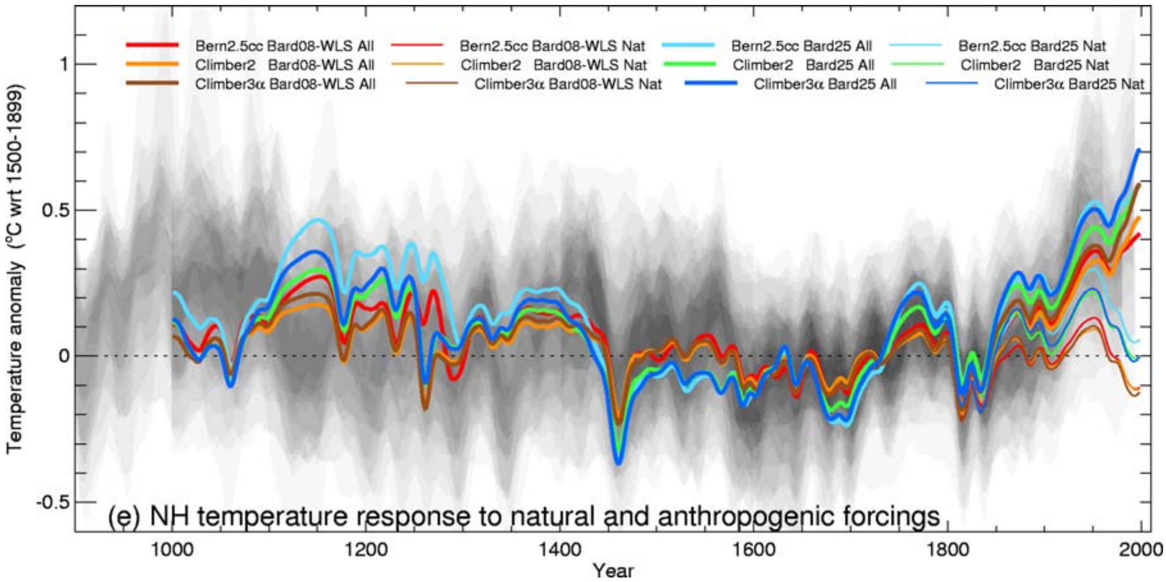

Figure 6.13. Radiative forcings and simulated temperatures during the last 1100 years. Global-mean radiative forcing (W m^{-2}) used to drive climate model simulations due to (a) volcanic activity, (b) solar irradiance variations (these values are indicated by the labeling on the right-hand axis), and (c) all other forcings (which vary between models, but always include greenhouse gases and, except for those with dotted lines after 1900, tropospheric sulphate aerosols). Annual-mean NH temperature (°C) simulated (d) under the range of forcings shown in (a)-(c) and (e) in a set of experiments designed to isolate the influences of anthropogenic and natural forcings, for two different estimates of solar irradiance variability (‘All’ [thick] used anthropogenic and natural forcings, ‘Nat’ [thin] used only natural forcings). The region of overlapping NH temperature reconstructions is shown by grey shading in panels (d) and (e) (modified from Figure 6.11c to account for the 1500–1899 reference period used here).

All forcings and temperatures are expressed as anomalies from their 1500–1899 means and then smoothed with a Gaussian-weighted filter to remove fluctuations on time scales less than 30 years; smoothed values are obtained up to both ends of each record by extending the records with the mean of the adjacent existing values.

The individual series are defined in Table 6.2 for (a) to (d), and in Table 6.3 for (e).

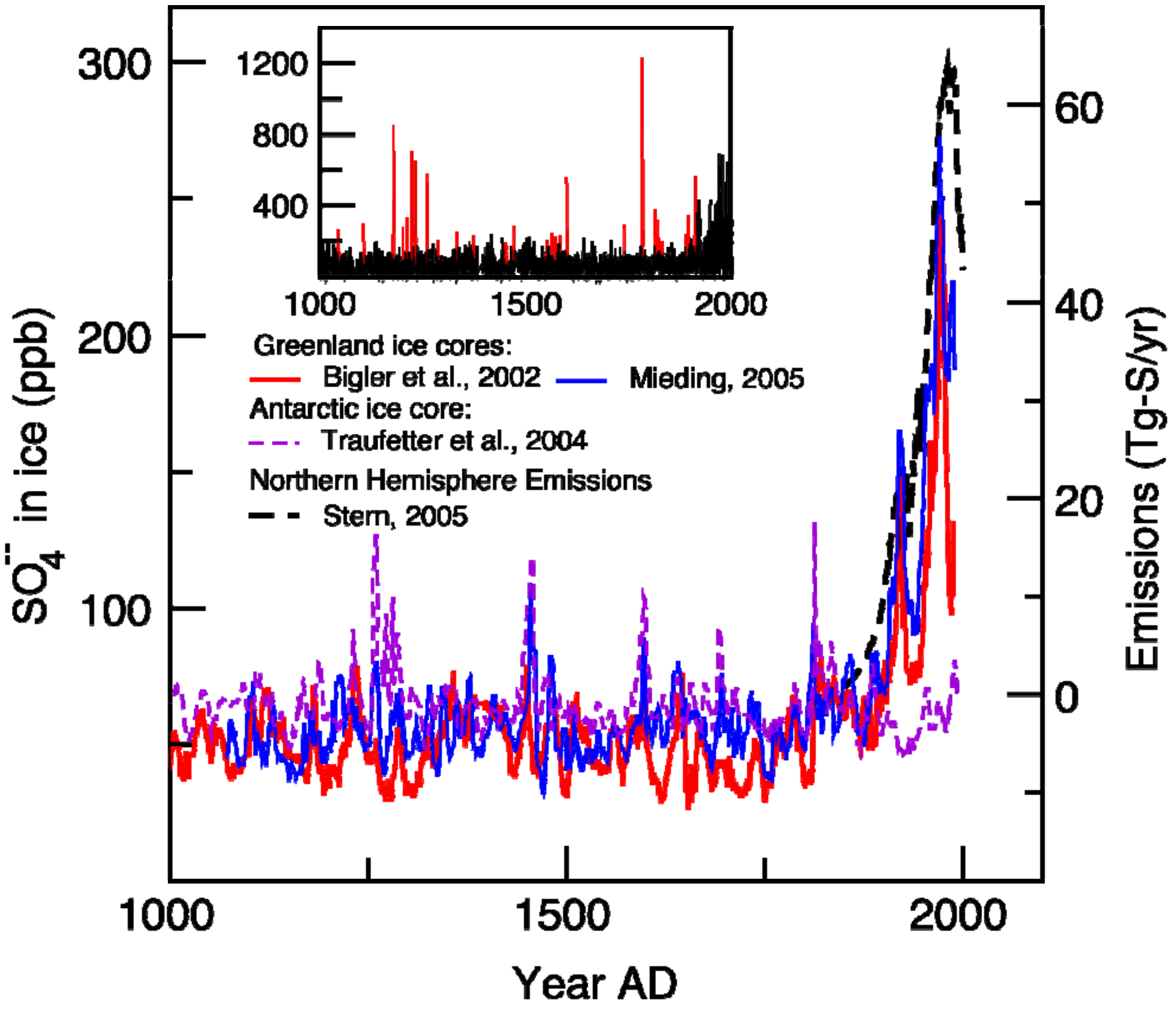

Figure 6.14. Sulfate concentrations in Greenland and Antarctic ice cores (Fischer et al., 1998; Bigler et al., 2002; Mieding, 2005) during the last millennium. Also shown are the estimated anthropogenic sulfur emissions for the Northern Hemisphere (Stern, 2005). The ice core data have been smoothed with a 10-year running median filter, thereby removing the peaks of major volcanic eruptions. The inset illustrates the influence of volcanic emissions and shows monthly data as measured (red) and with the volcanic spikes removed (black) (Bigler et al., 2002).

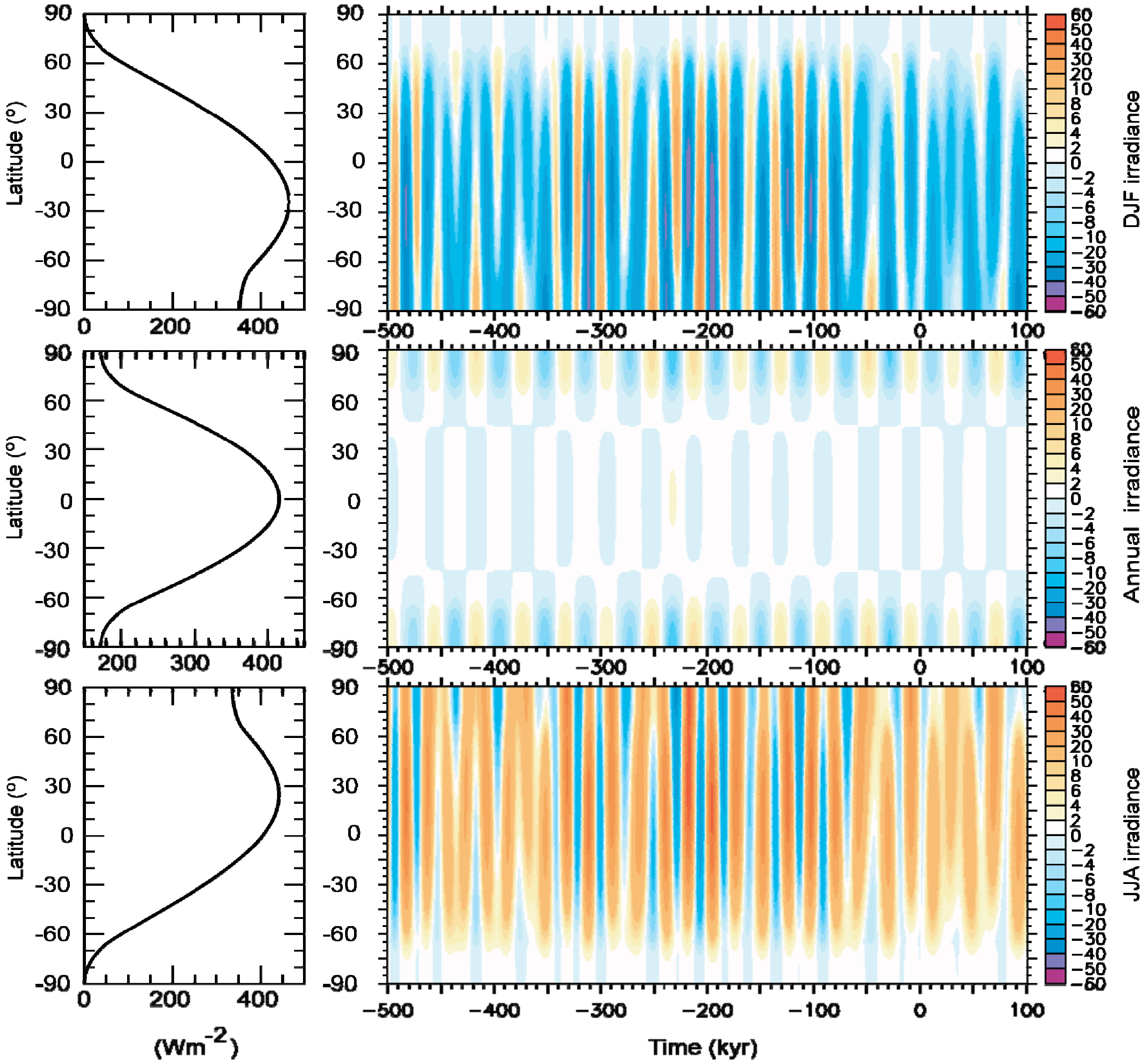

Box 6.1, Figure 1. December-January-February (top panel), annual mean (middle panel) and June-July-August (bottom panel) latitudinal distribution of present-day (year 1950) incoming mean solar radiation (W m^{-2}). Right side: deviations with respect to present-day of December-January-February (top panel), annual mean (middle panel) and June-July-August (bottom panel) latitudinal distribution of incoming mean solar radiation from the past 500 kyr to the future 100 kyr (W/m^{-2}) (Berger and Loutre, 1991; Loutre et al., 2004).

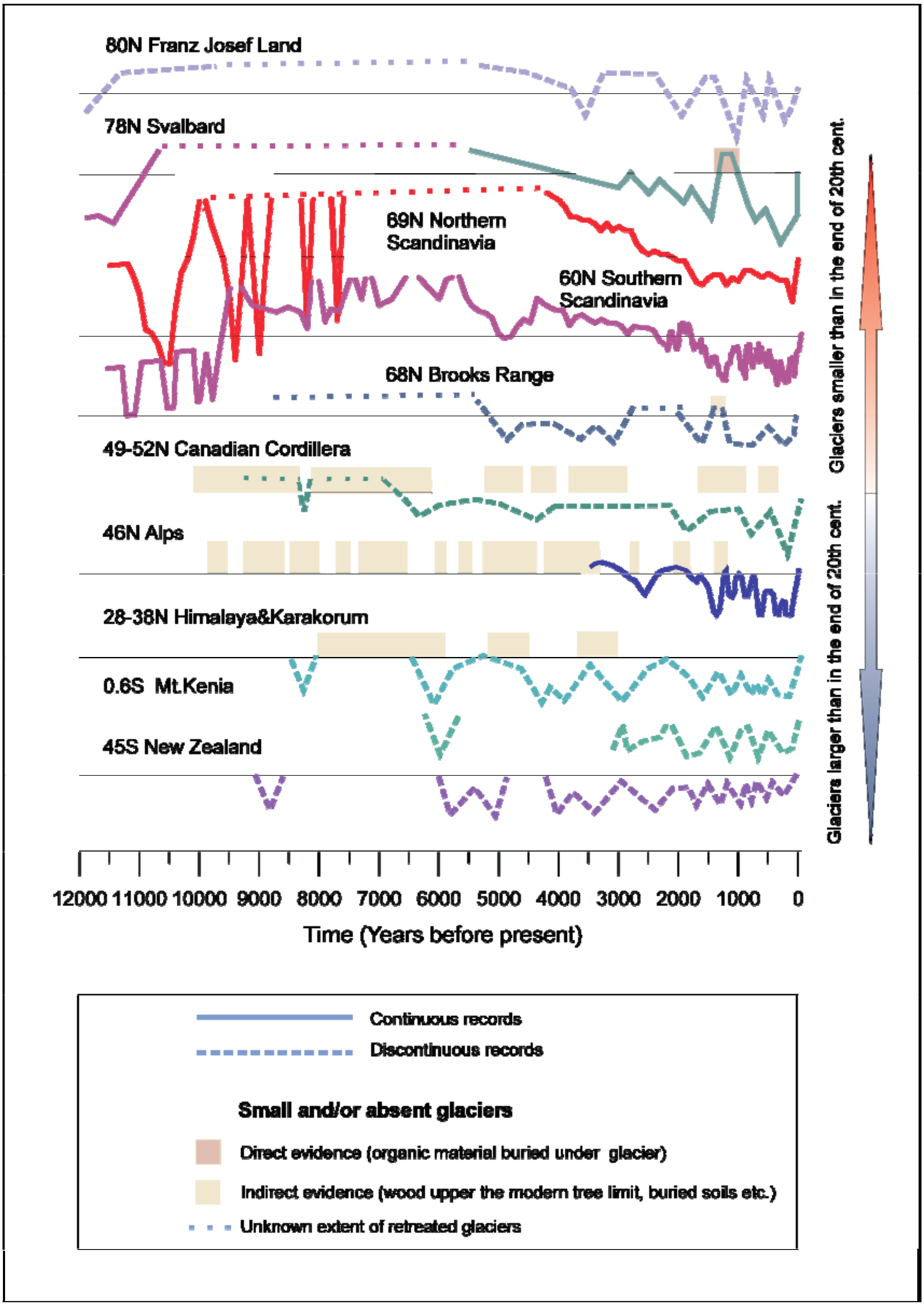

Box 6.3, Figure 1.
Franz Josef Land – (Lubinski et al., 1999), calibrated.
Svalbard – curve from (Svendsen and Mangerud, 1997) corrected with (Humlum et al., 2005).
Northern Scandinavia (Nesje et al, 2005; Bakke et al., 2005a; Bakke et al., 2005c).
Southern Scandinavia (Dahl et al, 1996; Matthews et al., 2000; Lie et al., 2004; Matthews et al., 2005).
Brooks Range – (Ellis and Calkin, 1984), calibrated.
Canadian Cordillera – (Luckman and Kearney, 1986; Osborn and Luckman, 1988), calibrated, (Koch et al., 2004; Menounos et al., 2004).

Alps – (Holzhauser et al., 2005; Joerin et al., accepted 2005).
Himalaya and Karakorum – (Roethlisberger and Geyh, 1985), calibrated, (Bao et al., 2003).
Mt Kenya – (Karlen et al., 1999).
New Zealand – (Gellatly et al., 1988), calibrated.

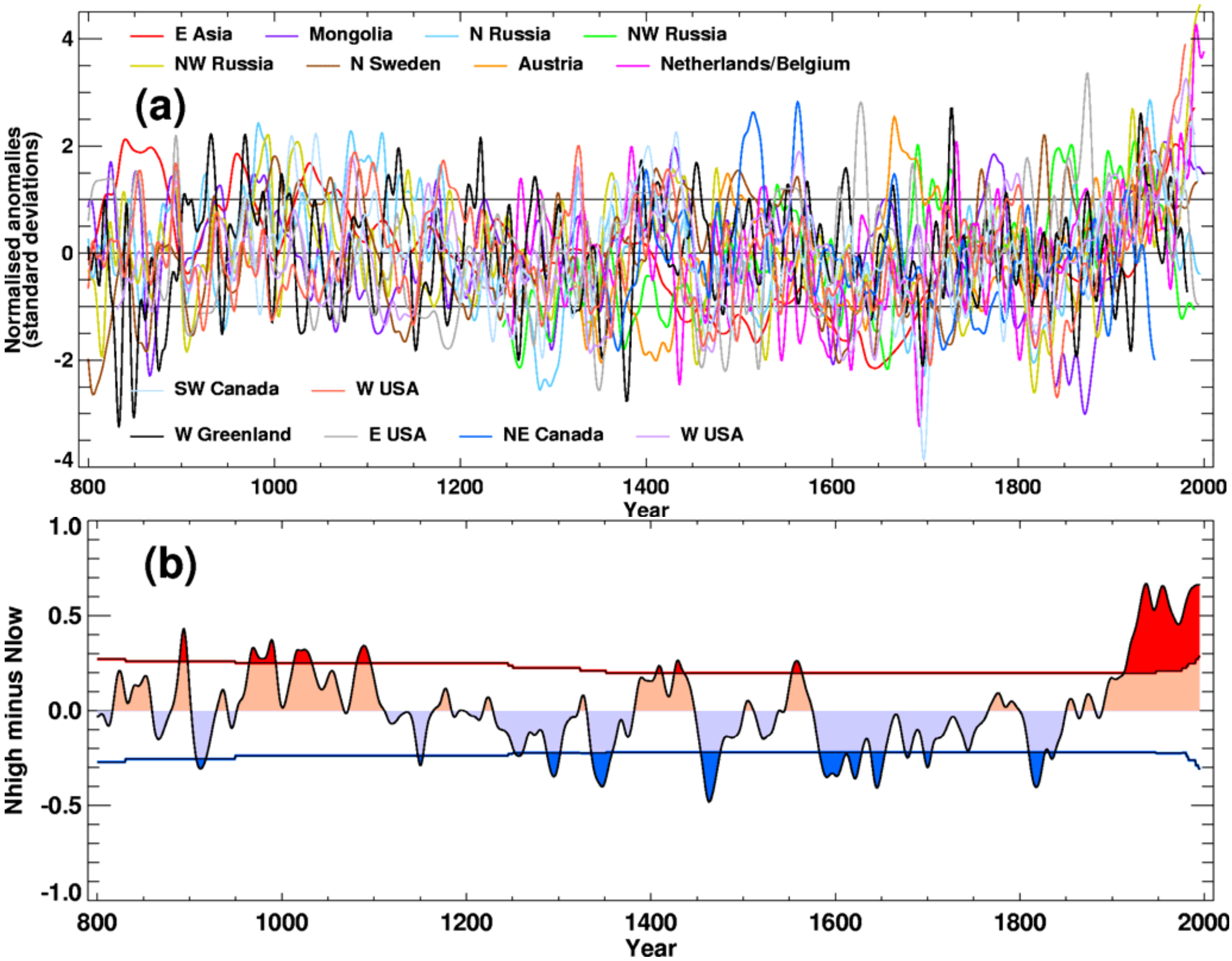

Box 6.4, Figure 1. (a) The heterogeneous nature of climate during the MWP is illustrated by the wide spread of values exhibited by the individual records that have been used to reconstruct NH-mean temperature. Individual, or small regional averages of, proxy records used in various studies (see Osborn and Briffa, 2006), (collated from those used by Mann and Jones (2003), Esper et al. (2002) and Luckman and Wilson (2005) but excluding shorter series or those with an ambiguous relationship to local temperature). These records have not been calibrated (though all show positive correlations with local temperature observations), but have been smoothed with a 20-year filter and scaled to have zero mean and unit standard deviation over the period 800–1995.

(b) The fraction of records shown in (a) that exceed the +1 standard deviation line, minus the fraction of records that are below the –1 standard deviation line (Osborn and Briffa, 2006). Horizontal lines indicate periods when the results differ significantly from those expected if the time series had no relationship to temperature (specifically, the 5th and 95th percentiles of the distributions of results obtained after shifting individual records randomly in time, thus destroying the calendar alignment between records).

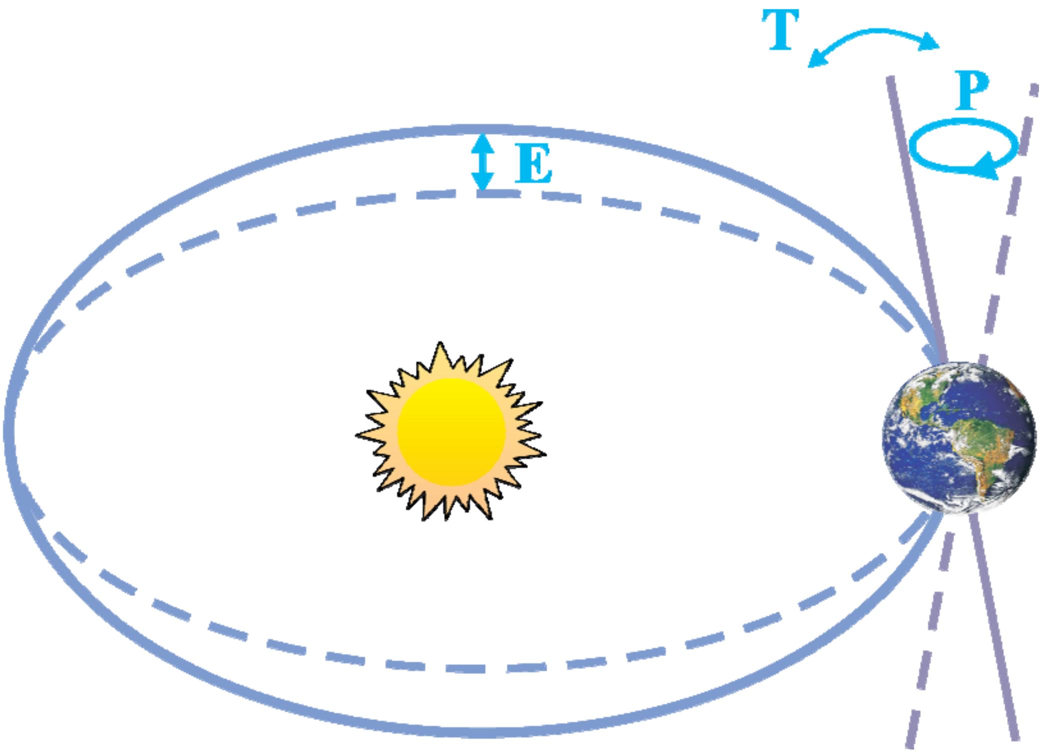

Question 6.1, Figure 1. Schematic of the Earth's orbital changes (Milankovich cycles) that drive the ice age cycles. "T" denotes changes in the tilt (or obliquity) of the Earth axis, "E" denotes changes in the eccentricity of the orbit, and "P" denotes precession, i.e., changes in the direction of the axis tilt at a given point of the orbit. Source: Rahmstorf and Schellnhuber (2006).